Recent Trends in Toll Transmission in the United States *

By EDWIN H. COLPITTS

YOUR country is advancing industrially and commercially with tremendous strides. Adequate telephone communication is of such great importance under these conditions that I felt a general statement as to methods in process of being applied to the plant of the Bell System would be interesting and possibly helpful. I am fully aware that, in some or even many respects, your problems will differ from ours. Much of what I have presented may, therefore, serve only to suggest research and development to meet your own requirements. Perhaps also, in some small way, this statement of progress in communication may stimulate research and development in other industries and services.

In the year 1885, only nine years after the telephone was invented, a Telephone Company was chartered in the United States for the following purpose: "to connect one or more points in each and every city, town, or place in the State of New York with one or more points in each and every other city, town or place in said State and in each and every other of the United States and in Canada and Mexico; and each and every of said cities, towns, and places is to be connected with each and every other city, town, and place in said states and countries, and also by cable and other appropriate means with the rest of the known world."

This was an ambitious program, and thirty years passed before the results of research and development could be embodied in apparatus and equipment to make it possible to talk between cities on the Atlantic and Pacific coasts of the United States, and about forty years passed before the establishment of telephone service between America and Europe. Telephone service was later extended to other parts of the world including your country, and it is now possible for a telephone subscriber in the United States to converse with a person at any one of thirty-four odd million subscriber stations in a large number of countries of the world. Further, it is possible to talk with persons on suitably equipped ships at sea. Expanding still further beyond the goal set in 1885, and departing from the idea of two-way conversation,

* One of three Iwadare Foundation lectures delivered during the past month in Japan by Dr. Colpitts.

this same company provides a portion of the facilities which make it possible for a person speaking at one place almost anywhere in the civilized world to have his voice heard at almost any other. I refer to broadcasting.

Figure 1 shows a wire map of a few of the principal toll lines in the United States. This toll plant affords facilities that, in connection with the local plant, enable any telephone subscriber at any point to communicate promptly with a subscriber at any other point in the United States, Canada, or Mexico.

With the growth of radio broadcasting, a service with which you are all familiar, it became necessary to provide circuits to interconnect radio broadcasting stations. Figure 2 shows a wire map of such interconnecting circuits commonly spoken of as "program circuits." Figure 3 shows schematically the radio-telephone circuits that connect the United States to foreign countries. Another extension of the service rendered by the Bell System is indicated by Fig. 4, which shows a wire map of circuits devoted to the telephotograph service.

It is not my purpose to take your time to discuss these past developments, since they have already been described quite fully in technical literature, which I know is available to you. I propose rather to discuss some of the more recent trends in toll circuit development in the United States, but the subject is so large that I can touch only upon the more salient factors, indicating to you the direction in which the art is moving.

This new art, or perhaps more accurately this extension of an older art, utilizes the results of continuing researches on vacuum tubes and their uses as amplifiers, modulators, and oscillators, on filters as a means of splitting up broad bands of frequencies into the relatively narrow bands required for telephony or the still narrower bands required for telegraphy, and on methods of electrically isolating a particular circuit so as to avoid crosstalk and noise. These are not all the factors requiring research, but are merely some of the more important ones.

In this connection, it should be emphasized that these new systems or methods are still under development, and that their development for commercial application will require continued effort over a considerable period. We have come to group these new systems or methods under the term "high-frequency broad-band wire transmission." Instead of confining ourselves to a frequency range extending to about 30,000 cycles, as used for our present carrier systems, we are setting for our objective the transmission and utilization of bands of frequencies a million or more cycles wide in the case of
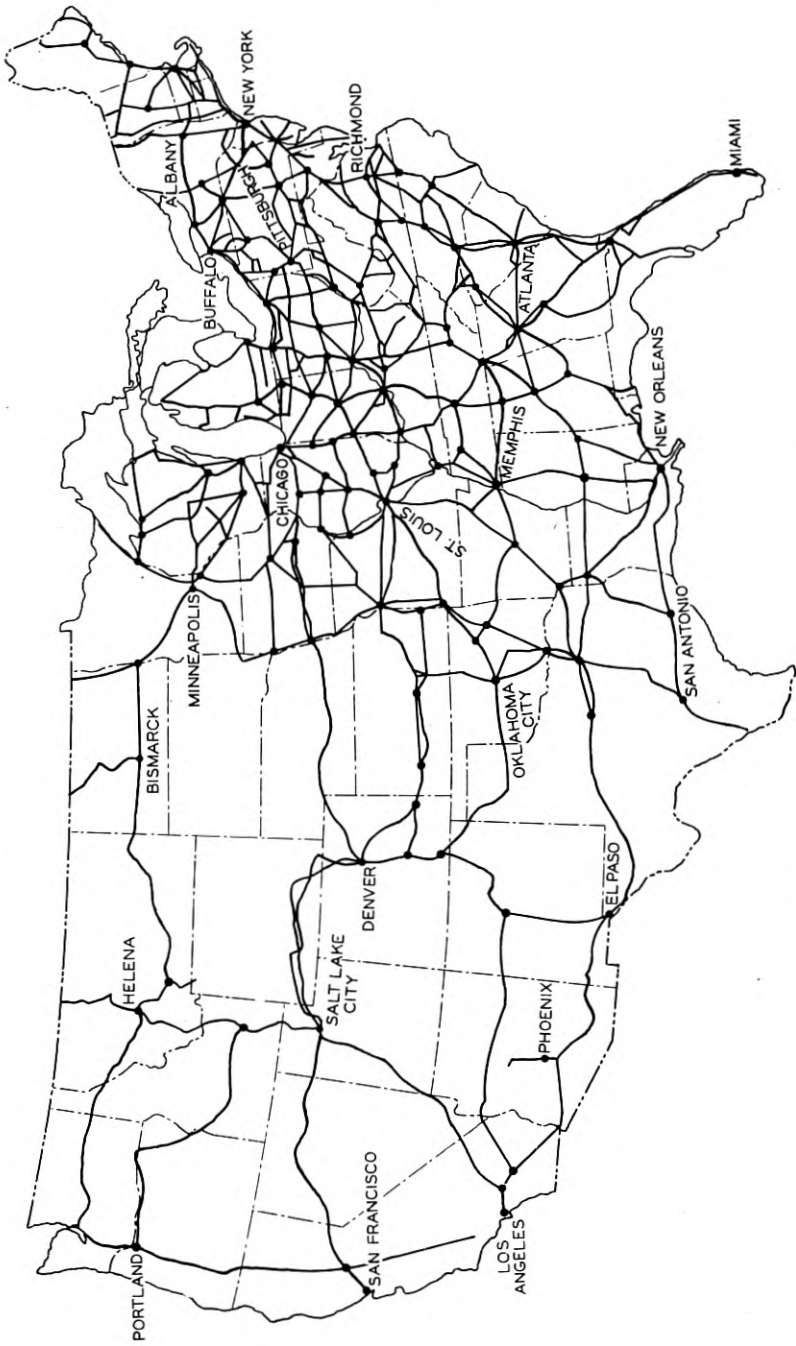
Fig. 1—Principal toll lines of the United States.
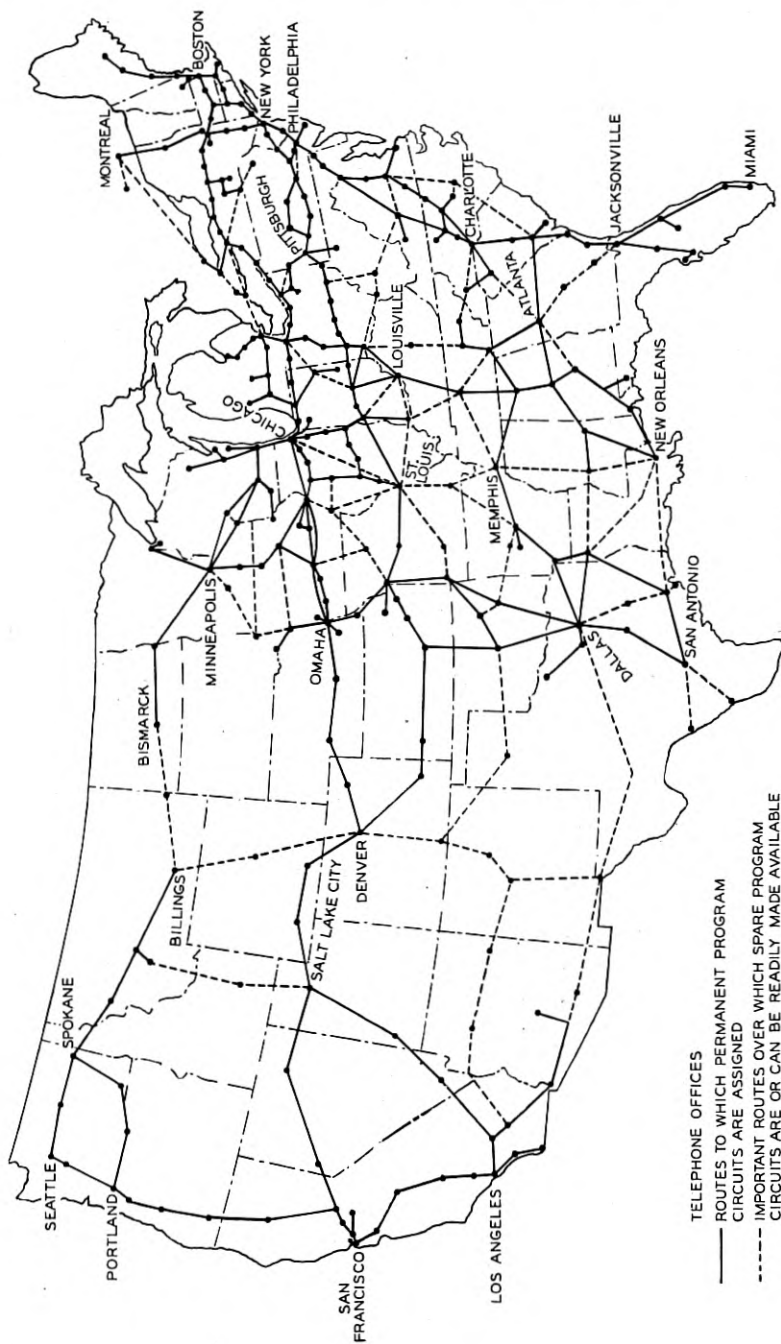
Fig. 2—Permanent and spare program circuits of the United States.
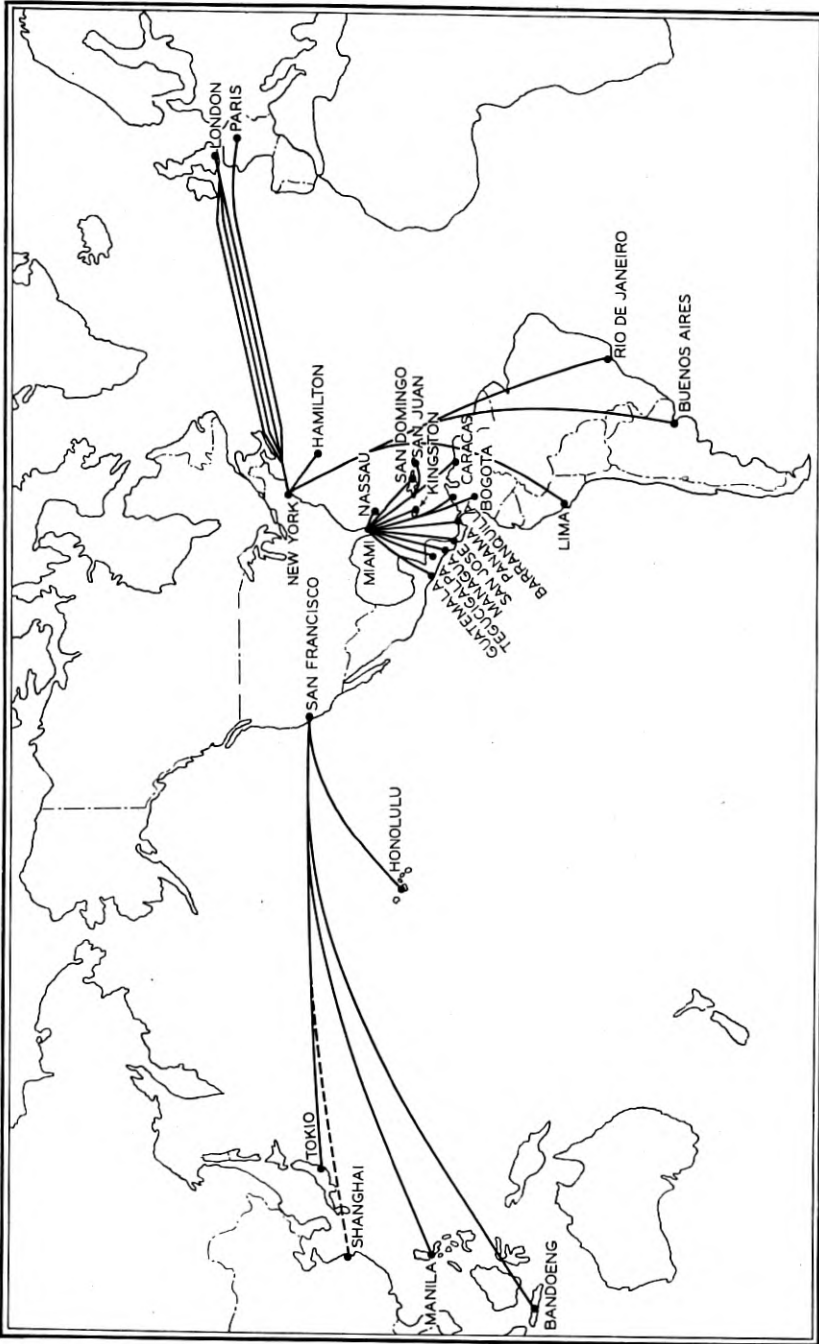
Fig. 3—Transoceanic radio telephone circuits operated by the Bell System.
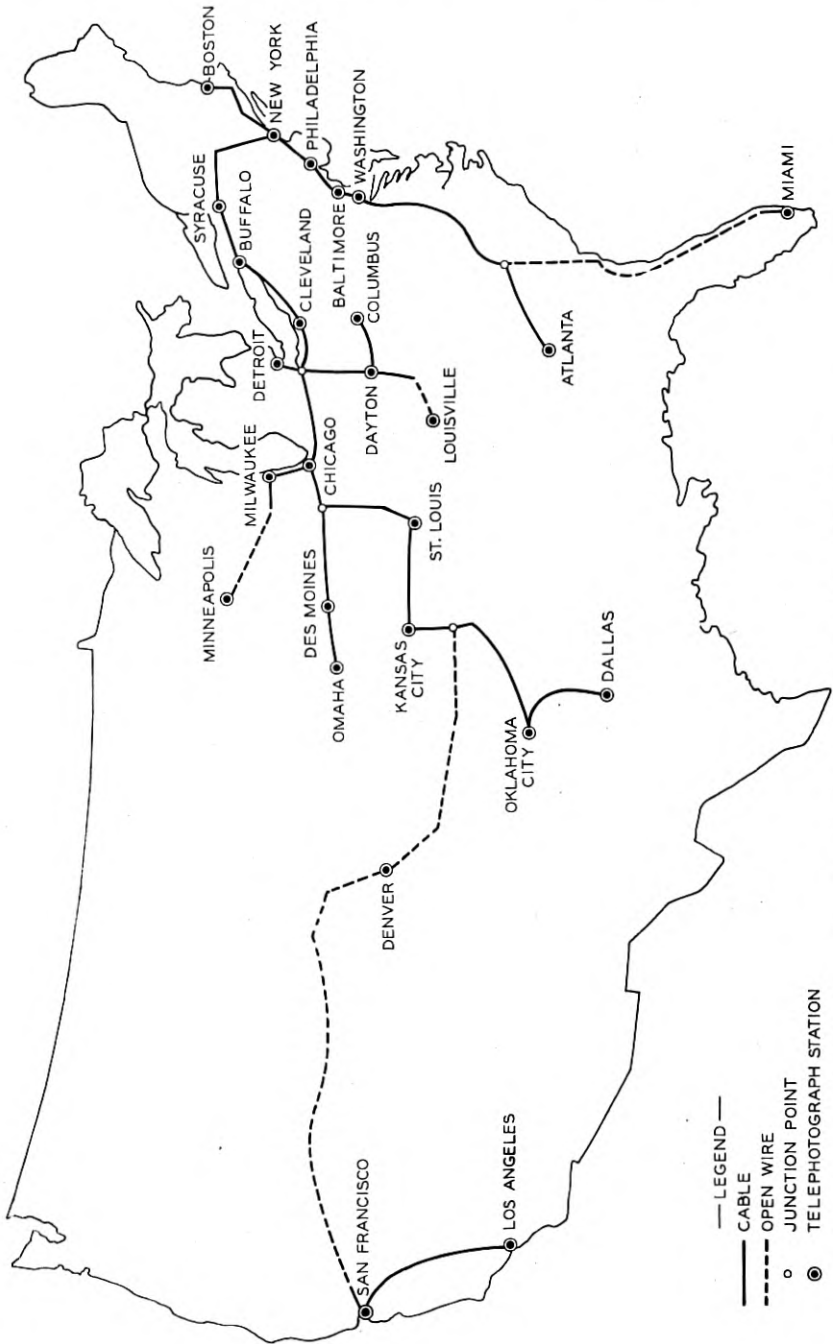
Fig. 4—Telephotograph circuits of the United States.

certain line structures. For other structures, the frequency range is narrower, but for all these systems the frequency range is transmitted as a single band, and split into communication channels for telephone or telegraph only at the terminals. If the transmission of television signals should become necessary, a very broad band—one or more million cycles—would, of course, be required. Although I have referred to television, our primary interest in broad-band wire transmission is for telephone transmission purposes, where the wide transmission band can be used to give a large number of talking channels.

You will recall that the idea of deriving more than one communication channel from a single pair of conductors, by what we now call carrier methods, is old—in fact, as old as the telephone itself. Until quite recently, however, physical devices and methods have not been available to make the carrier method utilizable in practice. Beginning about fifteen years ago, the Bell System began to install carrier systems, and since that time this method has had continued growth on open-wire lines, with the result that a substantial amount of toll traffic is now carried over carrier systems on open-wire lines. A relatively simple form of carrier equipment provides one two-way telephone circuit in addition to the usual voice frequency circuit, while more elaborate and refined equipment adds three two-way telephone circuits.

In addition to the economic urge to obtain the largest possible number of telephone channels over a given pair of wires, there is an additional factor that has influenced the development of broad-band systems, and that is, the speed of transmission. Even in the lowest-speed telephone circuits, the speed of transmission of voice waves, as judged by ordinary standards, is high, being from ten to twenty thousand miles per second (32,000 km. per sec.) in the loaded cable circuits that are now used for many of the long toll lines. For ordinary distances, moreover, the speed of transmission is not of any particular moment, but when the voice must be transmitted over distances of thousands of miles, it becomes important. Echo effects become exaggerated, and in a long connection, the actual time for speech to reach from the first subscriber to the second subscriber, added to the time required for the second subscriber to answer the first subscriber, may become an annoying factor. The broad-band transmission method furnishes circuits, however, in which the speed of transmission is raised from about 20,000 miles per second, as on loaded cable circuits, to a speed approaching that of light.

In developing a new toll system, there are many other factors, of course, that must be considered. In our case, just as in yours, there

is first, an existing toll telephone plant, which must be utilized to the maximum advantage. Also, distances between toll offices or toll centers vary, and particularly the number of circuits required between given toll centers varies over a wide range. It follows, therefore, that there is no one type of construction or method which can be economically utilized in all situations. Figure 5, for example, showing a pole line carrying open-wire circuits and circuits in cable, illustrates some of our present methods.

The high-frequency broad-band transmission development is being proposed for three uses: (1) for application on telephone toll cables already in existence, or on future toll cables of very similar type of
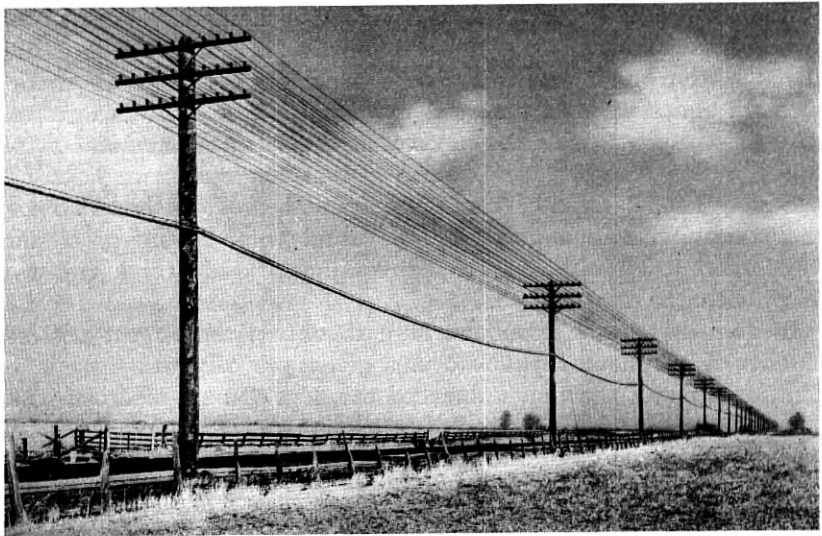

Fig. 5—A typical pole line carrying both open wire and cable.

construction; (2) for an extension to higher frequencies on open-wire telephone circuits, so as to secure more telephone channels on a given pair; (3) for application to new types of conductors capable of transmitting a very wide frequency band, such as the "coaxial" conductor, now being tried experimentally.

I need hardly point out to you that as the frequency of transmission is raised, the attenuation or line loss is greatly increased. This is due more particularly to two factors: an increase in series resistance due to skin effect, and an increase in shunt conductance due to increased dielectric losses. As the frequency increases, the currents transmitted tend more and more to avoid the inner parts of the conductor and to

concentrate on the surface, so increasing the effective series resistance. Dielectric losses in the insulation between the conductors also increase with the frequency, and so increase the effective shunt conductance. Figure 6 shows graphically the increase in attenuation with frequency,
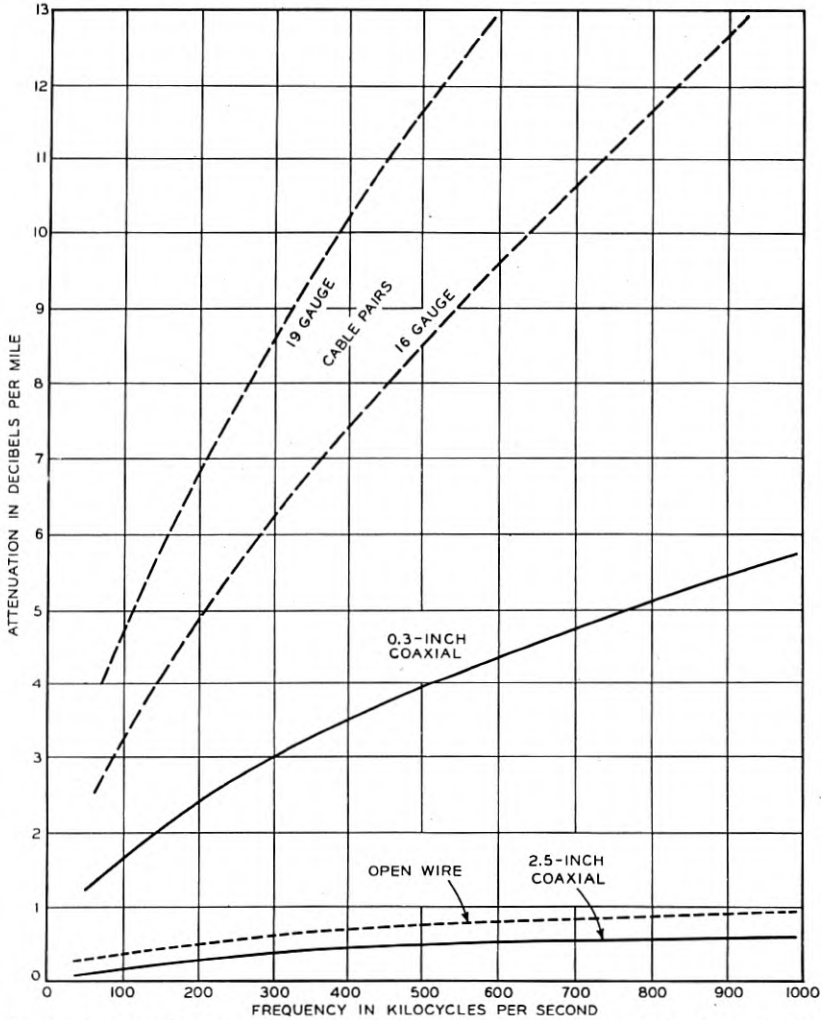

Fig. 6—Attenuation-frequency characteristics of various types of telephone circuits.

and also shows the relative attenuations of various types of construction.

Until the vacuum tube amplifier became available, the only practical method of overcoming high attenuation in a given type of line con-

struction was to provide larger conductors. With the development of the vacuum tube, high amplification became available as an alternative method. Since increasing the size of the conductor in order to decrease attentuation involves large expense, we are naturally led to consider the use of as much amplification as possible.

Before referring further to the utilization of high amplification, I wish to point out that at the present time for distances greater than about 150 miles (240 km.) in cable, we utilize the so-called 4-wire method to obtain two-way telephone transmission; that is, transmission in one direction is carried by one pair of wires, and transmission in the other direction is carried by a second pair of wires. What is in effect the same method is employed in our present carrier systems, transmission in one direction being superposed on one frequency, and transmission in the other direction being superposed on a different frequency.
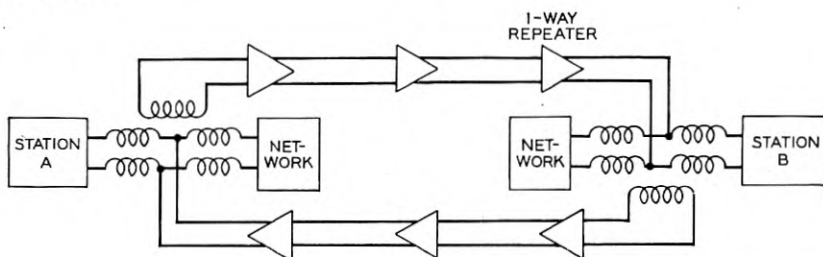

Fig. 7—Block schematic of a four-wire circuit showing two two-wire circuits with one-way repeaters.

Figure 7 shows diagrammatically a 4-wire telephone circuit in cable. You will note that one-way amplifiers are introduced in each pair of wires at points which in present practice are about fifty miles (80 km.) apart. The question naturally arises: Why not increase the distance between amplifiers and at the same time increase their amplification, and so reduce the cost? The answer is that two sources of noise disturbance have to be considered: first, induction from neighboring circuits; second, the noise of thermal agitation.

The line circuit, depending in degree upon the type of construction, receives unwanted interference from the outside, such as induced currents from power lines, lightning, and crosstalk from adjacent circuits, and it is not possible, as a result, to allow the transmitted speech signals to be attenuated below a certain level with respect to such noise interference. As a consequence, the amount which we can allow a speech signal to be attenuated before it reaches an amplifier,

depends on how completely the transmission system is free from external interference.

Two methods are commonly employed to minimize external interference: shielding, and a geometrical arrangement of the conductors of the circuit so as to balance out certain forms of interference. The open-wire line, which has no shielding, depends wholly on the symmetry of its conductors and the transpositions to balance out interference. Conductors surrounded by metal sheath, such as cable pairs, are less subject to interference than open-wire lines. The conductors of a pair are close together, are well transposed by twisting, and are shielded to a certain extent by the outside lead covering. As a result of this, the noise due to outside sources has a low level, and the telephone speech currents can be permitted to become attenuated to a relatively low value before reaching an amplifier where they are stepped up to their original value. It is evident, of course, that such cable pairs, being made up of small conductors close together and having paper dielectric, have correspondingly high attenuations.
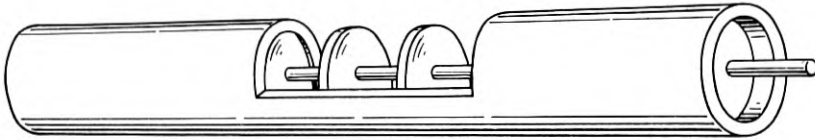

Fig. 8—Diagrammatic representation of the coaxial structure.

The ideal conductor would be one for which the attenuation over the whole operative frequency range was not too great, and at the same time one completely shielded from the influence of external electric or magnetic fields. The so-called coaxial conductor approximates to these requirements. This conductor transmits efficiently over a wide frequency band, and at the same time is well shielded from external influences, the degree of shielding being higher at the higher frequencies where greater amplification is needed to overcome the greater attenuation.

The coaxial conductor upon which we are experimenting consists of an inner wire and outer tube separated by spacing insulators. It is desirable to separate the two conductors by a minimum amount of solid insulation to the end that the dielectric will be largely air, and the losses at high frequencies be at a minimum. Figure 8 shows diagrammatically a coaxial structure. At high frequencies the current travels chiefly on the outside of the inner conductor, and on the inside of the outer conductor. It will be obvious to you that there is a wide latitude of choice in the dimensions of coaxial structures.

Although we are experimenting with a structure capable of transmitting a band of one or two million cycles in width, a coaxial structure capable of transmitting a band twenty million cycles in width is apparently not wholly unfeasible.

The question naturally arises whether, with interference from outside sources almost wholly or entirely eliminated, it is possible to allow speech currents to be attenuated to an unlimited degree before the introduction of amplification to bring them back to their original value. With all outside interference eliminated, however, noise arising within the conductor itself sets the limit. This interference is termed resistance noise or sometimes thermal-agitation noise because it is a function of the temperature of the conductor. It is apparently due to the continual moving around of the free electrons which exist in all conductors. Our Laboratories have investigated this phenomenon and determined its characteristics. This resistance noise varies in amount with the resistance of the conductor and with the temperature. It is uniformly distributed over the whole frequency range from lower voice frequencies up to the highest frequency which we have considered using. One ready means of observing this phenomenon is to provide an amplifier covering the voice range, with its input connected across the resistance, and to listen on the output of the amplifier with a telephone receiver. If the amplifier has an amplification of about 140 db, the noise heard in the telephone receiver is about as loud as would be heard in the receiver were it connected directly across the output from a telephone substation.

To prevent this thermal or resistance noise from being noticeable in a telephone conversation, we must limit the amount of amplification used at any one point in a long system, even though it were perfectly shielded, to an amount considerably less than 140 db. These considerations have led us to conclude that for a long circuit with many amplifiers distributed along the route, the amount of amplification at any one point should not exceed about 70 db.

The amount of amplification involved in present-day telephone circuits is illustrated by the 4-wire cable circuit, in which amplifiers are located in each pair at intervals of about 50 miles (80 kilometers) and each amplifier is set to give an amplification of about 25 db, or a power amplification of 300 times. For such a circuit between, say, New York and Chicago, a distance of about 900 miles (1450 km.), the total amplification is about 500 db, or a power amplification of 10^{50}. It is obviously necessary that these amplifiers must be made very *stable* so that the cumulative variations in the many amplifiers may not make it impossible to obtain the required degree of overall stability

of transmission. The total amplification is affected by the requirement that the New York-Chicago circuit is expected to have a net attenuation of not over 9 db, and to be stable within about ± 2 db.

These figures may seem large and the requirements difficult to meet, but with the systems under development, the magnitude of the high-amplification problem is even greater. In the carrier on cable development, the circuits will consist of non-loaded pairs, and it will be necessary to so space the amplifiers and adjust their amplification that the total amplification on, for example, a New York-Chicago circuit will be about 3000 db at the center of the frequency band, or a power ratio of 10^{300}. Obviously, the stability requirement has been made much more rigid. With a typical coaxial circuit, the overall amplification at a million cycles for a thousand-mile circuit (1600 km.) may well be 6500 db or a power ratio of 10^{650}.
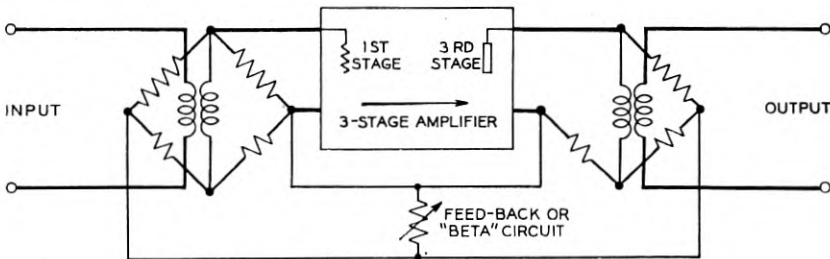

Fig. 9—Simplified schematic diagram of a feedback amplifier.

Furthermore, with the relatively simple circuit shown in Fig. 7, the amplifiers are called upon to handle merely the currents corresponding to one telephone conversation, while in the broad-band system an amplifier is required to handle simultaneously a large number of carrier telephone channels. To avoid the generation of extraneous frequencies or intermodulation products which would cause interference between the channels, an amplifier must be adopted which is more nearly perfect in this respect than any heretofore standard.

This problem of amplifier stability and perfection was solved some little time ago by an invention of one of our engineers. This engineer devised a new amplifier circuit which has been termed the "stabilized feedback amplifier." Some older types of amplifiers took some of their output and fed it back to the input for the purpose of *increasing* the amplification. This new feedback circuit controls the phases of the currents in the amplifier and feedback circuits so that the amplification is *decreased*. As a result, we have available an amplifier which is remarkably stable and closely *linear* in its performance. Figure 9

shows schematically the circuit of such an amplifier, but the actual detailed design is not simple and involves great technical skill.

Since the high amplifications just discussed are employed to offset the equally high attenuation of the line structures, careful consideration must be given to the stability or constancy of the attenuation caused by the line structure. The fact is that as the temperature changes, the attenuation of any line structure varies correspondingly. If the line structure is underground in cable, the temperature changes are slow in rate and the variations in line attenuation correspondingly slow, but if the structure is in aerial cable or consists of open wire, not only do we have variations in temperature with the season of the year, but large daily variations as well. With an aerial cable, for example, the change in loss of 19-gauge B & S non-loaded pairs throughout the year for a circuit 1,000 miles (1600 km.) in length amounts to approximately 500 db in the frequency band we propose to use. For our long cable circuits operated on voice frequencies, we have developed automatic regulating means, so that amplification is varied to compensate for changes in attenuation. With the much higher attenuations and equally higher amplifications involved in broad-band systems, more refined methods of compensating for temperature changes are under development. This is a very serious problem and sets one limit to the use of such systems.

I spoke of the new type of amplifier, employing negative feedback, which became available at a most fortunate time. It is almost equally fortunate that, due to continued research and development, new and simpler forms of electric wave filters became available. Time does not permit me to go into details, but in these newer types of electric filters suitably cut quartz crystals are utilized. Developments have also made it possible to use inductance coils with iron cores. As a result of these two changes the filter structure is simplified and its size reduced.

Fundamental to the whole broad-band transmission development, there are many other elements which have required much research and development effort such, for example, as modulators and demodulators, but I shall be able to discuss only the more striking problems underlying all broad-band systems as they pertain to certain specific applications.

Cable Carrier Systems

We plan as a first step to apply the cable carrier system to pairs in existing cables. These cables were designed and manufactured with the expectation that they would be required to transmit frequencies

only up to a few thousand cycles, that is, these cables were not designed to meet crosstalk requirements at high frequencies. Crosstalk between pairs in a cable arises from a lack of geometrical symmetry between each pair and every other. As a result of very careful research, we have developed a method of connecting small mutual inductance coils, or condensers, or both, between all the pairs concerned, and in this way reducing crosstalk to a satisfactory degree. At present coils alone are being used. Figure 10 shows schematically the balancing method.
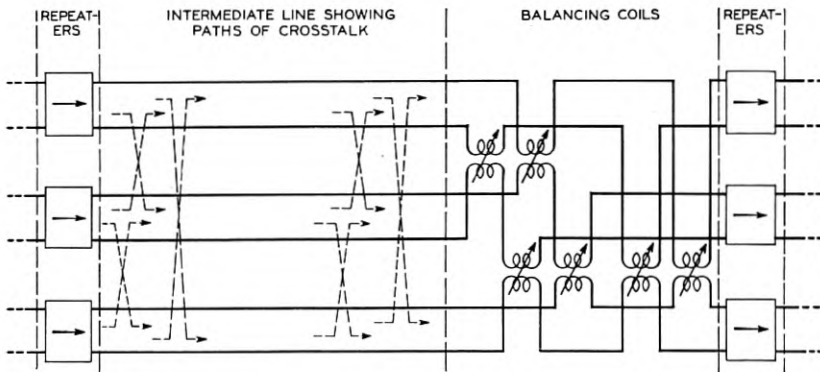

Fig. 10—Diagrammatic representation of method of balancing out cross-talk.

It is obvious that in this process of balancing out the crosstalk, the value given to the adjusting coil or condenser must be determined for each particular unit involved. When the balancing units have been installed and once adjusted, however, we feel that they will remain permanent. Present indications are that by adopting this procedure, we can employ frequency ranges up to 60,000 cycles upon our toll cables, and this will permit us to secure 12 one-way channels on each pair of conductors. With at least our present type of cables, we anticipate that it will be necessary to use separate cables in opposite directions to avoid the additional crosstalk that arises when adjacent pairs are used to transmit in opposite directions. Referring to our present cables, if the pairs which it is desired to utilize are loaded, it is necessary first to remove the loading coils. Repeaters will be spaced about 17 miles (27 km.) apart. Since the present repeater points on cables are about 50 miles (80 km.) apart, it will be necessary to add on the average two new repeater points between existing repeaters. The total amount of apparatus at these new repeater points, however, does not bulk very large, because a repeater handling 12 channels will be no larger than the older type voice repeaters
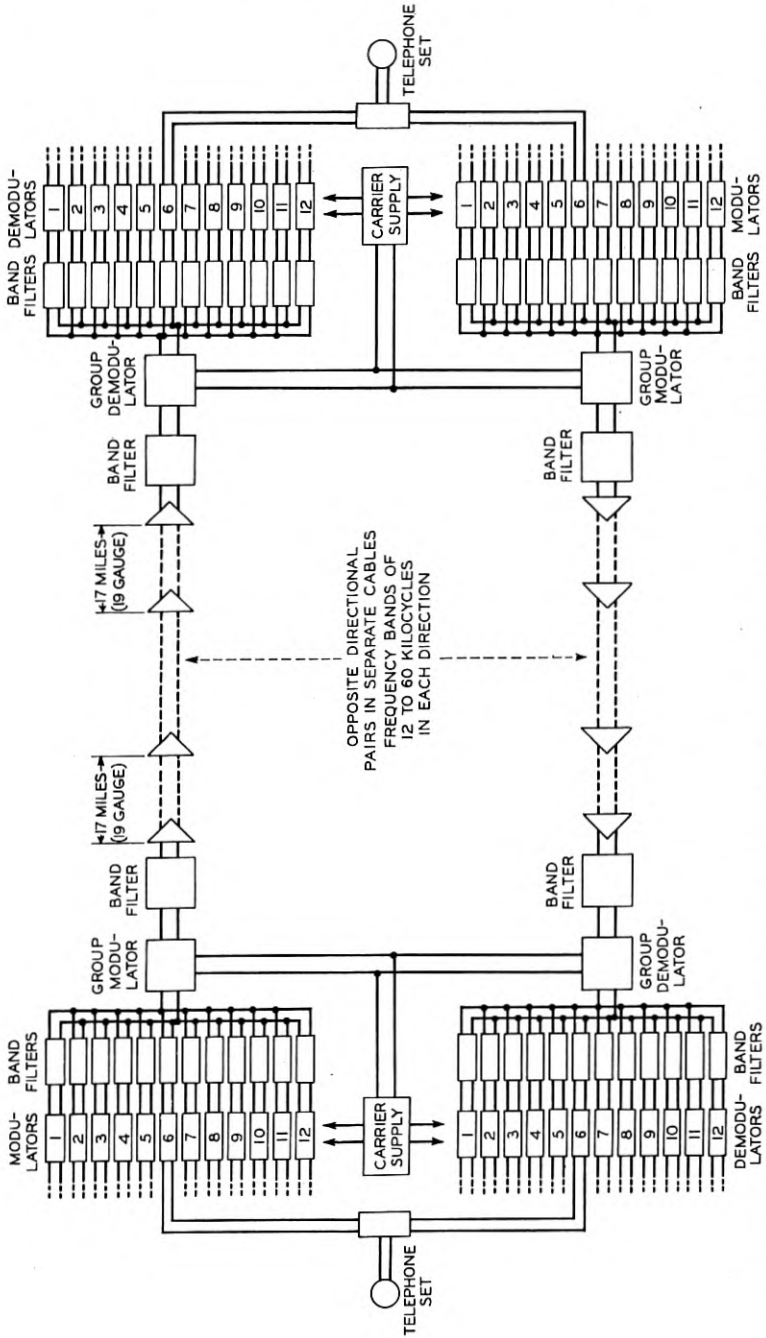
Fig. 11—Schematic representation of the broad-band cable carrier system, which supplies 12 channels in each direction.

handling only one channel. The present plans call for these intermediate repeater stations to be substantially non-attended. The electrical units employed in a cable carrier system are shown schematically in Fig. 11.

Some idea of the possibilities of this carrier cable system may be formed from the results of a trial installation made on a laboratory-scale. In one case, we had circuits as long as 7,500 miles (12,000 km.) set up, over which we carried on satisfactory conversations. The total attenuation over some of these circuits was such as to require power amplifications of 12,000 db, which corresponds to a power ratio of 10^{1200} to 1. This amplification was applied at nearly 400 points.

Broad-Band System for Open-Wire Lines

In the Bell System, as you know, along many toll routes, there is still much open-wire construction, aggregating tens of thousands of miles. At the present time, many thousands of miles of open-wire lines are equipped with 3-channel two-way carrier systems. These systems employ frequencies up to about 30,000 cycles, and with the regular voice frequency circuit provide facilities for four simultaneous conversations over one pair of wires. This might appear to be an efficient use of the wire plant, but the proposed system employs an additional frequency range from about 30,000 cycles to perhaps 150,000 cycles, adding 12 channels in each direction to a pair of wires. This will furnish a total of sixteen simultaneous conversations over a pair of wires.

Extending the frequency range accentuates the problem of crosstalk and some of the other problems of interference, but it is our present feeling that a substantial number of the pairs on a suitably constructed pole line can be rearranged for operation by this broad-band method. Figure 12 shows schematically the arrangement of apparatus at a terminal to provide these sixteen talking circuits, and Fig. 13 shows diagrammatically the arrangement of apparatus at a repeater station.

Since increased frequency means higher line attenuations with corresponding higher amplification, the use of higher frequencies means additional repeaters on the line, so that the line currents will not at any point be attenuated below a certain level. The present proposal is to provide repeater spacing of approximately 75 miles, instead of the 150 miles used on the present open-wire carrier systems.

Coaxial Cable System

This is the most radical of the broad-band developments that we have attempted to develop practically. Instead of several pairs
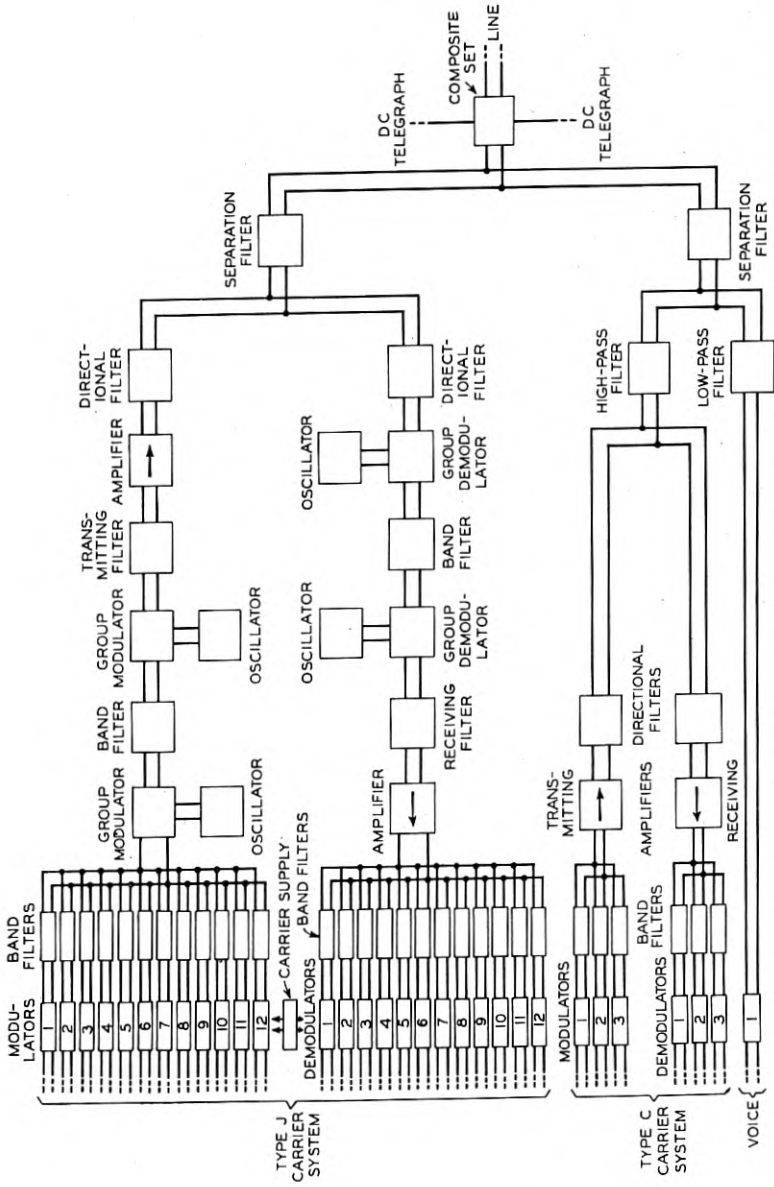
Fig. 12—The broad-band open-wire circuit superimposes twelve two-way circuits on a single pair of wires that also carries three two-way carrier channels at lower frequencies and a two-way voice circuit.
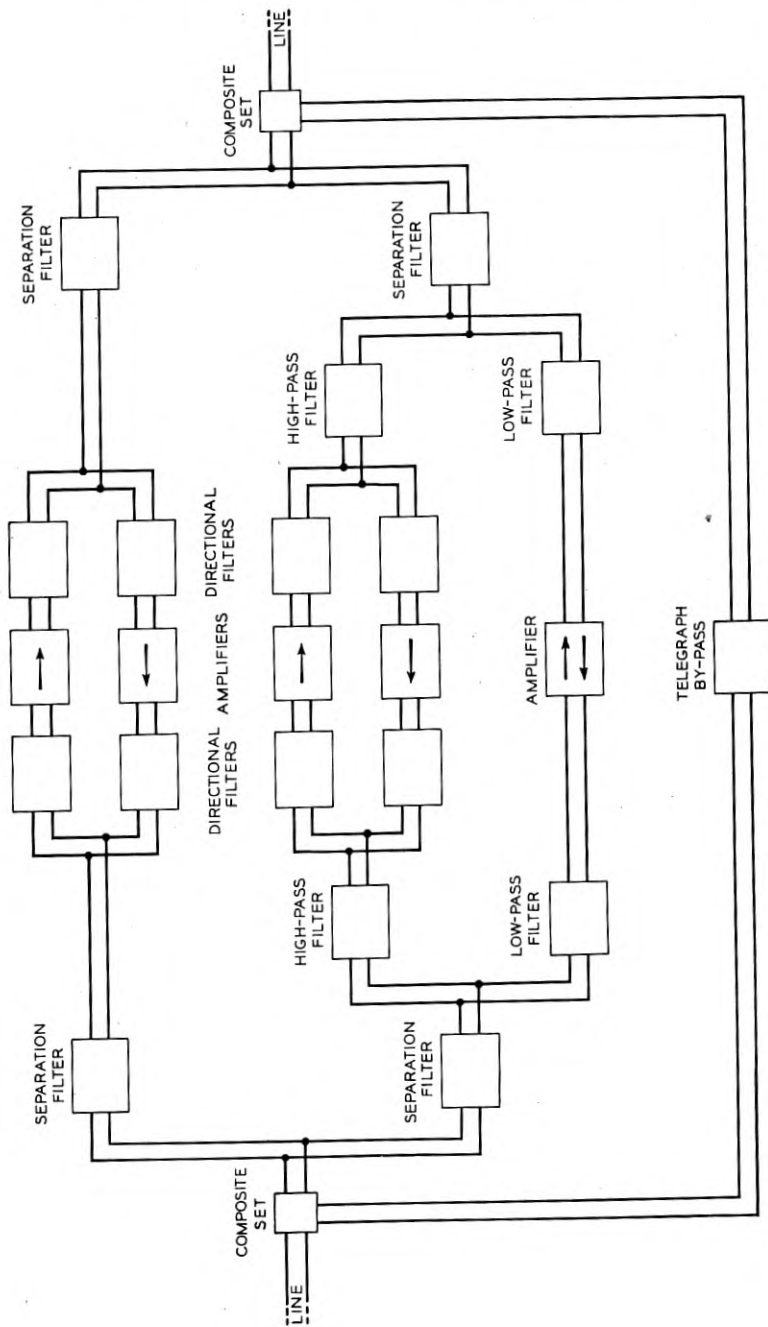
Fig. 13—Block schematic of a repeater station for a broad-band open-wire circuit.

carrying what are now considered moderately high frequencies, this new system employs a single circuit carrying a very broad frequency band. There are many ways in which conducting systems of this type may be constructed. In this connection, of course, facility of
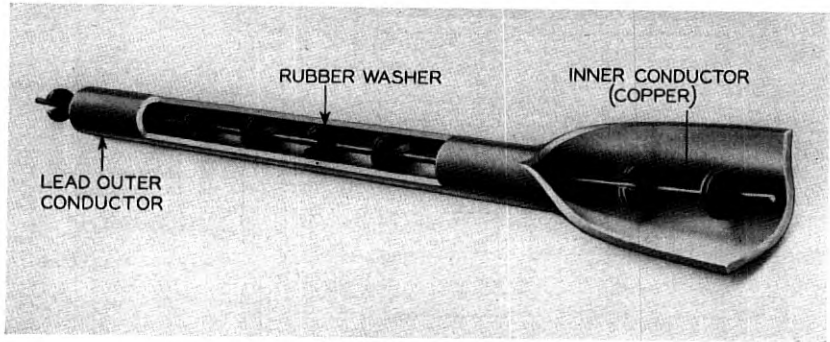
Fig. 14—One of the experimental coaxial structures.
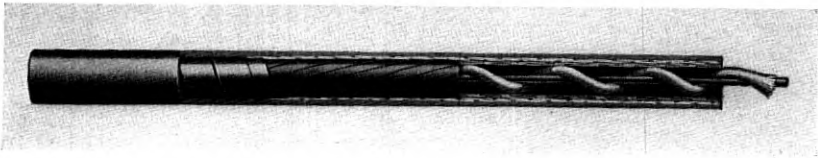
Fig. 15—Another experimental coaxial structure.
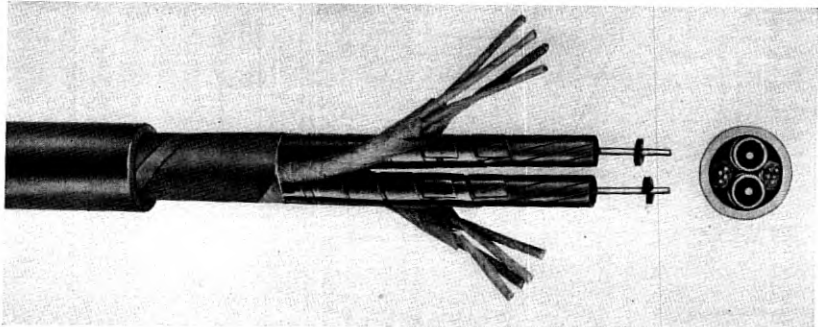
Fig. 16—The coaxial cable employed on the experimental installation between New York and Philadelphia.

manufacture and ability to withstand the handling incidental to installation, must be considered as well as electrical performance. Some of the experimental types of structure are shown in Figs. 14 and 15. In a field trial between New York and Philadelphia, over a
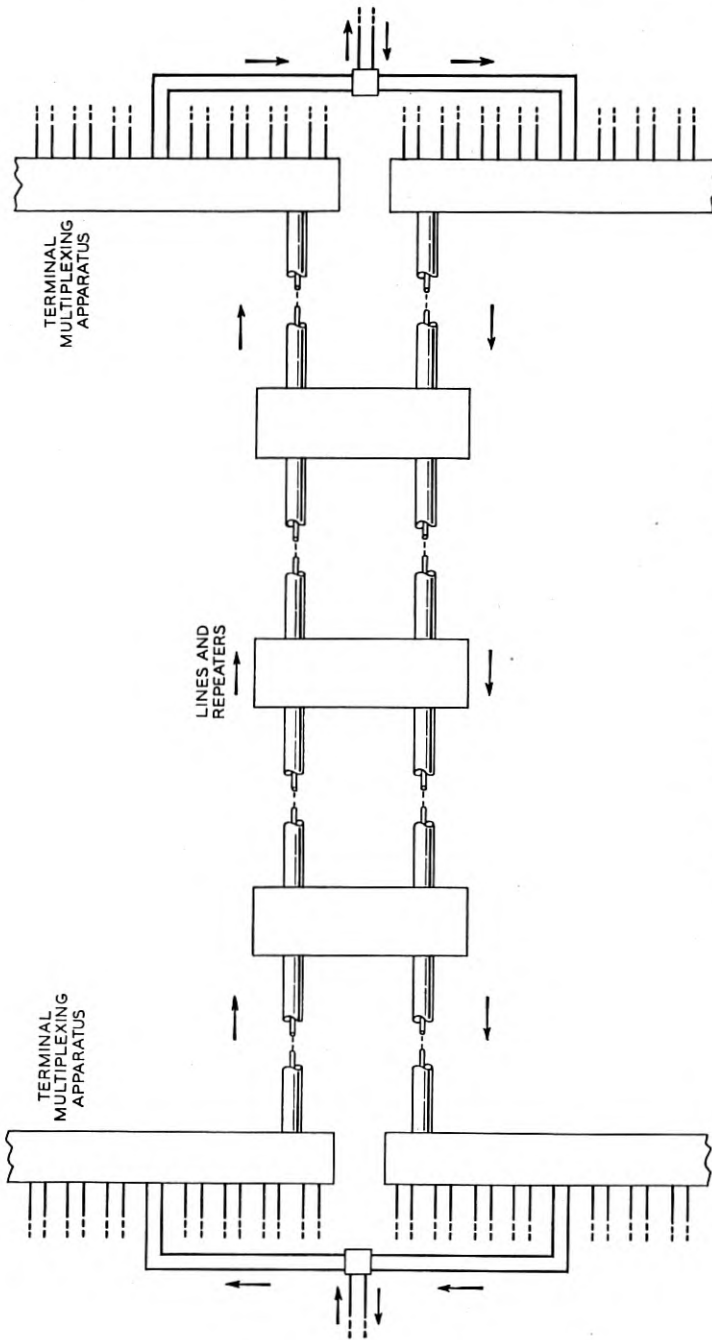
Fig. 17—Block schematic of the coaxial system.
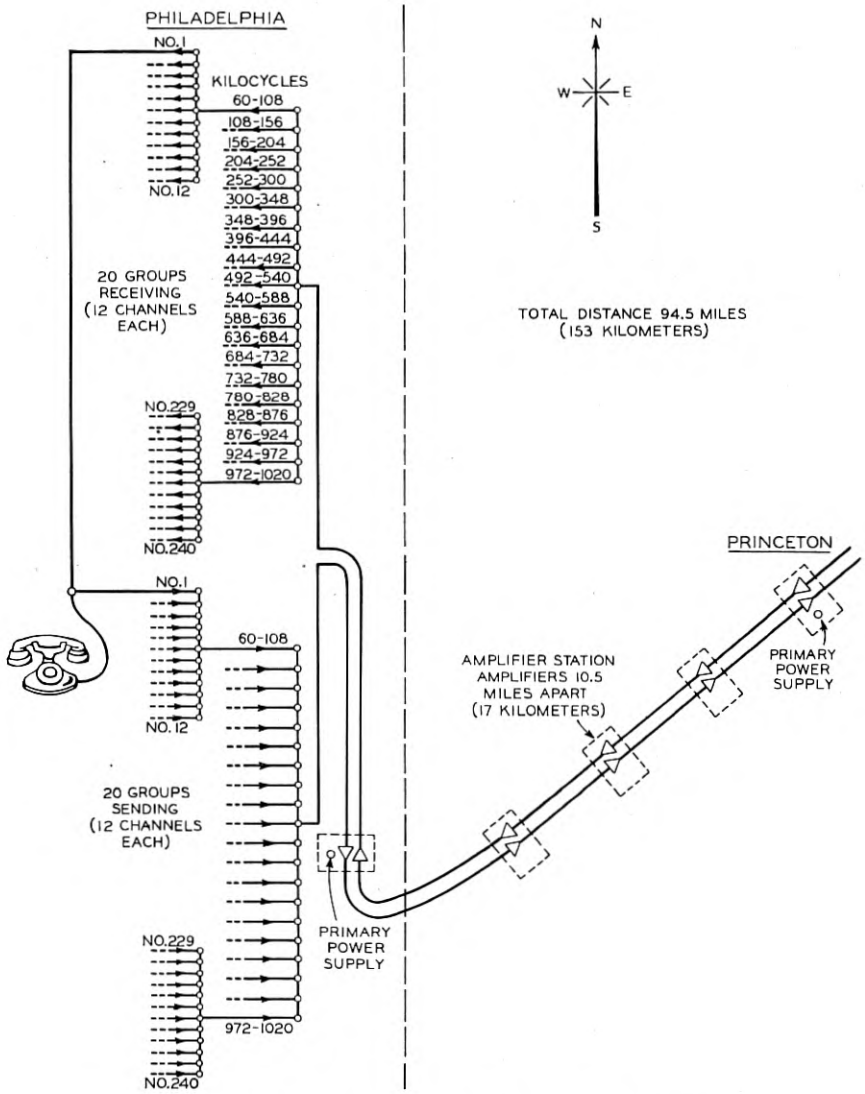
Fig 18—Schematic representation of the coaxial system.
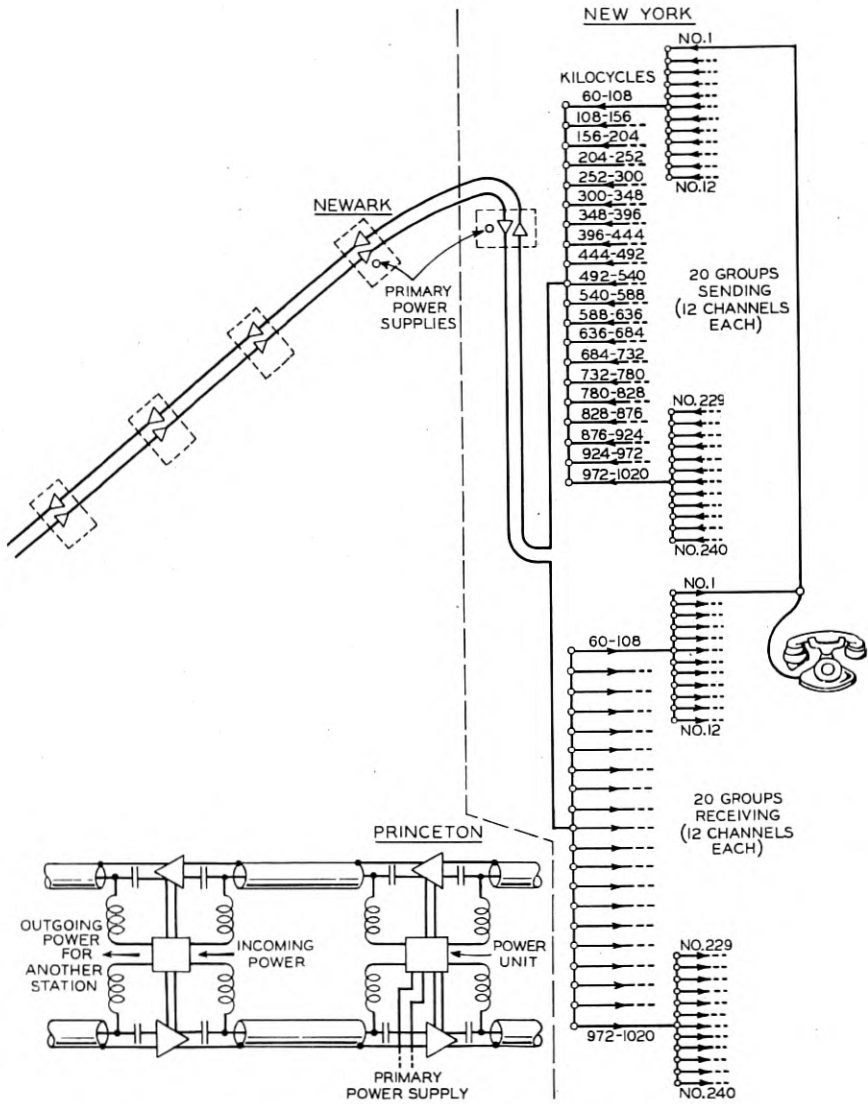
Fig. 18—*Continued from page 140.*

distance of about 95 miles (153 km.), we are employing two coaxial structures within a single lead sheath so as to provide transmission in each direction. The complete structure is shown in Fig. 16. Some of the space within the circular lead sheath is filled with ordinary cable pairs which are tapped out at repeater points for testing and trial purposes. Repeaters are being provided along this coaxial circuit at intervals of about 10 miles (16 km.), which allows frequencies up to about 1,000,000 cycles to be transmitted. Figures 17 and 18 show schematically this coaxial broad-band system.

At each repeater point there is a single amplifier for each coaxial unit, that is, one for each direction of transmission. This amplifier handles the entire number of simultaneous conversations obtainable, which is 240 for the million-cycle band. The amplifiers are equipped with automatic regulating arrangements to adjust the amplification to correspond to the attenuation of the cable as the temperature changes. As you would expect, the attenuation variations with temperature are not the same at different frequencies, but the regulating system meets this condition.

Development of means for combining and separating the channels at the terminals is an interesting feature. Some of our engineers have termed the means employed "unit group." The twelve carrier channels employed in both the cable and open-wire broad-band systems are provided in a unit called a "12-channel terminal." The coaxial system employs essentially the same 12-channel terminal, but it employs twenty of them to provide the total of 240 channels. The output of one 12-channel terminal is put directly on the line, but the outputs of the other nineteen are modulated a second time, and raised to successive positions in the frequency spectrum.

The use of double modulation has two principal advantages. In the first place it simplifies the apparatus by requiring fewer different carrier frequencies, and since it employs a channel terminal that is used by all broad-band systems, considerable economies in production are secured. The chief advantage of double modulation in the coaxial system, however, is that it simplifies the separation of the side-bands resulting from modulation, which is necessary because only one of the side-bands is transmitted. If only a single modulation were employed, the two sidebands of the upper carrier frequency would be separated by only about .05% of the carrier frequency, while with double modulation the narrowest separation is about ten times this amount.

With such a coordinated program of broad-band telephony, toll transmission takes on a new appearance. Not only will the provision

of additional channels be simplified by the availability of these new systems, but the cost per channel should be somewhat decreased. At the same time the quality of the circuits, from the standpoint of voice transmission, has been improved, so that a multiple gain is obtained.

Crosstalk Between Coaxial Transmission Lines

By S. A. SCHELKUNOFF and T. M. ODARENKO

The general theory of coaxial pairs was dealt with in an article on "The Electromagnetic Theory of Coaxial Transmission Lines and Cylindrical Shields" by S. A. Schelkunoff (*B. S. T. J.*, Oct., 1934). The present paper considers a specific aspect of the general theory, namely, crosstalk.

Formulae for the crosstalk are developed in terms of the distributed mutual impedance, the constants of the transmission lines and the terminal impedances. Some limiting cases are given special consideration. The theory is then applied to a few special types of coaxial structures studied experimentally and a close agreement is shown between the results of calculations and of laboratory measurements.

If the outer members of coaxial pairs are complicated structures rather than solid cylindrical shells, the crosstalk formulae still apply but the mutual impedances and the transmission constants which are involved in these formulae must be determined experimentally since these quantities cannot always be calculated with sufficient accuracy.

The crosstalk between coaxial pairs with solid outer conductors rapidly decreases with increasing frequency while the crosstalk between unshielded balanced pairs increases. In the low frequency range there is less crosstalk between such balanced pairs than between coaxial pairs but at high frequencies the reverse is true. The diminution of crosstalk between coaxial pairs with increasing frequency is caused by an ever increasing shielding action furnished by the outer conductors of the pairs.

Finally, crosstalk in long lines using coaxial conductors is discussed and the conclusion is reached that, unlike the case of the balanced structure, the far-end crosstalk imposes a more severe condition than the near-end crosstalk in two-way systems which involve more than two coaxial conductors.

A COAXIAL line consists of an outer conducting tube which envelops a centrally disposed inner conductor. The circuit is formed between the inner surface of the outer conductor and the outer surface of the inner conductor. Since any kind of high-frequency external interference tends to concentrate on the outer surface of the outer conductor and the transmitted current on the inner surface of the outer circuit, the outer conductor serves also as a shield, the shielding effect being more effective the higher the frequency.

Due to this very substantial shielding at high frequencies, this type of circuit has been a matter of increased interest for use as a connector

between radio transmitting or receiving apparatus and antennae, as well as a wide frequency band transmitting medium for long distance multiplex telephony or television.   It has been a subject of discussion in several articles published in this country and abroad.*

The purpose of this paper is to dwell at some length on the shielding characteristics of a structure exposed to interference from a similar structure placed in close proximity.   Such interference is usually referred to as crosstalk between two adjacent circuits, so that the purpose of this paper is a study of crosstalk between two coaxial circuits.   In what follows we shall give an account of the theory of crosstalk, the results of experimental studies, and application of these to long lines employing coaxial conductors.

GENERAL CONSIDERATIONS

Let us consider a simple case of two transmission lines (Fig. 1) and let us assume that both lines are terminated in their characteristic
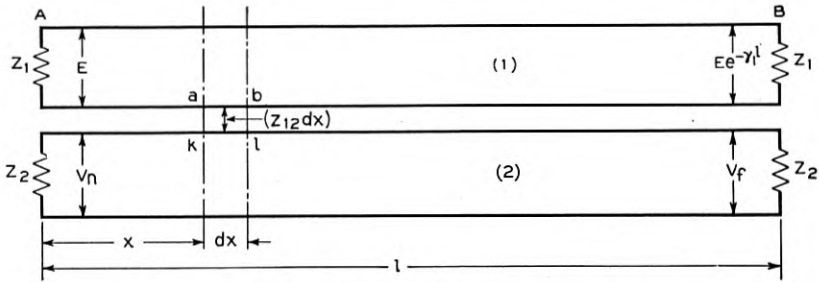
Fig. 1—Direct crosstalk between coaxial pairs.

impedances Z_1 and Z_2, and that their propagation constants per unit length are γ_1 and γ_2 respectively.   If the disturbing voltage E is applied to the left end of line (1) and the induced voltage V_n is measured at the corresponding end of line (2), the ratio V_n/E is called the near-end crosstalk ratio from circuit (1) into circuit (2).   Similarly, if V_f is the induced voltage as measured at the right end of line (2), when the disturbing voltage E is applied to the left end of circuit (1), we define the ratio $V_f/Ee^{-\gamma_1 l}$ as the far-end crosstalk ratio from circuit (1) into circuit (2).   For convenience, we shall speak of the near-end crosstalk and the far-end crosstalk whenever the voltage crosstalk ratios are actually involved.   Thus, the magnitude of crosstalk will be given by the absolute value of the corresponding crosstalk ratio.   It might be expressed either in decibels as is done in this paper or it might be given

* For references see end of paper.

in terms of crosstalk units, if the absolute value of the crosstalk ratio is multiplied by a factor 10^6.

It is well to observe at this point that, depending upon special conditions, the *significant* crosstalk ratio may be either the voltage ratio or the current ratio or the power ratio. The power ratio, or more commonly the square root of it, is usually the most important but if the outputs are impressed on the grids of vacuum tubes then the voltage ratio becomes the significant measure of crosstalk. However, if one crosstalk ratio is known, any other crosstalk ratio can be readily determined provided that the characteristics of both circuits are known. Thus for the conditions of Fig. 1 the value of far-end crosstalk as given by the ratio $V_f/Ee^{-\gamma_1 l}$ in the voltage ratio system will become $(V_f/Ee^{-\gamma_1 l})(Z_1/Z_2)$ in the current ratio system.

In general, the crosstalk between any two transmission lines depends upon the existence of mutual impedances and mutual admittances between the lines. Generally, then, one can differentiate between two types of crosstalk. The first is produced by an electromotive force in series with the disturbed line in consequence of mutual impedances between the lines, and can be appropriately designated as the "impedance crosstalk." The other is due to an electromotive force in shunt with the disturbed line, induced by virtue of mutual admittances, and can be designated as the "admittance crosstalk." The two types of crosstalk are frequently referred to either as "electromagnetic crosstalk" and "electrostatic crosstalk" or as "magnetic crosstalk" and "electric crosstalk"; the latter terminology is the better of the two.

The Mutual Impedance

Consider the simplest crosstalking system consisting of two circuits only, such as shown schematically in Fig. 1. The mutual impedance between two corresponding short sections of the two lines, between the disturbing section *ab* and the disturbed section *kl*, for instance, will be defined as the ratio of the electromotive force induced in the disturbed section to the current in the disturbing section. In what follows we shall assume that the coupling between the two transmission lines is uniformly distributed; that is, that the mutual impedance between two infinitely small sections, each of length dx is $Z_{12}dx$, where Z_{12} is independent of x. The constant Z_{12} is the mutual impedance *per unit length*.

The mutual impedance between coaxial pairs will be dealt with in a later section. For the present we need only assume that this impedance can be either calculated or measured. We shall find that the crosstalk is proportional to the mutual impedance, the remaining

factors depending upon the length of transmission lines and the character of their terminations.

DIRECT AND INDIRECT CROSSTALK

Let us now return to the circuits shown in Fig. 1. Because of the mutual impedance between the two circuits a certain amount of the disturbing energy is transferred from line (1) to line (2), producing voltages at both ends. The voltage at the end A determines the near-end crosstalk. The type of crosstalk present in a simple system of two circuits only in consequence of the direct transmission of energy from one circuit into another we shall call the direct crosstalk. Later on we shall discuss the case where three circuits are involved in such a way that the energy transfer takes place via an intermediate circuit, causing the crosstalk which we call the indirect crosstalk. Both direct and indirect types of crosstalk have a close correspondence to the types of crosstalk used in connection with work on the open-wire lines or the balanced pairs as discussed in the paper on open-wire crosstalk.[1] The direct crosstalk of the present paper is the direct transverse crosstalk; our indirect crosstalk is the total crosstalk due to the presence of the third circuit and as such is the resultant of the indirect transverse crosstalk and the interaction crosstalk of the above paper. Following the general method outlined in the present paper one can easily subdivide the indirect crosstalk into its components. Since only simple crosstalk systems consisting of two coaxial conductors are considered in our paper, the work has not been carried through.

DIRECT NEAR-END CROSSTALK

We proceed now to develop the formula for the direct near-end crosstalk. The line (1) being terminated in its characteristic impedance Z_1 the current through the generator is E/Z_1 and therefore the current in the section ab is

$$i_{ab} = \frac{Ee^{-\gamma_1 x}}{Z_1}.$$ (1)

Hence, by definition of the mutual impedance, the electromotive force induced in the section kl is

$$e_{kl} = i_{ab}Z_{12}dx = \frac{Ee^{-\gamma_1 x}}{Z_1}Z_{12}dx,$$ (2)

and the current in the section kl

$$i_{kl} = \frac{e_{kl}}{2Z_2} = \frac{Ee^{-\gamma_1 x}}{2Z_1Z_2}Z_{12}dx.$$ (3)

Therefore the current at the left end of line (2) due to the electromotive force e_{kl} is given by the expression

$$(i_{kl})_n = i_{kl}e^{-\gamma_2 x} = \frac{EZ_{12}}{2Z_1Z_2}e^{-(\gamma_1+\gamma_2)x}dx. \tag{4}$$

The contribution dV_n to the potential across the left end of line (2) due to crosstalk in the section dx, x cm. away from the left end of the line, is

$$dV_n = (i_{kl})_nZ_2 = \frac{E}{2Z_1}Z_{12}\,e^{-(\gamma_1+\gamma_2)x}dx. \tag{5}$$

Hence the total induced voltage at the near end is

$$V_n = \int_0^l dV_n = \int_0^l \frac{E}{2Z_1}Z_{12}\,e^{-(\gamma_1+\gamma_2)x}dx. \tag{6}$$

Integrating, we obtain

$$V_n = E\frac{Z_{12}}{2Z_1}\frac{1 - e^{-(\gamma_1+\gamma_2)l}}{\gamma_1 + \gamma_2}. \tag{7}$$

The near-end crosstalk is thus given by the expression

$$N_{12} = \left(\frac{V_n}{E}\right)_{12} = \frac{Z_{12}}{2Z_1}\frac{1 - e^{-(\gamma_1+\gamma_2)l}}{\gamma_1 + \gamma_2}. \tag{8}$$

If we reversed the procedure and considered the crosstalk from circuit (2) into circuit (1), we would similarly obtain

$$N_{21} = \left(\frac{V_n}{E}\right)_{21} = \frac{Z_{21}}{2Z_2}\frac{1 - e^{-(\gamma_1+\gamma_2)l}}{\gamma_1 + \gamma_2}. \tag{9}$$

By the reciprocity theorem, $Z_{21} = Z_{12}$. Incidentally, if instead of adopting as the definition of crosstalk the ratio of two voltages we regarded it as the ratio of the induced voltage to the current through the disturbing generator, we should have obtained $N_{21} = N_{12}$.

Finally, if the circuits are alike $Z_1 = Z_2 = Z_0$, $\gamma_1 = \gamma_2 = \gamma$ and the near-end crosstalk is given by the expression

$$N = \frac{V_n}{E} = \frac{Z_{12}}{2Z_0}\frac{1 - e^{-2\gamma l}}{2\gamma}. \tag{10}$$

We observe that the near-end crosstalk depends on length l. Two limiting cases are of importance here. For a length l so small, that for

a given frequency $2\gamma^2 l^2$ is negligible when compared with $2\gamma l$, we have

$$e^{-2\gamma l} = 1 - 2\gamma l + 2\gamma^2 l^2$$
$$= 1 - 2\gamma l, \tag{11}$$

and the expression (10) becomes

$$N = \frac{V_n}{E} = \frac{Z_{12}}{2Z_0} l. \tag{12}$$

The near-end crosstalk is therefore proportional to l.

For very large values of γl, that is, a very high frequency or extreme length or both, where the exponential expression is negligible as compared to unity, the expression (10) becomes

$$N = \frac{V_n}{E} = \frac{Z_{12}}{2Z_0} \frac{1}{2\gamma}, \tag{13}$$

which is independent of length.

The variation of the near-end crosstalk with length for intermediate values of γl can be best followed if instead of the expression (10) we use its absolute value

$$|N_{12}| = \left|\frac{V_n}{E}\right| = \frac{|Z_{12}|}{2|Z_1|} \frac{\sqrt{1 - 2e^{-2\alpha l}\cos(2\beta l) + e^{-4\alpha l}}}{\sqrt{\alpha^2 + \beta^2}}. \tag{14}$$

Here

$$\gamma = \alpha + i\beta, \tag{15}$$

α is the attenuation constant in nepers per unit length and β is the phase constant in radians per unit length.

We observe that for a given value of l one of the factors in (14) is oscillating with frequency. Thus, if we plot the crosstalk against frequency, the resulting curve is a wavy line superimposed upon a smooth curve, with the successive minimum points corresponding to the frequencies for which the given line is practically a multiple of half wave-lengths. The smooth curve is of course given by the magnitude of the expression (13). The curves on Fig. 2 illustrate the change of the near-end crosstalk with frequency for different lengths of a triple coaxial line made of copper conductors.

Direct Far-End Crosstalk

In order to determine the far-end crosstalk, we have to compute the induced voltage arriving at the far end of the system. Proceeding in a way similar to the derivation of the near-end crosstalk, we obtain the contribution dV_f to the potential across the right end of circuit (2), due
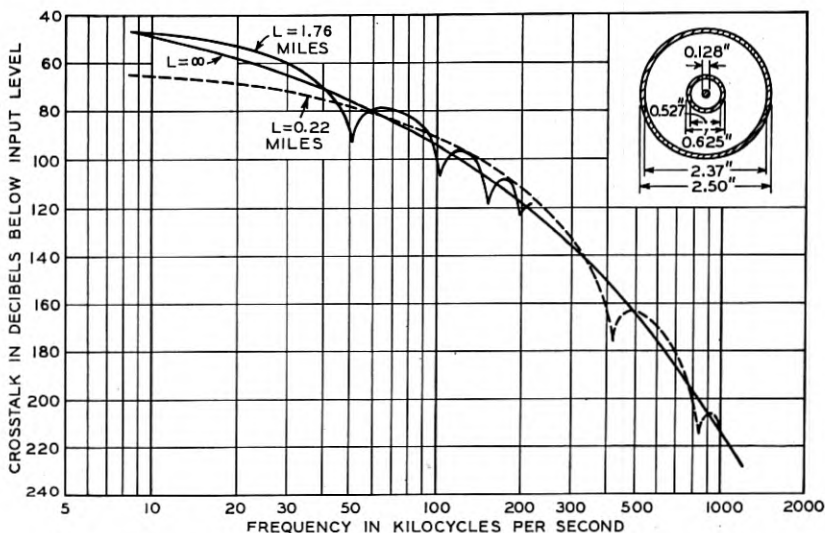
Fig. 2—Direct near-end crosstalk in a system of three coaxial conductors.

to the electromotive force in the section kl, to be given by the expression

$$dV_f = \frac{E}{2Z_1} Z_{12} e^{-\gamma_2 l} e^{(\gamma_2 - \gamma_1)x} dx. \tag{16}$$

Integrating this over the total length l we obtain the total voltage induced at the far end

$$V_f = E \frac{Z_{12}}{2Z_1} \frac{e^{-\gamma_2 l} - e^{-\gamma_1 l}}{\gamma_1 - \gamma_2}, \tag{17}$$

and the far-end crosstalk from circuit (1) into circuit (2) is

$$F_{12} = \frac{V_f}{Ee^{-\gamma_1 l}} = \frac{Z_{12}}{2Z_1} \frac{1 - e^{(\gamma_1 - \gamma_2)l}}{\gamma_2 - \gamma_1}. \tag{18}$$

If two similar lines are considered, with equal propagation constants and the characteristic impedances, equation (18) becomes

$$F = \frac{V_f}{Ee^{-\gamma l}} = \frac{Z_{12}}{2Z_0} l. \tag{19}$$

The far-end crosstalk is proportional to the length of the line at all frequencies.

Inasmuch as we have ignored the reaction of the induced currents upon the disturbing line, the foregoing equations must be regarded as approximations. Under practical conditions these approximations are

very good. Only equation (19) must not be pushed to its absurd implication, that for long enough transmission lines most energy will eventually travel via the disturbed line. The true limiting condition is that the energy will ultimately be divided equally between the two lines.

CROSSTALK VIA AN INTERMEDIATE CIRCUIT

The simplest case of the coaxial conductor system where the only crosstalk present is of the direct crosstalk type, as considered in the previous section, is the triple coaxial conductor. The mutual coupling in this case is due only to the transfer impedance between two circuits, as there are no other physical circuits involved. The case of two single coaxial conductors, the outer shells of which are in continuous electrical contact or strapped at frequent intervals, approximates the condition for the direct crosstalk if the system is sufficiently removed from any conducting matter. When two single parallel conductors in free space do not touch, an extra transmission line, an "intermediate circuit," is present consisting of the two outer shells of the coaxial conductors. Even two conductors, the shells of which are electrically connected, will form an intermediate circuit consisting of the outer shells and the other parallel conductors.

The voltage impressed on the disturbing coaxial circuit induces currents and voltages in the intermediate circuit, which now acts as a disturbing circuit for the second coaxial circuit, thus causing crosstalk. We shall now consider the near-end and far-end components of this indirect type of crosstalk.

INDIRECT NEAR-END CROSSTALK

Let us consider a system shown in Fig. 3. The circuit (3) is the
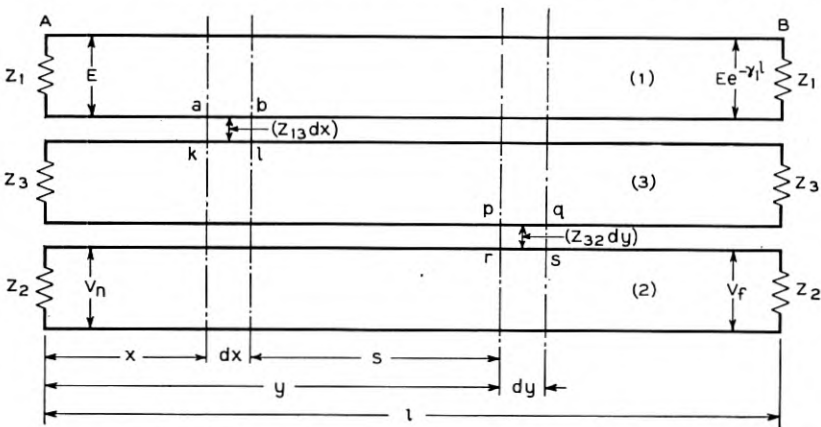
Fig. 3—Indirect crosstalk between two coaxial pairs.

intermediate circuit with an impedance Z_3 and propagation constant per unit length γ_3. Let the disturbing voltage E be applied at the A end of circuit (1). Then the current in the section kl is given by the expression similar to (3)

$$i_{kl} = \frac{EZ_{13}}{2Z_1Z_3} e^{-\gamma_1 x} dx. \tag{20}$$

The current in the section pq is

$$i_{pq} = i_{kl} e^{-\gamma_3 s}, \tag{21}$$

where

$$s = |y - x|. \tag{22}$$

The total current in the generic element of the intermediate transmission line due to coupling with circuit (1) is, then,

$$I_y = \int_0^l i_{pq} = \frac{EZ_{13}}{2Z_1Z_3} \int_0^l e^{-\gamma_3 s} e^{-\gamma_1 x} dx. \tag{23}$$

In carrying out the process of integration, we must keep in mind that from 0 to y, $s = y - x$ and from y to l, $s = x - y$.

Hence, we have

$$\int_0^l e^{-\gamma_3 s} e^{-\gamma_1 x} dx = e^{-\gamma_3 y} \int_0^y e^{(\gamma_3-\gamma_1)x} dx + e^{\gamma_3 y} \int_y^l e^{-(\gamma_3+\gamma_1)x} dx,$$

and

$$I_y = \frac{EZ_{13}}{2Z_1Z_3} \left[\frac{e^{-\gamma_1 y} - e^{-\gamma_3 y}}{\gamma_3 - \gamma_1} + \frac{e^{-\gamma_1 y} - e^{\gamma_3 y}e^{-(\gamma_3+\gamma_1)l}}{\gamma_3 + \gamma_1} \right]. \tag{24}$$

The elementary electromotive force induced in the second coaxial conductor by the current I_y is

$$E_y = Z_{32}I_y dy. \tag{25}$$

The contribution of this electromotive force to the voltage across the near-end of the second coaxial pair will be then

$$dV_n = \frac{1}{2} E_y e^{-\gamma_2 y} = \frac{Z_{32}}{2} I_y e^{-\gamma_2 y} dy. \tag{26}$$

The total induced near-end voltage will be given by the expression

$$V_n = \frac{1}{2} \int_0^l Z_{32}I_y e^{-\gamma_2 y} dy. \tag{27}$$

Using the expressions (23) and (24), we obtain

$$V_n = E \frac{Z_{13}Z_{32}}{4Z_1Z_3} S_n,$$ (28)

where

$$S_n = \int_0^l e^{-\gamma_2 y} \left[\frac{e^{-\gamma_1 y} - e^{-\gamma_3 y}}{\gamma_3 - \gamma_1} + \frac{e^{-\gamma_1 y} - e^{\gamma_3 y}e^{-(\gamma_3+\gamma_1)l}}{\gamma_3 + \gamma_1} \right] dy.$$ (29)

Integrating (29) we have

$$S_n = \frac{2\gamma_3}{\gamma_1 + \gamma_2} \frac{1 - e^{-(\gamma_2+\gamma_1)l}}{\gamma_3^2 - \gamma_1^2} - \frac{1 - e^{-(\gamma_3+\gamma_2)l}}{(\gamma_3 - \gamma_1)(\gamma_3 + \gamma_2)}$$
$$+ \frac{1 - e^{(\gamma_3-\gamma_2)l}}{(\gamma_3 + \gamma_1)(\gamma_3 - \gamma_2)} e^{-(\gamma_3+\gamma_1)l}.$$ (30)

Thus, the near-end crosstalk from circuit (1) into circuit (2) via the intermediate circuit (3) is given by the expression

$$N_{12}' = \frac{V_n}{E} = \frac{Z_{13}Z_{23}}{4Z_1Z_3} S_n.$$ (31a)

In a similar manner we can derive the following expression for the near-end crosstalk from circuit (2) into circuit (1) via the intermediate circuit (3):

$$N_{21}' = \frac{Z_{13}Z_{23}}{4Z_2Z_3} S_n.$$ (31b)

The factor S_n present in (31b) is the same as in (31a), being symmetrical with respect to the subscripts 1 and 2 as a close inspection of the formula (30) would prove. $Z_{13} = Z_{31}$ and $Z_{23} = Z_{32}$ by the reciprocity theorem.

For the case of two similar coaxial pairs with equal characteristic impedances Z_0 and propagation constants γ, and symmetrically placed with respect to the intermediate line, so that $Z_{13} = Z_{32}$, we have

$$N' = \frac{(Z_{13})^2}{4Z_0Z_3} \left[\frac{\gamma_3}{\gamma} \frac{1 - e^{-2\gamma l}}{\gamma_3^2 - \gamma^2} - \frac{1 - 2e^{-(\gamma_3+\gamma)l} + e^{-2\gamma l}}{\gamma_3^2 - \gamma^2} \right].$$ (32)

Now for short lengths we may use again the approximation

$$e^{-a} = 1 - a + \tfrac{1}{2}a^2.$$ (33)

The expression in the brackets of (32) then becomes equal to l^2 and the

near-end crosstalk is given by the expression

$$N' = \frac{(Z_{13})^2}{4Z_0Z_3} l^2, \tag{34}$$

which is proportional to the second power of length.

For γl very large we can rewrite expression (32) as follows:

$$N' = \frac{(Z_{13})^2}{4Z_0Z_3} \frac{1}{\gamma(\gamma_3 + \gamma)} . \tag{35}$$

Thus, for a system sufficiently long the near-end crosstalk via an intermediate line is independent of length.

If the intermediate transmission line is short-circuited a large number of times per wave-length, its propagation constant γ_3 becomes very large on the average and we have approximately

$$S_n = \frac{2[1 - e^{-(\gamma_2+\gamma_1)l}]}{(\gamma_1 + \gamma_2)\gamma_3}, \tag{36}$$

and

$$N_{12}' = \frac{V_n}{E} = \frac{Z_{13}Z_{23}}{2Z_1Z_3\gamma_3} \frac{1 - e^{-(\gamma_1+\gamma_2)l}}{\gamma_1 + \gamma_2} . \tag{37}$$

But $Z_3\gamma_3 = Z$, the distributed series impedance of the intermediate transmission line. Hence the "indirect" cross-talk becomes direct with the mutual impedance given by

$$Z_{12} = \frac{Z_{13}Z_{23}}{Z} .$$

INDIRECT FAR-END CROSSTALK

Using the method outlined in the previous section we arrive at the following expression for the far-end crosstalk from circuit (1) into circuit (2) via the intermediate circuit (3); see Fig. 3.

$$F_{12}' = \frac{V_f}{Ee^{-\gamma_1 l}} = \frac{Z_{13}Z_{32}}{4Z_1Z_3} S_f. \tag{38a}$$

The crosstalk from circuit (2) into circuit (1) will be given by a similar expression with Z_2 replacing Z_1 in the denominator, namely

$$F_{21}' = \frac{Z_{13}Z_{32}}{4Z_2Z_3} S_f. \tag{38b}$$

The factor S_f used in the above formulae is given by the expression

$$S_f = e^{-(\gamma_2-\gamma_1)l} \left[\frac{2\gamma_3}{\gamma_1 - \gamma_2} \frac{1 - e^{-(\gamma_1-\gamma_2)l}}{\gamma_3{}^2 - \gamma_1{}^2} - \frac{1 - e^{-(\gamma_3-\gamma_2)l}}{(\gamma_3 - \gamma_1)(\gamma_3 - \gamma_2)} \right.$$
$$\left. + \frac{1 - e^{(\gamma_3+\gamma_2)l}}{(\gamma_3 + \gamma_1)(\gamma_3 + \gamma_2)} e^{-(\gamma_3+\gamma_1)l} \right]. \quad (39)$$

When both coaxial pairs are similar and placed symmetrically with respect to the intermediate conductors we obtain the following expression for the far-end crosstalk between two coaxial conductors via an intermediate circuit:

$$F' = \frac{(Z_{13})^2}{4Z_0Z_3} \left[\frac{2\gamma_3 l}{\gamma_3{}^2 - \gamma^2} - \frac{1 - e^{-(\gamma_3-\gamma)l}}{(\gamma_3 - \gamma)^2} - \frac{1 - e^{-(\gamma_3+\gamma)l}}{(\gamma_3 + \gamma)^2} \right]. \quad (40)$$

For small l the expression for the far-end crosstalk becomes

$$F' = \frac{(Z_{13})^2}{4Z_0Z_3} l^2, \quad (41)$$

which is the same as (34) for the near-end crosstalk.

For large l and provided the attenuation of the intermediate circuit is greater than that of the coaxial circuit we have

$$F' = \frac{(Z_{13})^2}{4Z_0Z_3} \left[\frac{2\gamma_3 l}{\gamma_3{}^2 - \gamma^2} - \frac{2(\gamma_3{}^2 + \gamma^2)}{(\gamma_3{}^2 - \gamma^2)^2} \right]. \quad (42)$$

Finally, letting γ_3 approach γ and considering a limiting case when attenuation of the intermediate circuit is equal to attenuation of either of the coaxial conductors we obtain

$$F' = \frac{(Z_{13})^2}{4Z_0Z_3} \left[\frac{l}{2\gamma} + \frac{1}{2} l^2 - \frac{1 - e^{-2\gamma l}}{4\gamma^2} \right]. \quad (43)$$

If the intermediate transmission line is short-circuited a large number of times per wave-length its propagation constant γ_3 becomes very large on the average. The equation (37) becomes, then,

$$S_f = \frac{2[1 - e^{-(\gamma_2-\gamma_1)l}]}{(\gamma_2 - \gamma_1)\gamma_3}, \quad (44)$$

and

$$F_{12}' = \frac{Z_{13}Z_{32}}{2Z_1Z_3\gamma_3} \frac{1 - e^{(\gamma_1-\gamma_2)l}}{\gamma_2 - \gamma_1}. \quad (45)$$

The indirect crosstalk becomes direct with the mutual impedance given by the expression

$$Z_{12} = \frac{Z_{13}Z_{23}}{Z_3\gamma_3} = \frac{Z_{13}Z_{23}}{Z}, \quad (46)$$

where $Z = Z_3\gamma_3$ is the distributed series impedance of the intermediate transmission line.

COMPARISON BETWEEN DIRECT CROSSTALK AND CROSSTALK VIA INTERMEDIATE CIRCUIT FOR TWO PARALLEL COAXIAL CONDUCTORS

We have already seen that two parallel coaxial conductors in free space form actually three transmission circuits, the third circuit being formed by two outer shells of the coaxial conductors. When this third line is shorted by direct electrical contact or by frequent straps only direct crosstalk is present. When the third circuit is terminated in its characteristic impedance we have crosstalk via the third circuit. In this last case, however, the crosstalk via the third circuit is also the total crosstalk, since the only available path for the transfer of interfering energy is via the third circuit. Thus, we can directly compare the values of crosstalk for the system for both conditions.

We have shown that for sufficiently short lengths of the crosstalk exposure the direct type of crosstalk is given by (12) or (19), namely,

$$F = N = \frac{Z_{12}}{2Z_0} l. \tag{47}$$

We have also found that the crosstalk via an intermediate circuit is given by (34) or (41) provided that the length of conductors is small enough. Thus

$$F' = N' = \frac{Z_{13}^2}{4Z_0 Z_3} l^2. \tag{48}$$

Consequently

$$\frac{F'}{F} = \frac{N'}{N} = \frac{Z_{13}^2}{2Z_{12} Z_3} l. \tag{49}$$

In seeking an experimental verification of equation (49) a series of measurements were taken on a pair of coaxial conductors of varying lengths, separations, and different terminating conditions of the third circuit. The results agreed fully with the theory.

MUTUAL IMPEDANCE

Like the other constants of transmission lines the distributed mutual impedance can be measured. In certain cases, however, it is possible to obtain simple formulae for this impedance. For details of such calculations the reader is referred to a paper by one of the authors.[2]

In this paper the mutual impedance is expressed in terms of *surface*

transfer impedances. Consider a coaxial pair whose outer conductor is either a homogeneous cylindrical shell or a shell consisting of coaxial homogeneous cylindrical layers of different conducting substances. The transfer impedance from the inner to the outer surface of the outer conductor is then defined as the voltage gradient on the outer surface per unit current in the conductor. In a triple coaxial conductor system this transfer impedance is evidently the mutual impedance between two transmission lines, one comprised of the two inner conductors and the other of the two outer conductors. On the other hand the mutual impedance has a quite different value if one line consists of the two inner conductors while the other is comprised of the innermost and the outermost conductors.

The surface transfer impedance of a homogeneous cylindrical shell is given by the following expression, good to a fraction of a per cent for all frequencies up to the optical range if the thickness t is smaller than 20 per cent of the average radius

$$Z_{ab} = \frac{\eta}{2\pi\sqrt{ab}} \operatorname{csch}(\sigma t). \tag{50}$$

In this equation:

a is the inner radius of the middle shell in cm.
b is the outer radius of the middle shell in cm.
t is the thickness of the middle shell in cm.
$\sigma = \sqrt{2\pi g\mu f i}$ nepers per cm.
$\eta = \dfrac{\sigma}{g} = \sqrt{\dfrac{2\pi\mu f i}{g}}$ ohms
g is the conductivity in mhos per cm.*
μ is the permeability in henries per cm.*
f is the frequency in cycles per second.

If the ratio of the diameters of the shell is not greater than 4/3 the following formula correct to 1 per cent at any frequency will hold for the absolute value of the transfer impedance

$$|Z_{ab}| = R_{DC} \frac{u}{\sqrt{\cosh u - \cos u}}, \tag{51}$$

where

R_{DC} = the dc resistance of the shell,
$u = t\sqrt{4\pi\mu g f}.$

* As in the previous paper by Schelkunoff we adhere throughout this article to the practical system of units based on the c.g.s. system. For copper of 100 per cent conductivity

$g = 5.8005 \times 10^5$ mhos/cm. and $\mu = 4\pi 10^{-9}$ henries/cm.

The expression (51) is plotted in Fig. 3, p. 559 of Schelkunoff's paper.[2]

As it has been already mentioned, (50) and (51) represent the mutual impedance in a triple conductor *coaxial* system. One might anticipate that if the arrangement is not coaxial the mutual impedance has a different value. This is indeed the case if all three conductors have different axes. But if one transmission line is a strictly coaxial pair, then its own current remains substantially uniform around its axis and from equation (81) of Schelkunoff's paper we immediately conclude that the mutual impedance will be the same as if *all three* conductors were coaxial. *Both* transmission lines must be eccentric before their mutual impedance becomes affected by their eccentricities. Thus the mutual impedance Z_{13} between a coaxial circuit and the circuit consisting of its outer shell and a cylindrical shell parallel to it is given very accurately by (50) and (51).

The surface transfer impedance across a shell consisting of two coaxial homogeneous layers is given by

$$Z_{12} = \frac{(Z_{ab})_1(Z_{ab})_2}{Z},$$ (52)

where Z_{ab} is the transfer impedance for each layer and Z is the series impedance per unit length of the circuit consisting of the two layers insulated from each other by an infinitely thin film, when one layer is used as the return conductor for the other.

The mutual impedance between two coaxial pairs the outer conductors of which are short-circuited at frequent intervals is also given by (52) provided Z is interpreted as the distributed series impedance of the intermediate transmission line comprised of the outer shells of the given coaxial pairs. This Z is the sum of the internal impedances of the two shells $(Z_{bb})_1$ and $(Z_{bb})_2$ and of the external inductive reactance ωL_e due to the magnetic flux between the shells. If the proximity effect is disregarded, the internal impedance of a single cylindrical shell is the same as that with a coaxial return and various expressions for it are given in equations (75) and (82) in the previous paper.[2] The inclusion of the proximity effect does not complicate the formulae if the separation between the shells is fairly large by comparison with their radii, but in this case the proximity effect is not very large either. The more accurate determination of Z leads to complicated formulae; for these the reader is referred to a paper by Mrs. S. P. Mead.[6] However, at high frequencies the important factors in the mutual impedance are the transfer impedances in the numerator of (52).

Under certain conditions it is easy to obtain approximate values of the denominator of (52) and use them for gauging the limits between which the mutual impedance must lie. If the frequency is so high that the proximity effect has almost reached its ultimate value the external inductance and the internal impedance of the intermediate line are approximately

$$L_e = \frac{\mu}{2\pi} \cosh^{-1} \frac{l^2 - b_1^2 - b_2^2}{2b_1 b_2},$$

$$(Z_{bb})_1 + (Z_{bb})_2 = \frac{1}{2\pi} \sqrt{\frac{i\omega\mu}{g}} \frac{\left(\frac{1}{b_1} + \frac{1}{b_2}\right) + \frac{b_1^2 - b_2^2}{l^2}\left(\frac{1}{b_1} - \frac{1}{b_2}\right)}{\sqrt{\left[1 - \frac{(b_1 + b_2)^2}{l}\right]\left[1 - \frac{(b_1 - b_2)^2}{l}\right]}}, \quad (53)$$

where b_1 and b_2 are the external radii and l is the interaxial separation. Usually $b_2 = b_1 = b$ and consequently

$$L_e = \frac{\mu}{2\pi} \cosh^{-1}\left(\frac{l^2}{2b^2} - 1\right),$$

$$(Z_{bb})_1 + (Z_{bb})_2 = \frac{1}{\pi b} \sqrt{\frac{i\omega\mu}{g}}\left[1 - 4\frac{b^2}{l^2}\right]^{-\frac{1}{2}}. \quad (54)$$

If the proximity effect is disregarded then the external inductance is simply

$$L_e = \frac{\mu}{\pi} \log_e \frac{l}{\sqrt{b_1 b_2}} . \quad (55)$$

For this case, then, the mutual impedance is given by the expression

$$Z_{12} = \frac{(Z_{ab})_1 (Z_{ab})_2}{(Z_{bb})_1 + (Z_{bb})_2 + \frac{i\omega\mu}{\pi} \log_e \frac{l}{\sqrt{b_1 b_2}}} . \quad (56)$$

For two identical coaxial conductors the expression is further simplified to

$$Z_{12} = \frac{(Z_{ab})^2}{2Z_{bb} + \frac{i\omega\mu}{\pi} \log_e \frac{l}{b}} . \quad (57)$$

MEASURING METHOD

As defined above, crosstalk between two transmission lines terminated in their characteristic impedances is given by the ratios of the induced and disturbing voltages. Consequently, if the input voltage into the disturbing circuit is known and the induced voltage at one of

the ends of the disturbed pair is measured, the far-end or near-end crosstalk values are obtained readily. In fact, the magnitude of the near-end crosstalk is given by the expression

$$|N| = \left|\frac{V_n}{E}\right| \tag{58}$$

and the magnitude of the far-end crosstalk is given by the expression

$$|F| = \frac{|V_f|}{|E|e^{-\alpha l}} . \tag{59}$$

Taking $20 \log_{10} \frac{1}{|N|}$ and $20 \log_{10} \frac{1}{|F|}$, we obtain an equivalent loss in db between the disturbing and disturbed levels of the two crosstalking circuits. This consideration determined the method of measurements used in our experimental studies.
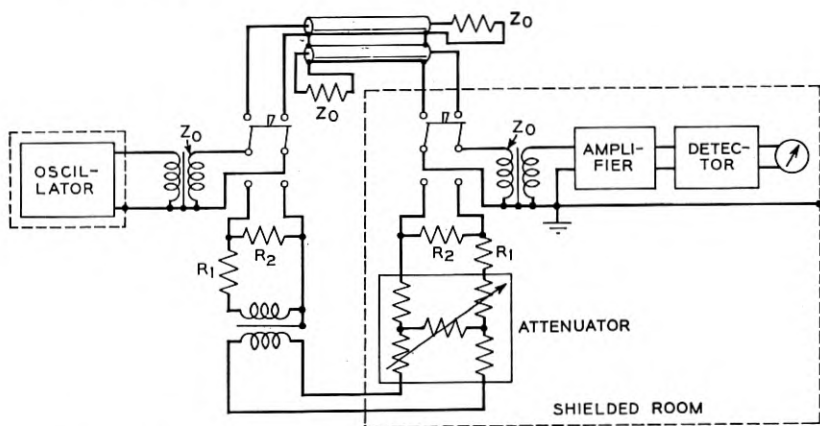
Fig. 4—Crosstalk measuring circuit arranged for far-end measurements.

The circuit used is given in Fig. 4. The two branches of the measuring set are the comparison circuits, the upper containing the crosstalking system and the lower including adjustable attenuators. The input and output impedances of both branches are kept alike by adjusting the resistances R_1 and R_2. Thus, when the lower branch of the circuit is adjusted to produce the same input into the detector as through the crosstalking branch the loss in the calibrating branch gives an equivalent crosstalk loss in db. These values of crosstalk in db below the input level in the disturbing circuit are plotted on all our sketches.

Both coaxial circuits were terminated in resistances closely equal to the absolute values of their characteristic impedances. The terminations were carefully shielded to prevent any crosstalk at these points. Careful shielding and grounding were found necessary to reduce errors due to longitudinal currents, unbalances, and interference between different parts of the measuring circuit. The overall accuracy of the measuring circuit attained was better than .5 db when the difference in input to output levels amounted to 150 db.

AGREEMENT BETWEEN THEORY AND EXPERIMENTS

The general agreement between the theory and the experiments is indicated by the curves in Fig. 5 and Fig. 6, which give the crosstalk values for cases of two small coaxial pairs with solid outer shells in
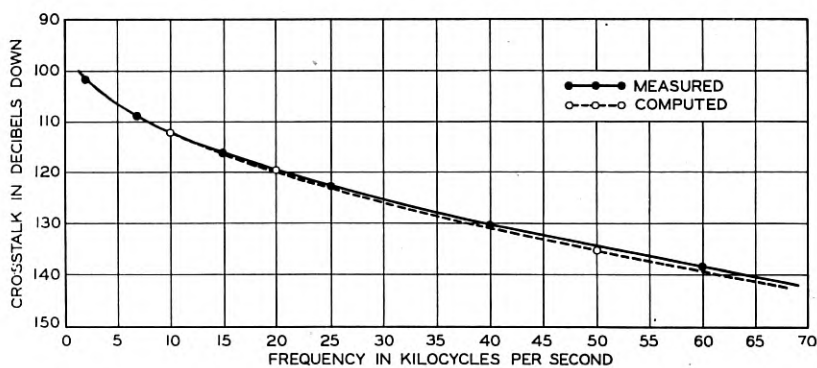

Fig. 5—Crosstalk between two coaxial pairs 20 ft. long using refrigerator pipe .032 inch thick for outer conductors. Both coaxial pairs terminated in 70 ohms. Outer conductors in contact.
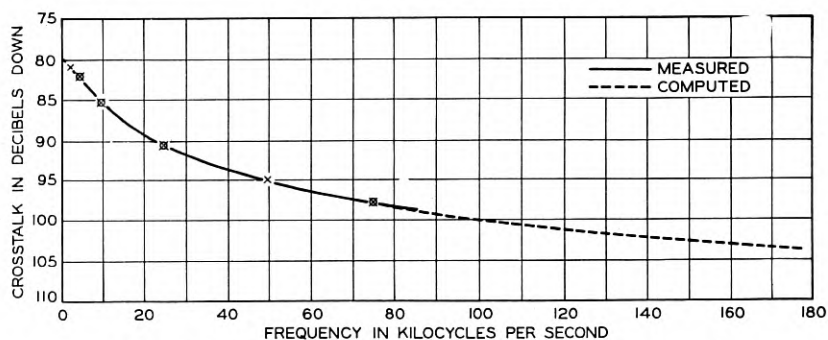

Fig. 6—Crosstalk between two coaxial pairs 25 ft. long. Outer conductor made of copper .008 inch thick, .232 inch inner diameter. Both coaxial pairs terminated in 40 ohms. Outer conductors in contact.
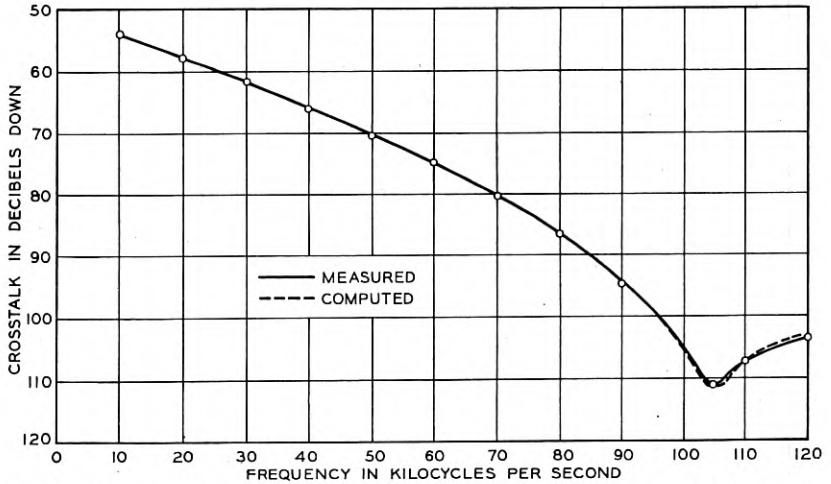
Fig. 7—Near-end crosstalk on a triple coaxial system of conductors at Phoenixville, Pa. Outer to inner circuits. Length .088 mi.

continuous contact. The curves in Fig. 7 show a comparison between measured and computed values of near-end crosstalk for a system of three coaxial conductors .88 mile long as installed at Phoenixville, Pennsylvania.

Also, as was already stated above, full agreement between theory and experiments was established as to validity of equation (49).

CROSSTALK IN LONG LINES EMPLOYING COAXIAL CONDUCTORS

In a system consisting of two coaxial pairs, where two outer conductors are in contact, essentially only one kind of crosstalk is present depending on the direction of transmission on both pairs. It is near-end crosstalk when transmitting in opposite directions and far-end crosstalk for transmission in the same direction. Where more than two coaxial conductors are grouped together and transmission is in both directions both types of crosstalk are present.

Although for a sufficiently short length of crosstalk exposure near-end and far-end crosstalk are identical, in a sufficiently long system the transmission characteristics of the line and associated repeaters will make a marked difference between them. It has been a common experience that in a long system using unshielded balanced structures near-end crosstalk imposes more severe requirements on balance between crosstalking circuits than far-end crosstalk.

We shall now consider a coaxial pair. Here, the magnitude of the far-end crosstalk was found to be given by expression (19). The

magnitude of the near-end crosstalk is given by expression (14), which for equal level points becomes

$$|N| = \left|\frac{Z_{12}}{2Z_0}\right| \frac{e^{\alpha l}\sqrt{1 - 2e^{-2\alpha l}\cos(2\beta l) + e^{-4\alpha l}}}{2\sqrt{\alpha^2 + \beta^2}} . \tag{60}$$

Thus, the ratio of the corrected near-end to the far-end crosstalk is obtained by combining equations (60) and (19):

$$\left|\frac{N}{F}\right| = \frac{e^{\alpha l}\sqrt{1 - 2e^{-2\alpha l}\cos(2\beta l) + e^{-4\alpha l}}}{2\sqrt{(\alpha l)^2 + (\beta l)^2}} . \tag{61}$$

The curve in Fig. 8 gives the db difference between near-end and far-end crosstalk for different frequencies on a 10-mile length of two
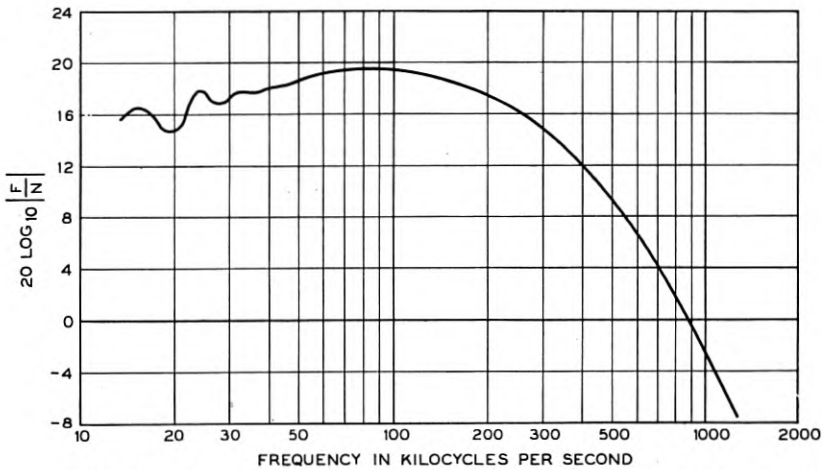
Fig. 8—Values of $20 \log_{10} |F/N|$ for a 10 mi. repeater section of two parallel coaxial pairs in continuous contact. Coaxial pairs consist of No. 13 AWG solid copper wire, .267 in. inner diameter copper outer conductor .020 in. thick, and rubber disc insulation.

parallel coaxial pairs with hard rubber disc insulation. Each pair consists of a copper outer conductor of .267″ inner diameter and .020″ thick, and a .072″ solid copper inner conductor. It is evident that in a single repeater section far-end crosstalk is higher than near-end crosstalk up to about 900 kc.

When a number of repeater sections are connected in tandem the near-end crosstalk contribution from a single repeater section will reach the terminal of the system modified both in magnitude and in phase due to transmission through intervening sections of crosstalking circuits. At the terminal the phase changes will distribute the crosstalk from all sections in a random manner, which, in accord with both the theory and

experimental evidences, will result in a root-mean-square law of addition. Thus, the overall near-end crosstalk from m sections will be equal to the crosstalk from a single section multiplied by the square root of m.

On the contrary, in a system using similar coaxial pairs transmitting in the same direction and employing repeaters at the same points, the far-end crosstalk is affected mostly by the phase differences of the repeaters. If these do not vary from the average by more than a few degrees, the far-end crosstalk in a system involving even a comparatively large number of repeaters will change proportionally to the first power of the number of repeater sections m. Only with a very large number of repeater sections (perhaps 500 or more) and random phase differences of repeaters and line of perhaps 5°–10° will the far-end crosstalk from single sections tend to approach random distribution. In this case the root-mean-square law will hold reasonably well.

Thus, far-end crosstalk will grow faster than near-end crosstalk as the number of repeater sections increases. This, combined with the relationship between the far-end and the near-end crosstalk in a single repeater section as given by equation (61) and Fig. 8, leads us to conclude that in long systems with both near- and far-end crosstalk present the limiting factor will be the far-end crosstalk. This is contrary to the experience with balanced structures stated above.

REFERENCES

1. A. G. Chapman, "Open-Wire Crosstalk," *Bell System Technical Journal*, Vol. XIII, January 1934, pp. 19–58, and April 1934, pp. 195–236.
2. S. A. Schelkunoff, "The Electromagnetic Theory of Coaxial Transmission Lines and Cylindrical Shields," *Bell System Technical Journal*, Vol. XIII, October 1934, pp. 532–579.
3. L. Espenschied and M. E. Strieby, "Systems for Wide-Band Transmission Over Coaxial Lines," *Bell System Technical Journal*, Vol. XIII, October 1934, pp. 654–769.
4. E. J. Sterba and C. B. Feldman, "Transmission Lines for Short-Wave Radio Systems," *Bell System Technical Journal*, Vol. II, July 1932, pp. 411–450.
5. H. F. Mayer and E. Fisher, "Breitband Kabel mit Neuartige Isolation," *E.T.Z.* No. 46, Nov. 14, 1935.
6. S. P. Mead, "Wave Propagation Over Parallel Tubular Conductors: The Alternating Current Resistance," *Bell System Technical Journal*, pp. 327–338, April 1925.
7. John R. Carson and J. J. Gilbert, "Transmission Characteristics of the Submarine Cable," *Journal Franklin Institute*, December 1921.
8. John R. Carson and Ray S. Hoyt, "Propagation of Periodic Currents over a System of Parallel Wires," *Bell System Technical Journal*, July 1927.
9. H. Kaden, "Das Nebensprechen Zwischen Parallelen Koaxialen Leitungen," *Electrische Nachrichten Technik*, Band 13, Heft 11 (1936), pp. 389–397.
10. M. E. Strieby, "A Million-Cycle Telephone System," *Electrical Engineering*, January 1937; *Bell System Technical Journal*, January 1937.

Sound Recording on Magnetic Tape

By C. N. HICKMAN

This paper describes an improved method of recording sound magnetically on a steel tape, similar in principle to that of the Poulsen telegraphone. In the latter a longitudinal magnetic pattern of the voice current is imprinted on a steel wire by drawing it rapidly past recording pole pieces. The high speed used by Poulsen and subsequent investigators has been directly and indirectly a limiting factor in the application of magnetic recording to commercial uses. The system here described makes use of perpendicular magnetization. This method makes it possible, with suitable equalization, to obtain a substantially uniform frequency-response characteristic up to 8000 cycles per second with a tape speed of only 16 inches per second. In many cases a speed of 8 inches per second is adequate for recording speech. At the same time the ratio of signal to background noise has been substantially increased.

The decrease in efficiency resulting from the use of perpendicular instead of longitudinal magnetization is offset to a great extent by the use of a better design and construction of the pole-pieces and a more suitable recording medium. The recording medium is a steel tape having a thickness of about 1.0 to 2.0 mils (0.025 to 0.051 mm.) and a width of about 50 mils (1.3 mm.).

INTRODUCTION

A SYSTEM of recording speech magnetically on a steel wire was invented by Poulsen almost forty years ago. The wire was drawn past a pair of pole-pieces surrounded by coils carrying a speech current. A magnetic pattern corresponding to the current was thus impressed on the wire. When the wire thus magnetically treated was again drawn past the pole-pieces a current corresponding to the recording current was induced in the surrounding coils. It was common practice to place the pole-pieces on opposite sides of the wire and offset with respect to each other. The magnetic pattern in the wire thus consisted mainly of a variation in the intensity of magnetization, the direction of the magnetization being substantially parallel to the axis of the wire. This method of putting the record on the wire is known as longitudinal magnetization. With such a system the wire must travel at a very high speed if high frequencies are to be recorded and reproduced. It was customary to use speeds of from six to ten feet per second. By using tape instead of wire, the recording and re-

producing pole-pieces may be placed directly opposite each other so that the magnetic pattern consists of variations in the intensity of magnetization, the direction of the magnetization being substantially perpendicular to the surface of the tape. This type of magnetization will be called perpendicular magnetization. There is another method of recording in which the magnetization is in a direction perpendicular to an edge and parallel to the surface of the tape which has been called cross or transverse magnetization.

In spite of the fact that the principle of magnetic recording has been known for a long time, there has been very little literature on the subject until recently. Several papers [1] which deal almost entirely with the longitudinal method of magnetization have been published abroad during the past two years. Cross magnetization is discussed briefly in one of the papers. Apparently, perpendicular magnetization has not been seriously considered. This paper will treat mainly the perpendicular method of magnetization with which a good frequency-response characteristic may be obtained with a tape speed of only 16 inches per second.

FORMS OF RECORDING MEDIA

Steel wire has been used as a recording medium in most of the telegraphones. This was probably because it was easier to obtain. When wire is used it is necessary to make the longitudinal separation of the pole-pieces rather large. This is done in order to minimize the distortion caused by the continual rotation of the wire about its axis. Such rotations change the relation of the magnetic patterns in the wire with respect to the reproducing pole-pieces from that which existed at the time the record was made.

When the pole-pieces have a wide separation, high linear speed must be used in order to record and reproduce high frequencies. The high speed required in this method of recording gives rise to a number of mechanical difficulties. The contacting pole-pieces wear away rapidly and it is difficult if not impossible to construct and hold them so that they will ride smoothly against the wire. These variations in contact with the wire change the magnetic reluctance of the flux path so that the signal strength varies and an excessive amount of noise is introduced.

Recording on steel discs has been investigated from time to time but no practical results have yet been reported.

[1] See list at end of this article of recently published papers dealing with magnetic recording.

Steel tape as a recording medium was suggested by V. Poulsen in his U. S. patent No. 661,619–1900. Its use eliminates many of the objectionable features of the wire recording system. The magnetic patterns in the tape pass the pole-pieces during reproducing in the same relative positions as at the time they were made. It is practical to wind the tape on reels of pancake shape. Snarling difficulties encountered when using wire are thereby avoided. Thin tape permits the use of smaller pulleys without exceeding the bending fatigue limit of the metal. The use of tape permits the perpendicular method of magnetization to be employed. High frequencies may therefore be recorded and reproduced with a relatively low linear tape speed.

METHODS OF MAGNETIZATION

There are two methods of longitudinal magnetization in use, one and two pole-piece recording. A detailed description of these methods is given in two of the papers which have been mentioned. It will be sufficient here to consider them only briefly.
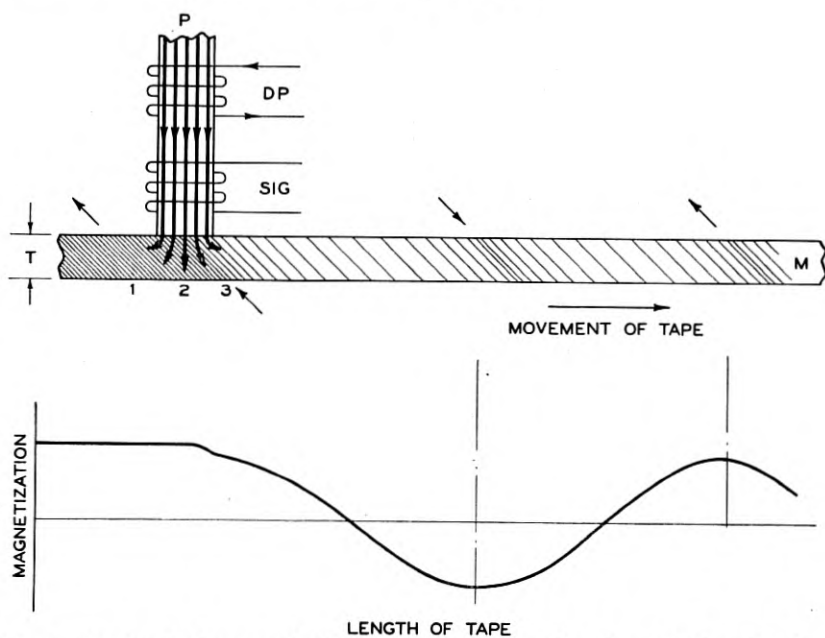

Fig. 1—Longitudinal magnetization of a recording medium by a single pole piece.
SIG = Signal coil; DP = Depolarizing coil.

Figure 1 shows the action taking place in recording with one pole-piece. *M* is the recording medium and *P* is the recording pole-piece.

It will be assumed that the recording medium has been previously magnetized by drawing it past a pole-piece so that the residual magnetization in it has a direction as indicated by the upper arrow at the left.[2] In this method of recording the magnetization is principally parallel to the axis of the medium but in order to simplify the drawing, the direction of magnetization in Fig. 1 is shown at a considerable angle. If the pole-piece P carries a steady flux in the direction indicated by the heavy lines, this flux will spread in the medium. At the point 2 in the middle of the pole-face, the flux will be substantially perpendicular to the axis of the medium. On either side it will be approximately parallel to the axis of the medium but of opposite directions. As the elements of the recording medium approach the pole-piece P, they will first be subjected to the flux 1 which is in approximately the same direction as the residual magnetization in the medium so that no appreciable change will take place. When the elements are directly opposite the face of the pole-piece they will be acted on by a flux 2 which is nearly perpendicular to the residual magnetization of the medium. When the elements reach the position 3, the flux will be in opposition to the original magnetization within the medium. If it were not for these changes in the direction of the flux while the elements are passing from the position 1 to the position 3 a signal record without appreciable distortion could be left on the medium at the point 3 by superimposing a signal flux on the steady flux in the pole-piece P. It will be realized that the positions 1, 2 and 3 are not discrete points but that they cover an appreciable distance. The spreading of the flux at 3 will be considerable so that it will be necessary for the medium to travel at high speed in order to get the recorded signals away from the recording flux before the record is distorted by subsequent signals.

Figure 2 shows a similar diagram for two pole-piece recording. Where two pole-pieces are relatively close to each other, the flux will not spread so much in the medium and the direction of magnetization will be approximately the same as that of the recording flux. It is again assumed that the residual magnetization within the medium is mainly in the opposite direction to the motion of the medium as indicated by the upper arrow at the left. The flux 1 will have no appreciable effect on the residual magnetization. The flux 3 is in the opposite direction to the residual magnetization and were it not for

[2] In Figs. 1, 2, 3, 4 and 6, the heavy lines passing through the pole-pieces represent the instantaneous recording flux. The density of the fine lines in the recording medium represents the intensity of magnetization. The arrows above and below the medium show the direction of this magnetization. The curve below represents the nature of the signal that has been recorded on the tape.

these changes in the direction of the flux while passing from 1 to 3, a modulation of the flux 3 might be expected to leave an undistorted record on the medium as was the case with one pole piece recording. However, in the case of two pole-pieces, the elements still must pass the pole-piece P_2 where the flux 4 is approximately perpendicular to the medium. After passing the pole-piece P_2 the record is subjected to the flux 5 which is in the opposite direction to the recorded flux. The record which was made by the flux 3 is therefore distorted by fluxes 4 and 5. This distortion is greater than it is for one pole-piece
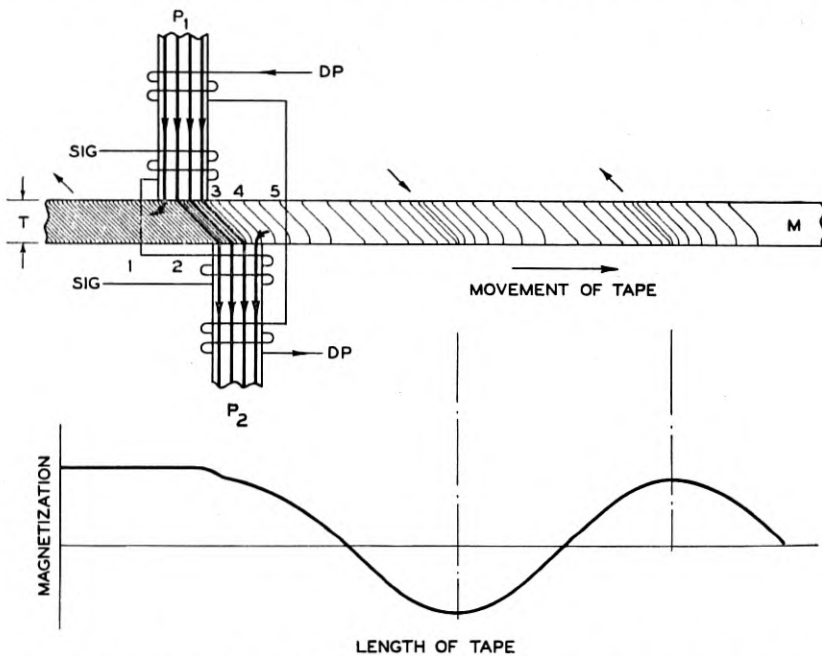
Fig. 2—Longitudinal magnetization of a recording medium by two pole pieces.

recording. In practice the stray fluxes 4 and 5 are sufficiently small so that the distortion introduced may be tolerated in exchange for the improved frequency response which is obtained with two pole-piece recording.

Figure 3 shows the action taking place where cross-magnetization is used. It is here assumed that the recording medium has been previously magnetized so that the residual magnetization is in the direction indicated by the upper arrows at the left. W represents the width of the recording medium which in this case is a steel tape. It will readily be seen that if W is very large there will be considerable spread-
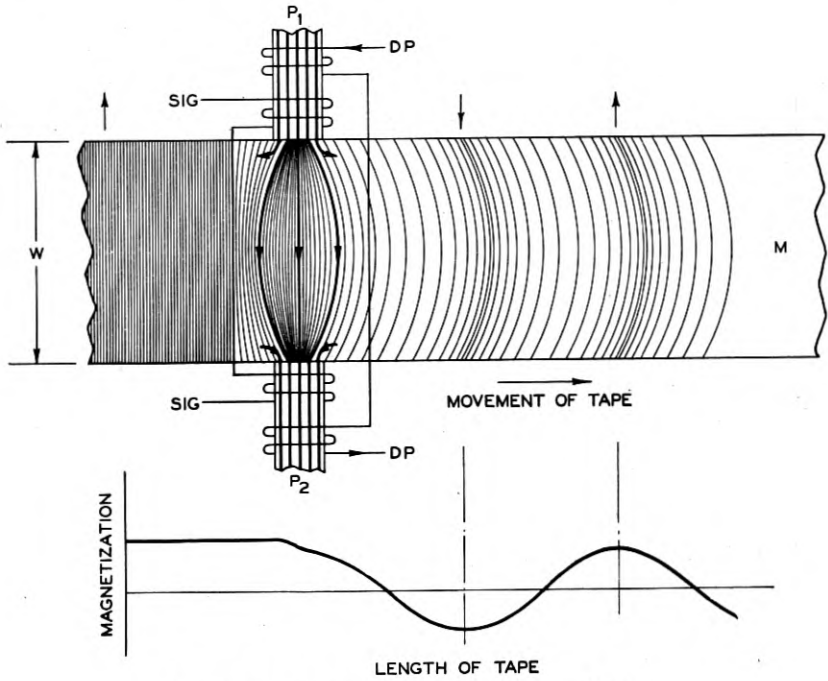
Fig. 3—Transverse magnetization of a steel tape.
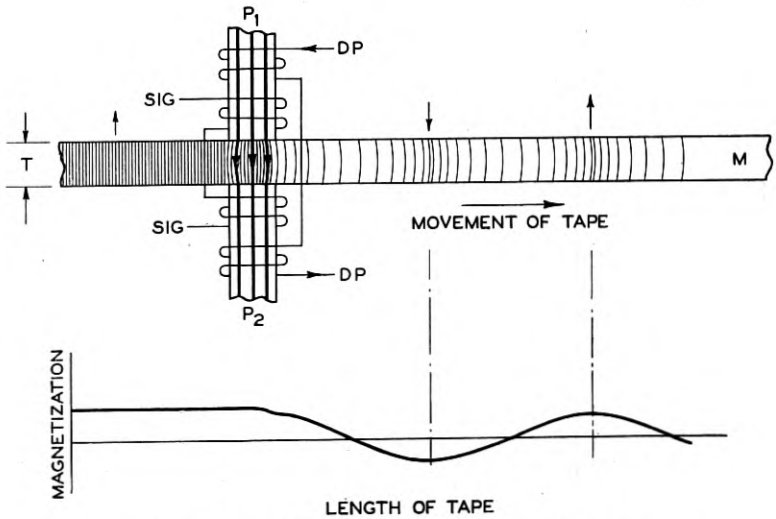
Fig. 4—Perpendicular magnetization of a steel tape.

ing of the recording flux within the tape. The recording flux is always at substantially right angles to the axis of the tape and parallel to its surface and is in the opposite direction to the residual magnetization.

If W is made quite small or in other words if the pole-pieces P_1 and P_2 are directly opposite each other with the thin dimension of the tape between them, we have the conditions shown in Fig. 4. The tape is so thin that there is very little spreading of the flux so that the width of the flux path is not appreciably dependent on the strength of the signal. This type of recording is called perpendicular magnetization in order to distinguish it from cross-magnetization, where the width of the tape instead of the thickness determines the pole-piece separation. The perpendicular method of magnetization permits a relatively low tape speed. The thickness of the pole-piece tips determines the frequency response for a given tape speed.

Method of Recording with Perpendicular Magnetization

If the tape is first subjected to a saturation flux which is at right angles to the surface of the tape, it will be left with one side of north and the other of south polarity. If the tape in this condition is passed between recording pole-pieces carrying only AC flux, it is obvious that only half cycles will be recorded. The record is therefore much distorted. The current reproduced from such a record is similar to the alternating current which may be obtained from a single wave rectifier.

If on the other hand the tape is passed through an alternating high-frequency field which is strong enough to erase the record, it is left in a substantially neutral condition. If it is then passed between the recording pole-pieces, both half cycles will be recorded but there will be amplitude distortion. Figure 5 shows a magnetization curve for iron which has previously been demagnetized with alternating current. The slope of the first part of the curve is small in either direction of magnetization and then increases with increase in the flux and finally becomes smaller again. Small signals will therefore be recorded weakly and strong signals will be recorded relatively higher. Both will have wave form distortion. The same effects would be obtained with longitudinal or cross magnetization. In the past, investigators have often utilized only one side of the magnetization curve. A direct current was used as a bias to bring the recording flux to the most suitable part of the curve such as at n, Fig. 5.

The method employed here will be made clear from Figs. 6 and 7. As the tape elements enter the field of the polarizing pole-pieces P_1, P_2 (Fig. 6) they are subjected to an increasing magnetizing force. The
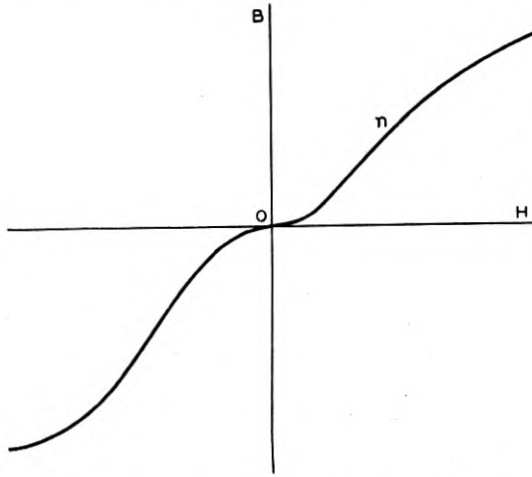
Fig. 5—Typical magnetization curve for steel.
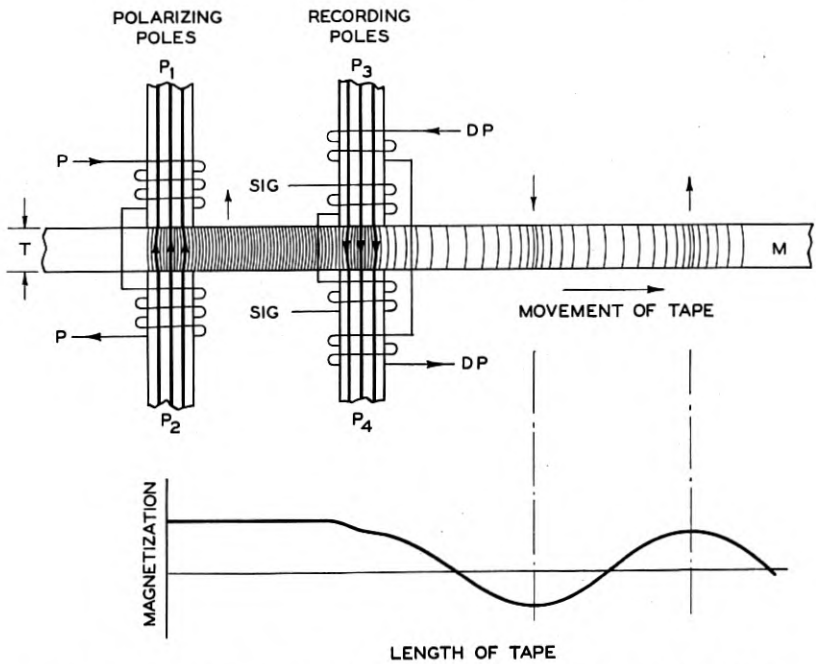
Fig. 6—Perpendicular magnetization method of recording on steel tape.
SIG = Signal coil; P = Polarizing coil; DP = Depolarizing coil.

elements are magnetized to the saturation point P as shown by curve a, Fig. 7. As the elements leave the polarizing field they are subjected to a field of decreasing strength so that the magnetic induction drops along the curve **b** to R, this point being reached when the applied field is zero. In Fig. 7, the magnetizing force H refers to the externally applied field. The tape elements then pass between the recording pole-pieces which carry a flux in opposite direction to that of the polarizing pole-pieces. If there is no signal current present, the magnetic induction will be brought down to the point N by the biasing field. As the elements pass out from between the pole-pieces, the field will decrease to zero and the magnetic induction will change from
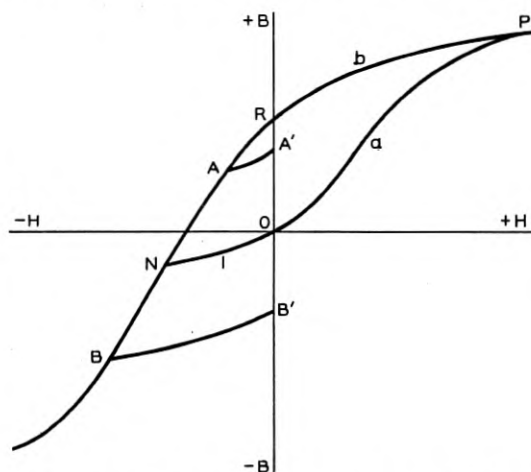
Fig. 7—Diagram showing the cycles of magnetization through which the elements of a steel tape may pass during the process of recording.

N to O, which is a substantially neutral condition. However, if there is a signal current present at the time the tape elements are passing between the recording pole-pieces, the magnetization will be reduced to a point A higher than N if the cycle is in opposition to the bias flux or to the point B lower than N if the signal flux is in the same direction as the bias flux. In either case the elements will retain a magnetization value corresponding to A' or B' respectively. This system makes it possible to record over a longer portion of the magnetization curve without appreciable distortion.

Unless the proper value of biasing field is used to bring the magnetization approximately to the point N when no voice current is present, the maximum recording range cannot be obtained without excessive amplitude distortion. For example if no bias is used, it has been found

that the output plotted against input will be too steep as shown in the curve 1, Fig. 8. If the bias is too great, the output input curve will be inclined too much as shown in curve 2 of the same figure. When the
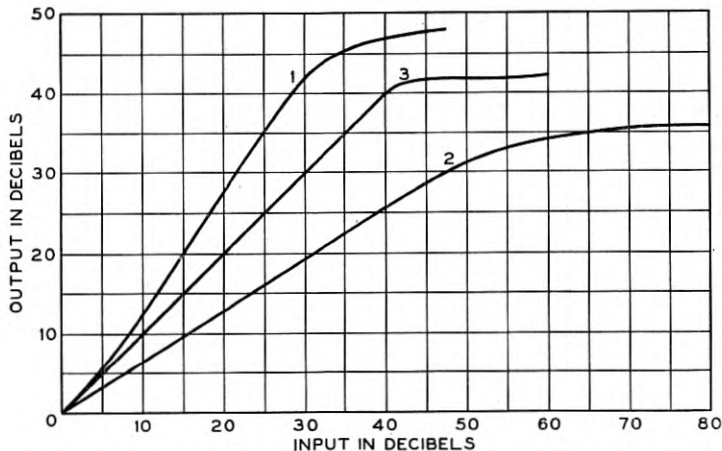
Fig. 8—The effect of the biasing current on the slope of the output-input level curves.

proper value of bias is used the curve 3 is obtained which is inclined at 45 degrees. Measurements of output versus input may therefore be used to determine the proper bias current.

Another method of determining the proper amount of bias is to plot the output obtained from records of very weak signals as a function of
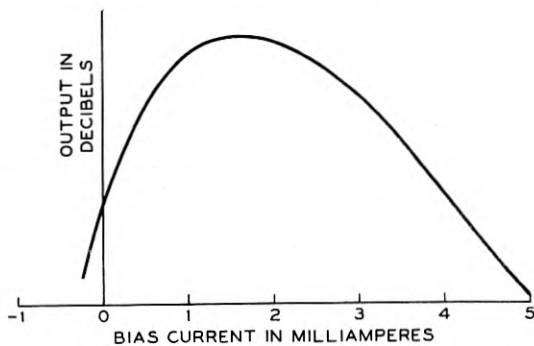
Fig. 9—Effect of the biasing current on the intensity of weak signals.

the bias current used during recording. Figure 9 shows such a curve for a 1000-cycle record. In selecting the proper bias current from the curve, the point at the crest gives the most efficient value but it is

better to favor some point slightly to the right of the crest in order to avoid the danger of very strong signals operating too far down on the left side of the curve. The recording current for the 1000 cycles had a value 30 db below the overload so that only a small amplitude was used in obtaining the data for this curve.

If the same set of pole-pieces is used both for recording and reproducing, there is no question of getting the reproducing pole-pieces in the same alignment as the recording pole-pieces. If different sets are used care must be taken to get the same alignment.

In order to keep the signal high above the tape noise, it is desirable to record so that the flux or current amplitude is independent of the frequency. Since the impedance of the recording coils rises rather sharply with frequency, it is necessary either to place a high resistance in series with the recording coils or to connect them to a high impedance. The later method is of course the more efficient. Since the energy present in the higher frequencies of voice and music is usually less than in the 1000-cycle region, an amplifier having a rising characteristic may be used in order to record these frequencies at a higher level. A corrective network may be used in reproducing to obtain the desired frequency response. Such a procedure increases the apparent ratio of signal to the tape noise.

REPRODUCING

If the thickness of the pole-piece tips is small with respect to the wave length of the signal on the tape, the voltage generated in the reproducing coils is proportional to frequency, so that the coils may be matched to favor the lower frequencies. If a straight line frequency characteristic is desired, a corrective network may be used.
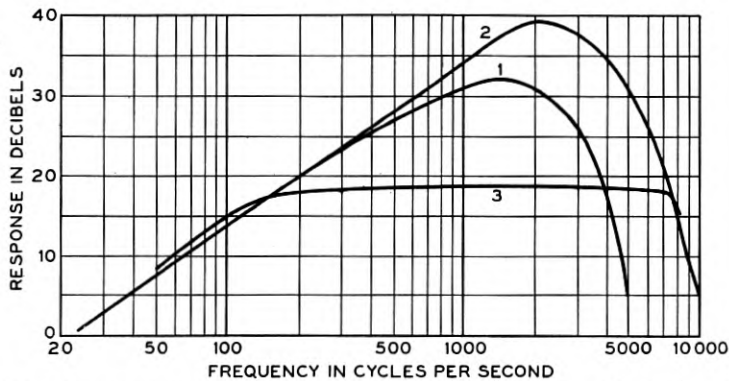
Fig. 10—Frequency response curves obtained with the perpendicular method of magnetization.

Figure 10 shows several frequency response curves. Curve 1 shows a response without the use of equalization for a tape speed of 8 inches per second. Curve 2 shows the response under the same conditions for a tape speed of 16 inches per second. Curve 3 shows the same signals of curve 2 reproduced through a suitable equalizer.

The ratio of the maximum reasonably undistorted 1000-cycle signal to the noise with typical good tape is about 38 db. The transfer loss is approximately 60 to 70 db. The maximum power required in recording is about 0.3 milliwatt.

Characteristics of Magnetic Recording

Magnetic recording differs from other methods in several respects. Since no processing is required, the record may be reproduced without a long delay. The recording medium may be used over and over again for new records. It is only necessary to subject the tape to a strong magnetic field in order to obliterate a record. The obliteration is conveniently done at the same time that the new record is being made. Where temporary records are desired, magnetic recording therefore has some advantages over other methods. On the other hand it should be fully appreciated that the records may be kept, filed away, or reproduced thousands of times with no appreciable deterioration in the quality.

The magnetic system is very convenient for use where short delays are desired. A short loop of tape in conjunction with recording, reproducing, and obliterating pole-pieces is all that is required. Instead of a loop of tape, a disc or cylinder rotating at high speed may be used to carry the recording medium. The latter method makes it possible to obtain very short delays. Where perpendicular magnetization is used, very long records may be obtained from a medium which occupies a relatively small amount of space. For example, a thin coil of 2 mil tape 9 inches in diameter will give a playing time of 1/2 hour with a tape speed of 16″ per second.

There are no moving parts in the modulating unit. The difficulties of obtaining high frequencies due to the inertia of the cutting stylus in mechanical recording are therefore not present. The system is subject to the same difficulties of eliminating flutter that we find in other methods of recording; however, mechanical vibrations due to the motor and other moving parts of the recording system do not have to be filtered out as is the case with mechanical recording. There are of course no shavings. The recording medium cannot be easily scratched and may be handled in any kind of light and subjected to large variations in temperature. When properly wound on reels it is not liable to breakage or damage during transportation.

LITERATURE

Stille, K., "Die Electromagnetische Schallaufzeichnung," *E. T. Z.*, 1930, p. 449.

Hormann, E., "Zur Theorie der Magnetischen Tonaufzeichnung," "On The Theory of Magnetic Sound Recording," *E. N. T.*, Vol. 9, pp. 388–403, Oct., 1932.

Meyer, E. and Schuller, E., "Magnetische Schallaufzeichnung auf Stählbander," "Magnetic Sound Recording on Steel Ribbons," *Zeits. f. Techn. Physik*, Vol. 13, No. 12, pp. 593–599, 1932.

Begun, S., "Die Diktiermaschine im Grossbetrieb," *E. T. Z.*, 1932, p. 204.

Hickman, C. N., "Delayed Speech," *Bell Labs. Record*, Vol. 11, pp. 308–310, June, 1933.

"Magnetic Recording and Reproducing," The Marconi-Stille apparatus described, *Wireless World*, Vol. 34, pp. 8–10, Jan. 5, 1934.

Rust, N. M., "Marconi-Stille Recording and Reproducing Equipment," *Marconi Rev.*, No. 46, pp. 1–11, Jan.–Feb., 1934.

Frederick, H. A., "Recording and Reproducing Sound," *Rev. Sci. Instruments*, Vol. 5, pp. 177–182, May, 1934.

Braunmühl, H. J. von, "Magnetische Schallaufzeichnung im Rundfunkbetrieb," "Magnetic Sound Recording in Broadcasting Service," *Funktechnische Monatshefte*, No. 12, pp. 483–486, Dec., 1934.

Mallina, R. F., "A Mirror for the Voice," *Bell Labs. Record*, Vol. 13, pp. 200–202, Mar., 1935.

Volk, T., "Magnetophon, ein Neues Tonaufzeichnungsgerät," "Magnetophone, a New Sound Recording Apparatus," *Filmtechnik*, Vol. 11, pp. 229–231, Oct. 26, 1935.

Hansen, W. H., "Das Magnetophon," "The Magnetophone," *E. T. Z.*, Vol. 56, p. 1232, Nov. 7, 1935.

Schuller, E., "Magnetische Schallaufzeichnung," "Magnetic Sound Recording," *E. T. Z.*, Vol. 56, pp. 1219–1221, Nov. 7, 1935.

Schrage, W. F., "Sound Recording on Magnetic Materials," *Radio Craft*, Vol. 7, pp. 537–562, March, 1936.

Constant Resistance Networks with Applications to Filter Groups

By E. L. NORTON

The problem investigated is the determination of two finite networks such that, when connected in parallel, they will have a constant resistance at all frequencies. The admittance of any network may be written as the ratio of two polynomials in frequency. A network to be one of a constant resistance pair must have certain restrictions imposed on its admittance. In case the two networks are both filters of negligible dissipation, the expression for the input conductance of each may be written from a knowledge of the required loss characteristic.

The poles of the expression for the conductance are then found. They will be identical for the two networks. The networks are then built up by synthesis from those poles of the conductance which have negative real parts, these corresponding to real network elements.

The methods which have been developed for this last process are described in detail.

ONE of the most useful principles available to the network design engineer is that of constant resistance networks. The use of these networks is widespread in the telephone system for purposes of loss equalization and distortion correction, where they have the advantage of providing a means for altering the transmission properties
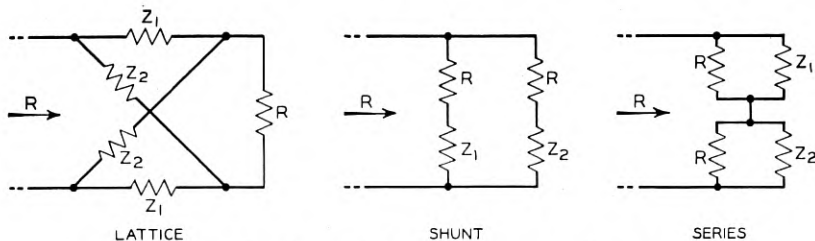
Fig. 1—The three fundamental forms of constant resistance networks.

of a circuit without affecting its impedance.[1] The three usual types of constant resistance networks are shown in Fig. 1, where, in all cases, $Z_1 Z_2 = R^2$, a relationship which is always possible to fulfill if

[1] "Distortion Correction in Electrical Circuits with Constant Resistance Recurrent Networks," Otto J. Zobel, *Bell Sys. Tech. Jour.*, July 1928.

Z_1 and Z_2 are built up of resistive and reactive elements in the usual way.

The lattice type will not be considered here. The first step in extending the other two is shown in Fig. 2, where the networks shown

SHUNT   SERIES
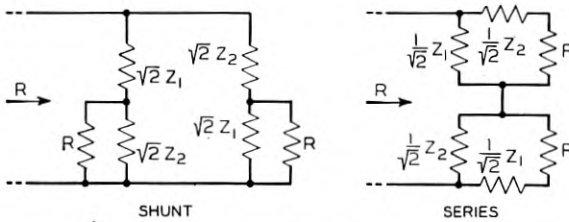
Fig. 2—The first step in extending the fundamental forms of the constant resistance networks.

have a constant resistance if $Z_1 Z_2 = R^2$. The networks have now taken on the form of two half-section filters in parallel or series, provided that Z_1 and Z_2 are purely reactive. This suggests the possibility of an extension to more complicated configurations having the general properties of wave filters with constant resistance. Since the shunt and series types are analytically the same, only the former will be considered in detail.

Use will be made of the following theorem:

Any finite network of linear elements having a constant conductance at all frequencies, and no purely reactive shunt across its terminals, has zero susceptance.

The admittance may be written [2]

$$Y(\lambda) = \frac{A_0 + A_1 \lambda + \cdots + A_m \lambda^m}{B_0 + B_1 \lambda + \cdots + B_n \lambda^n},$$

where $\lambda = i(\omega/\omega_0)$ and m is equal to or one greater or one less than n. ω_0 is a constant which fixes the frequency scale. If the real part of Y is to be a constant other than zero, A_0 cannot be zero and m must be equal to or greater than n. If there is no purely reactive shunt across the terminals, B_0 cannot be zero and m cannot be greater than n. The expression for the admittance may then be written

$$Y(\lambda) = G \frac{1 + A_1 \lambda + \cdots + A_n \lambda^n}{1 + B_1 \lambda + \cdots + B_n \lambda^n}.$$

[2] See "Synthesis of a Finite Two Terminal Network Whose Driving Point Impedance is a Prescribed Function of Frequency," Otto Brune, *M. I. T. Journal of Mathematics and Physics*, vol. 10, 1931.

By elementary methods it may be shown that if the real part of this expression is constant for all real frequencies then $A_1 = B_1$, $\cdots A_n = B_n$, and the imaginary part is zero. All other possibilities involve special relations between the B's, which correspond to a $Y(\lambda)$ with poles on the imaginary axis. This has been excluded by the condition of no purely reactive shunt across the terminals. The study of networks of constant admittance may then be restricted to the study of the conditions for constant conductance.

We will consider, then, the problem of designing two passive networks of linear elements such that, when connected in parallel, they will have constant conductance. The value of the constant conductance may be taken as unity without loss of generality.

The conductance of a finite network may be written as a ratio of two polynomials in frequency. Its value must always be positive for real frequencies, and for the case under consideration it may never exceed unity, since otherwise the conductance of the second network to make up the constant resistance pair would be required to be negative. The expression for the conductance of the first network may be written in the form

$$G_1 = \frac{1}{1 + F(\lambda)}, \tag{1}$$

where λ may be $i(\omega/\omega_0)$ as above, or it may be taken as any imaginary function of frequency which may be realized by the impedance of a reactive network, and $F(\lambda)$ is the ratio of two polynomials in even powers of λ. By subtracting G_1 from unity the required expression for G_2 may be obtained:

$$G_2 = \frac{1}{1 + \dfrac{1}{F(\lambda)}}. \tag{2}$$

An investigation of general networks of an arbitrary number of resistance and reactance elements fulfilling the relations (1) and (2) would take the present investigation too far from its main objective. If the networks are to have the general properties of wave filters with a minimum of loss in a band, they may be restricted to reactive networks having a single resistance. Furthermore, both resistances may be taken as unity, for, in cases where this is not necessary, a transformation to some other value may be made after the design is completed on the unit resistance basis. We assume, too, that when $\lambda = 0$, $F(\lambda) = 0$ and $G_1 = 1$, $G_2 = 0$. This implies the proper choice of the expression for λ.

With a voltage E_0 applied to the common terminals the power absorbed by the first network is $E_0^2 G_1$ and by the second is $E_0^2 G_2$. Since in both cases the power delivered to the network must be absorbed in the single resistance, the two insertion losses are given by

$$e^{-2\alpha_1} = G_1 = \frac{1}{1 + F(\lambda)}, \tag{3}$$

$$e^{-2\alpha_2} = G_2 = \frac{1}{1 + \dfrac{1}{F(\lambda)}}. \tag{4}$$

Since $F(\lambda)$ must be an even function of λ, the poles of (3) may be written $\pm c_m \pm id_n$ and (3) is

$$e^{-2\alpha_1} = -D^2 \frac{1}{\lambda + c_0} \frac{1}{\lambda - c_0} \prod_1^{m=(n-1)/2} \frac{1}{\lambda + c_m \pm id_m} \frac{1}{\lambda - c_m \pm id_m} \tag{5}$$

if the degree of $F(\lambda)$ is $2n$. If n is even, the terms $\lambda + c_0$ and $\lambda - c_0$ are omitted and the product taken from $m = 1$ to $m = n/2$. The quantity D^2 is the denominator of $F(\lambda)$, a polynomial in λ^2.

Let β_1 be the phase angle between E_0 and the voltage E_1 across the resistance in the first network. The left side of equation (3) may then be factored in the form $e^{-2\alpha_1} = e^{-(\alpha_1 + i\beta_1)} e^{-(\alpha_1 - i\beta_1)}$. Similarly half of the factors on the right belong with $e^{-(\alpha_1 + i\beta_1)}$ and half with $e^{-(\alpha_1 - i\beta_1)}$. Now the terms with poles having a negative real part[3] must belong with $e^{-(\alpha_1 + i\beta_1)}$ so that:

$$e^{-(\alpha_1 + i\beta_1)} = D \frac{1}{\lambda + c_0} \prod \frac{1}{\lambda + c_m \pm id_m}$$

$$= D \frac{1}{\lambda + c_0} \prod \frac{1}{c_m^2 + d_m^2 + \lambda^2 + 2c_m\lambda}. \tag{6}$$

Since λ is an imaginary function of frequency, say $\lambda = ix$, and D is real if λ or x is real, the phase β_1 is given by

$$\beta_1 = \tan^{-1} \frac{x}{c_0} + \sum_{m=1}^{m=(n-1)/2} \tan^{-1} \frac{2c_m x}{c_m^2 + d_m^2 - x^2}. \tag{7}$$

If n is even the expression is

$$\beta_1 = \sum_{m=1}^{m=n/2} \tan^{-1} \frac{2c_m x}{c_m^2 + d_m^2 - x^2}. \tag{7a}$$

[3] These being the factors that correspond to physically realizable network elements, they belong with the physically realizable factor of the exponent.

The network can be designed from equation (6) or by making use of both (3) and (7). Both methods will be illustrated in two types of networks giving filter characteristics.

FILTERS WITH CHARACTERISTICS SIMILAR TO THE "CONSTANT K" TYPE OF FILTER

As the simplest form of $F(\lambda)$ take $F(\lambda) = [(\lambda)/(i)]^{2n}$. The poles of (3) are then simply the $2n$ roots of $(-1)^{n-1}$, which may be written $\pm \cos (m\pi/n) \pm i \sin (m\pi/n)$ if n is odd, and $\pm \cos [(2m-1)\pi/2n] \pm i \sin [(2m-1)\pi/2n]$ when n is even. In the first case m varies between zero and $(n-1)/2$ and in the second case between unity and $n/2$. For the case of n being odd, equation (6) may then be written

$$e^{-(\alpha_1 + i\beta_1)} = \frac{1}{1+\lambda} \prod_{m=1}^{m=(n-1)/2} \frac{1}{1 + \lambda^2 + 2 \cos \dfrac{m\pi}{n} \lambda} \tag{8}$$

where the polynomial D is unity in this case. The last equation expanded is in the form

$$e^{\alpha_1 + i\beta_1} = 1 + A_1\lambda + A_2\lambda^2 + \cdots + A_n\lambda^n, \tag{9}$$

which is the form for the ratio E_0/E_1 for the network shown in Fig. 3. By writing out the ratio E_0/E_1 for this network and comparing terms with equation (8) expanded in the form of (9) the values of the a's may be found to be [4]

$$a_1 = \sin \frac{\pi}{2n},$$

$$a_2 = \frac{\sin \dfrac{3\pi}{2n} \sin \dfrac{\pi}{2n}}{a_1 \cos^2 \dfrac{\pi}{2n}},$$

$$\cdot \quad \cdot \quad \cdot \quad \cdot \quad \cdot \quad \cdot \quad \cdot \quad \cdot \quad \cdot \tag{10}$$

$$a_m = \frac{\sin \dfrac{2m-1}{2n}\pi \sin \dfrac{2m-3}{2n}\pi}{a_{m-1} \cos^2 \dfrac{m-1}{2n}\pi},$$

$$a_n = n \sin \frac{\pi}{2n}.$$

[4] By the evaluation of the finite sums and products of the trigonometric terms. No short method has been found for obtaining the results.

The second network, which when connected in parallel with Fig. 3 will give a constant resistance, is obtained from the first by replacing λ by $1/\lambda$.   It is shown in Fig. 4.

These structures have been designed on the basis of λ being a pure imaginary.   Note, however, that the two structures will have a constant resistance provided that λ is any function realizable by a combination of resistances and reactances.   Equations (8) and (9) will still hold but (3) and (7) will no longer be true.   Note, too, that for the simplest case of $n = 1$ the structures reduce to the usual form for constant resistance networks as shown in Fig. 1.
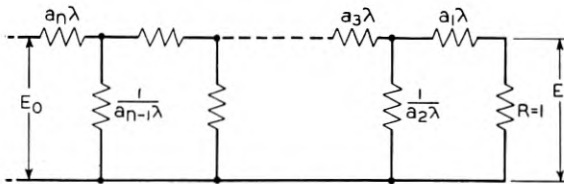
Fig. 3
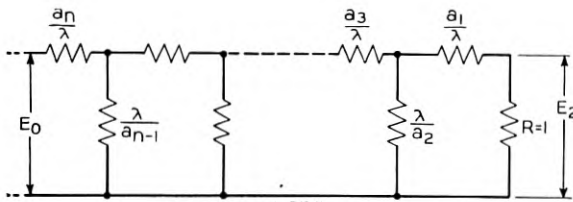
Fig. 4

Figs. 3–4—A pair of constant resistance networks of "constant K" configuration.

If λ is taken of the form $i(f/f_0)$, the structure of Fig. 3 will be made up of series coils and shunt condensers in the form of a low-pass filter. The structure of Fig. 4 will be of the form of a high-pass filter with series condensers and shunt inductances.   The loss of the first network is

$$e^{2\alpha_1} = 1 + \left(\frac{f}{f_0}\right)^{2n}$$

and of the second

$$e^{2\alpha_2} = 1 + \left(\frac{f_0}{f}\right)^{2n}.$$

With $f < f_0$ the loss of the first network will be small and the loss of the second network large.   With $f > f_0$ the reverse is true.   At $f = f_0$ each of the networks takes half of the available power, illustrating a

necessary property of constant resistance networks of this type, of a three db loss at the cross-over frequency.

If λ is taken of the form $i\dfrac{\left(\dfrac{f}{f_m} - \dfrac{f_m}{f}\right)}{\left(\dfrac{f_2}{f_m} - \dfrac{f_m}{f_2}\right)}$ the networks become band-pass

and band-elimination filters, respectively. By taking other functions for λ multiple band structures may be designed, subject always to the limitation that the combined bands of both filters must extend over the whole frequency range, with a three db loss at each cross-over point.

The evaluation of the elements is easily done from equations (10). The impedance denoted by $a_1\lambda$, for example, in the low-pass filter would have the value $i(f/f_0) \sin (\pi/2n)$, which is an inductance of a value $(1/2\pi f_0)[\sin (\pi/2n)]$. For a terminating resistance different from unity the value of the first inductance is $L_1 = (R_0/2\pi f_0)[\sin (\pi/2n)]$ or in general any inductance is $L_m = a_m L_0$ where $L_0 = R_0/2\pi f_0$. Similarly, any capacitance is $C_m = a_m C_0$ where $C_0 = 1/2\pi f_0 R_0$. The corresponding formulas for the second network are $C_m = C_0/a_m$ and $L_m = L_0/a_m$. The same formulas hold for n even; in that case the networks of Fig. 3 and Fig. 4 would terminate on the right in a shunt arm with impedances of $1/a_1\lambda$ and λ/a_1, respectively. This is illustrated by Fig. 2 for $n = 2$.

Filters with Characteristics Similar to Those of the "M-derived" Type

The networks shown in Fig. 3 and Fig. 4 have the same configuration and similar characteristics to constant K filters. They are subject to the same objection of a relatively slow rate of cut-off and an excessive loss at frequencies remote from the cut-off. A type of characteristic similar to that obtained with M-derived filters, with points of infinite loss at finite frequencies, is necessary for an economical design in the majority of cases.

The loss characteristic of the network is of course fixed by the function $F(\lambda)$, a ratio of two polynomials in λ. It may be written

$$F(\lambda) = A_0\lambda^2 \frac{1 + A_1\lambda^2 + \cdots + A_n\lambda^{2n-2}}{1 + B_1\lambda^2 + \cdots + B_n\lambda^{2n-2}}.$$

Now the first filter will have infinite loss points when the denominator is zero, and the second filter when the numerator is zero. If these

peaks are to occur at real frequencies, $F(\lambda)$ must have poles at $\lambda^2 = -1/S_m{}^2$ and zeros at $\lambda^2 = -P_m{}^2$. Moreover, since $1/[1 + F(\lambda)]$ and $1/[1 + (1/F(\lambda)]$ must always be positive for real frequencies, the expression for $F(\lambda)$ when all its zeros and poles occur at real frequencies must be a perfect square. It may then be written

$$F(\lambda) = A_0\lambda^2 \frac{(P_1{}^2 + \lambda^2)^2 \cdots (P_{n-1}{}^2 + \lambda^2)^2}{(1 + S_1{}^2\lambda^2)^2 \cdots (1 + S^2{}_{(n-1)/2}\lambda^2)^2}.$$

In order to get an idea of the significance of the expression, let $\lambda = i(f/f_0)$ and restrict the P's and the S's to values less than unity. The first network will then have zero loss points at $f = 0$ and $f = P_m f_0$ and infinite loss points at $f = f_0/S_m$ and $f = \infty$. The second network will have infinite loss points when the loss of the first is zero, and zero loss points when the loss of the first is infinite. The first network is therefore a low-pass filter and the second a high-pass filter.

The following work is considerably simplified if $S_m = P_m$. This implies that the characteristic of the second filter is the same function of $1/\lambda$ that the first is of λ. If the cross-over point is fixed at $\lambda^2 = -1$, the value of A_0 is -1 and in order to write equation (6) or (7), it is necessary to find those zeros with a negative real part of

$$1 - \lambda^2 \frac{(P_1{}^2 + \lambda^2)^2 \cdots (P^2{}_{(n-1)/2} + \lambda^2)^2}{(1 + P_1{}^2\lambda^2)^2 \cdots (1 + P^2{}_{(n-1)/2}\lambda^2)^2}$$

$$= \left[1 + \lambda \frac{(P_1{}^2 + \lambda^2) \cdots}{(1 + P_1{}^2\lambda^2) \cdots} \right] \left[1 - \lambda \frac{(P_1{}^2 + \lambda^2) \cdots}{(1 + P_1{}^2\lambda^2) \cdots} \right].$$

Now since the zeros of the second factor on the right are the negatives of the zeros of the first factor, it will be sufficient to find all of the zeros of the first factor and reverse the signs when necessary to secure negative real parts. Consider, then, the equation

$$1 + \lambda \frac{(P_1{}^2 + \lambda^2) \cdots (P^2{}_{(n-1)/2} + \lambda^2)}{(1 + P_1{}^2\lambda^2) \cdots (1 + P^2{}_{(n-1)/2}\lambda^2)} = 0.$$

One root is $\lambda = -1$. It may be shown further that the magnitude of all of the roots is unity. Writing $\lambda = \rho e^{i\theta}$ as a root, the magnitude of the typical product term $(P^2 + \lambda^2)/(1 + P^2\lambda^2)$ may be written

$$\left| \frac{P^2 + \lambda^2}{1 + P^2\lambda^2} \right|^2 = 1 + \frac{\left(\dfrac{1}{P^2} - P^2 \right) \left(\rho^2 - \dfrac{1}{\rho^2} \right)}{\left(P\rho + \dfrac{1}{P\rho} \right)^2 - 4\sin^2\theta}.$$

Now since the denominator of the expression on the right is always positive, and all of the P's are less than unity, the magnitude of each of the product terms is greater than unity if ρ is greater than unity and less than unity if ρ is less than unity. Since, however, the magnitude of the complete product must be unity, the value of ρ must be unity.

After dividing through by the factor $1 + \lambda$, the remaining function is a reciprocal equation in λ and may be written as an equation in $p = \lambda + (1/\lambda)$. Since the magnitudes of the roots in λ are all unity, the roots in p must all be real and be in the region $-2, +2$.

The degree of the polynomial in p is $(n - 1)/2$. It may be shown further that if $(n - 1)/2$ is even there are an equal number of positive and negative real roots, if the degree is odd there is one more positive than negative root.

The equations in p for various values of $(n - 1)/2$ are

$$\frac{n-1}{2} = 1, \qquad p - (1 - \Sigma_1) = 0$$

$$= 2, \qquad p^2 - (1 - \Sigma_2)p - (1 - \Sigma_1 + \Sigma_2) = 0$$

$$= 3, \qquad p^3 - (1 - \Sigma_3)p^2 - (2 - \Sigma_1 + \Sigma_3)p$$
$$+ (1 - \Sigma_1 + \Sigma_2 - \Sigma_3) = 0$$

$$= 4, \qquad p^4 - (1 - \Sigma_4)p^3 - (3 - \Sigma_1 + \Sigma_4)p^2$$
$$+ (2 - \Sigma_1 + \Sigma_3 - 2\Sigma_4)p$$
$$+ (1 - \Sigma_1 + \Sigma_2 - \Sigma_3 + \Sigma_4) = 0,$$

where the Σ's are the symmetric functions of the P^2's, that is,

$$\Sigma_1 = P_1^2 + P_2^2 + \cdots P^2_{(n-1)/2},$$
$$\Sigma_2 = P_1^2 P_2^2 + \cdots + P^2_{(n-3)/2} P^2_{(n-1)/2}.$$

The equations in p may also be written in trigonometric form as follows:

$$\frac{n-1}{2} = 1, \qquad \cos \frac{3}{2}\theta + \Sigma_1 \cos \frac{\theta}{2} = 0$$

$$= 2, \qquad \cos \frac{5}{2}\theta + \Sigma_2 \cos \frac{3}{2}\theta + \Sigma_1 \cos \frac{\theta}{2} = 0$$

$$= 3, \qquad \cos \frac{7}{2}\theta + \Sigma_3 \cos \frac{5}{2}\theta + \Sigma_1 \cos \frac{3}{2}\theta + \Sigma_2 \cos \frac{\theta}{2} = 0$$

$$= 4, \qquad \cos \frac{9}{2}\theta + \Sigma_4 \cos \frac{7}{2}\theta + \Sigma_1 \cos \frac{5}{2}\theta + \Sigma_3 \cos \frac{3}{2}\theta$$
$$+ \Sigma_2 \cos \frac{\theta}{2} = 0.$$

These equations include the root at $\lambda = -1$ corresponding to $\theta = \pi$. Excluding this they will each have $(n-1)/2$ roots between $\theta = 0$ and $\theta = \pi$. The roots in p will then be given by $p = 2 \cos \theta$. Equation (7) becomes

$$\beta_1 = \tan^{-1} x + \sum_1^{(n-1)/2} \tan^{-1} \frac{p_m x}{1 - x^2}, \tag{11}$$

where the quantities p_m are the roots of the above equations, without regard to sign.

We require also the value of $d\beta_1/dx$, which may be written

$$\frac{d\beta_1}{dx} = \frac{1}{1 + x^2} \left[1 + \sum_1^{(n-1)/2} \frac{p_m}{1 - \dfrac{(4 - p_m^2)x^2}{(1 + x^2)^2}} \right]. \tag{12}$$

A possible configuration for the first network is shown in Fig. 5 and for the second in Fig. 6.
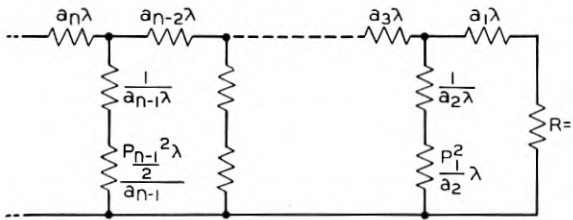
Fig. 5
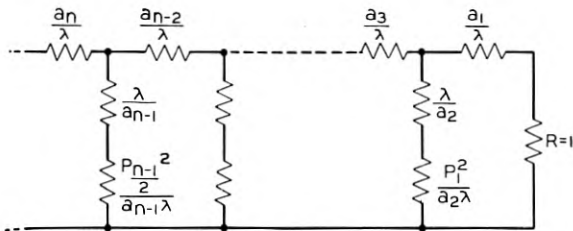
Fig. 6

Figs. 5–6—A pair of constant resistance networks of the "M-derived" configuration.

To find the elements it would be possible to expand the voltage ratio and solve for the a's as was done in the constant K illustration. Another method would be to find the input admittance of the network from the known input conductance, and find the a's from this expression. A simpler method, however, takes advantage of the fact

that each structure is a purely reactive network with the exception of the terminating resistance and finds the network elements in terms of the short circuit reactance as measured from the resistance end of the network.

Use may be made of the following theorem:

With any four-terminal reactive network the reactance measured at terminals 3–4 with terminals 1–2 short-circuited is equal to the tangent of the phase shift between a voltage E_0 applied to terminals 1–2 and the resultant voltage E_1 across a unit resistance connected to terminals 3–4.

The open-circuit voltage across 3–4 due to E_0 would be $\pm kE_0$, where k is a real quantity, if the network contains only reactances. By Thévenin's Theorem, then,

$$E_1 = \frac{\pm kE_0}{1 + iX},$$

where X is the reactance of the network from terminals 3–4. If β is the phase shift between E_0 and E_1, $X = \tan \beta$.

Since this phase shift is given by (11) the short-circuit reactance is known. At a value of $\lambda = i(1/P_1)$ or $x = 1/P_1$, the impedance of the first shunt arm from the right of Fig. 5 is zero, so that the reactance of the filter is simply the reactance of the arm $a_1\lambda$, which gives the value of a_1 directly as

$$a_1 = P_1(\tan \beta_1)_1,$$

where $(\tan \beta_1)_1$ denotes the value of $\tan \beta_1$ when $x = 1/P_1$. The reactance of the network after subtracting a_1x is $\tan \beta_1 - P_1(\tan \beta_1)_1 x$. At values of x very close to $1/P_1$ this is the reactance of the first shunt arm, or

$$a_2 = \frac{\dfrac{d}{dx}\left(P_1^2 x - \dfrac{1}{x}\right)}{\dfrac{d}{dx}(\tan \beta_1 - a_1 x)},$$

where, after differentiation, $x = 1/P_1$. Carrying through the differentiation,

$$a_2 = \frac{2P_1^2}{(1 + \tan^2 \beta_1)_1 \left(\dfrac{d\beta_1}{dx}\right)_1 - a_1}.$$

Similar formulas may be found for the rest of the elements. If X_m denotes the reactance starting with the series arm $a_m\lambda$ or with the

shunt arm $(P_{m/2}{}^2\lambda^2 + 1)/a_m\lambda$, then for m odd, that is, for a series element,

$$a_m = P_{(m+1)/2}X_m \quad \left(x = \frac{1}{P_{(m+1)/2}}\right)$$

and for a shunt arm, m even,

$$\frac{1}{a_m} = \frac{1}{2P_{m/2}{}^2}\frac{dX_m}{dx} \quad \left(x = \frac{1}{P_{m/2}}\right).$$

When $m = n$, or for the last series arm, a special relation is necessary, readily obtained by the limiting value of reactance as x approaches zero. This gives

$$(a_1 + a_3 + \cdots + a_n)x = (1 + \Sigma p_m)x$$

or

$$a_n = 1 + \Sigma p_m - (a_1 + a_3 + \cdots + a_{n-2}).$$

To use these relations it is necessary to know the expression for X_m, the reactance to the left from the successive points in the network. To determine this in terms of the elements already known use may be made of the following theorem:

If the impedance looking to the left into a network is Z, the impedance to the left from A, any point within the network is the negative of the impedance to the right from A when the network is terminated on the right by an impedance $- Z$.

For example, referring to Fig. 5, to determine a_3 it is necessary to know the reactance to the left starting with a_3x. By the theorem this is

$$X_3 = \frac{1}{\dfrac{a_2x}{1 - P_1{}^2x^2} - \dfrac{1}{a_1x - \tan \beta_1}}$$

and when $x = 1/P_2$ we have for a_3

$$\frac{1}{a_3} = \frac{a_2}{P_2{}^2 - P_1{}^2} - \frac{1}{a_1 - P_2(\tan \beta_1)_2}.$$

The impedance at that end of the filter terminated by the resistance is of interest. Its value of course depends upon the terminating impedance at the junction of the two filters, but assuming that this impedance and the separate terminating resistances are all R_0, the impedance from the load of the first filter is $R_0 \tanh (\alpha_2 + i\beta_2)$ if terminated in a series arm and $R_0 \coth (\alpha_2 + i\beta_2)$ if terminated in a shunt arm. Note that the impedance of the first filter depends upon

the transfer constant of the second. The impedance from the load of the second filter depends in the same way upon the transfer constant of the first. The proof of these relations is based upon both networks being purely reactive.

APPLICATIONS

The use of the constant resistance pairs of filters is indicated wherever the impedance at the junction of two filters is of major importance. Another application which is of some importance is that of separating the energy in a band of frequencies into two or more channels, delivering all of the energy into one or the other of the loads.

The method may be extended to more than two networks in parallel or series to give a constant resistance. For example, the combination

$$G_1 = \frac{1}{[1 + F_1(\lambda)]\left[1 + \dfrac{1}{F_2(\lambda)}\right]},$$

$$G_2 = \frac{1}{\left[1 + \dfrac{1}{F_1(\lambda)}\right]\left[1 + \dfrac{1}{F_2(\lambda)}\right]},$$

$$G_3 = \frac{1}{1 + F_2(\lambda)},$$

will give a constant resistance for the three networks. Designs have been carried through on this basis where the networks are low-pass, high-pass and band-pass, respectively. This is one method of avoiding the limit of three db in the loss of the low-pass and the high-pass filters at their cross-over point, since in this case the band-pass filter will take up the power. A second method is to use a pair of low and high-pass filters, each terminated in another pair with different cross-over points. This method requires the use of both a low-pass and a high-pass filter as power absorbing networks but they would be simple structures and together would require no more elements than the single band-pass filter in a three-filter combination.

The two methods are illustrated in Fig. 7 and Fig. 8, respectively. The structures for the second type are given by Fig. 9. Note that the filters designated L.P. II, L.P. III, H.P. II and H.P. III have one series arm missing and are apparently terminated at a shunt point at the load end of the filter. This is a consequence of selecting the two P's in such a way that the coefficient a_1 becomes zero, a matter of no particular difficulty in the case of a two-section filter.
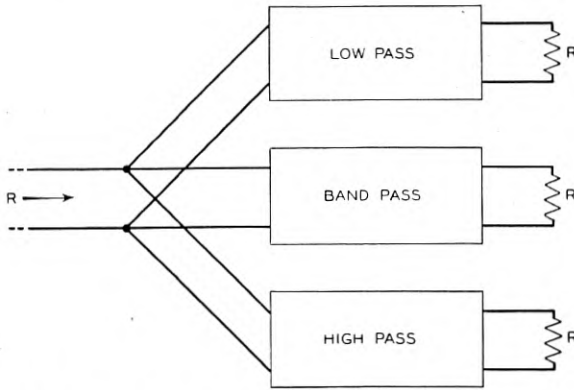
Fig. 7—A three-filter constant resistance combination.
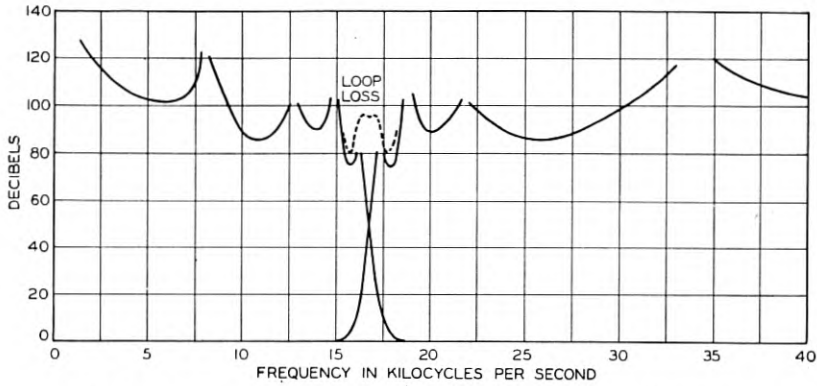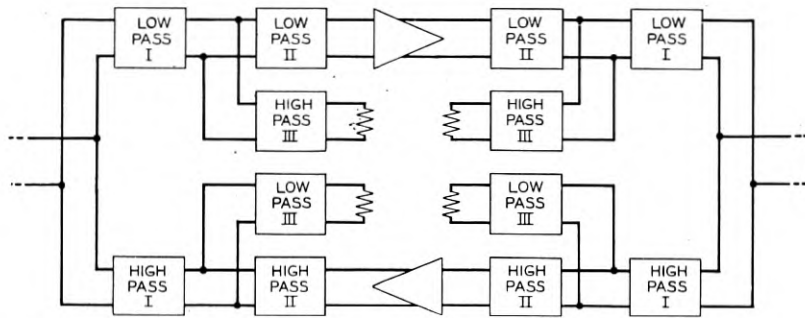
Fig. 8—Constant resistance networks used as directional filters.

It will be found that a filter of several sections of the type described in this paper will have somewhat less loss in the attenuated band than the usual type of design. On the other hand the loss in the band will, in general, be less unless additional elements are used in the standard type of filter to reduce reflection losses. A design for a pair of constant

LOW PASS I   HIGH PASS I

LOW PASS II AND III   HIGH PASS II AND III
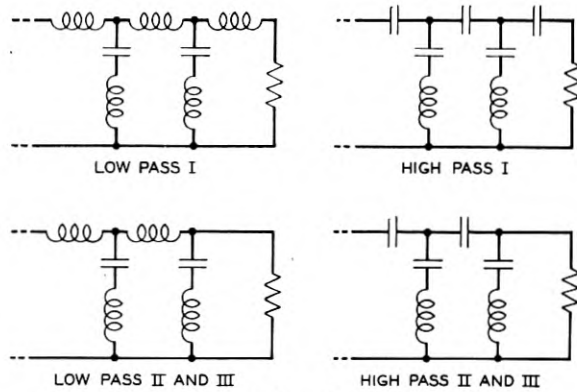
Fig. 9—The configuration of the filters of Fig. 8.

STANDARD

CONSTANT RESISTANCE
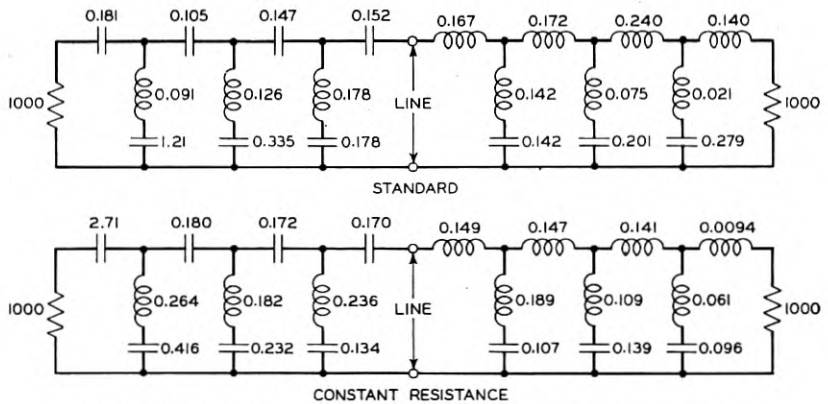
Fig. 10—Comparison of the elements of typical standard and constant resistance filters.

resistance filters having a cross-over frequency of 1000 cycles is compared with a design for a pair of standard filters in Fig. 10. No additional elements have been added to the standard type to improve the impedance.[5] The loss characteristics for the two low-pass filters

[5] "Impedance Correction of Wave Filters," E. B. Payne, and "A Method of Impedance Correction," H. W. Bode, *Bell Sys. Tech. Jour.*, October 1930.
"Extensions to the Theory and Design of Electric Wave Filters," Otto J. Zobel, *Bell Sys. Tech. Jour.*, April 1931.

are compared in Fig. 11. Note that in this case the constant resistance filters have only about sixty per cent of the loss of the standard
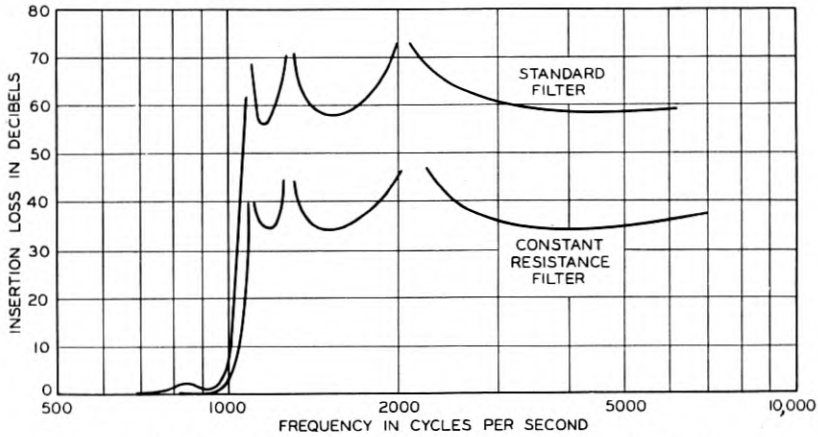
Fig. 11—Loss characteristics obtained by the filters of Fig. 10.

filters. The difference would not be as great for filters of less sharp discrimination.

A Laboratory Evaluation of Wood Preservatives

By R. E. WATERMAN, JOHN LEUTRITZ and CALEB M. HILL

Evolution of a simple laboratory technique for the assay of materials proposed for use in the preservation of wood is reported in this paper. This test involves a measurement of the actual decay resistance of the treated wood. Included are a resumé of the limitations imposed by current test-methods and a discussion of the adaptations of this new technique to the numerous variables inherent in laboratory simulations of outdoor exposure.

FUNDAMENTAL scientific discoveries in the biological sciences during the latter part of the nineteenth century slowly brought organized knowledge out of the chaos of conflicting theories as to the character of many natural phenomena. This was especially true in the field of fermentation where these accumulated findings and observations finally served as the basis for the proof that the filamentous fungi were the causal agents in the decay of wood. This knowledge of the decay mechanism, together with increased demand for wood products due to industrial expansion and the concomitant depletion of our best stands of naturally rot-resistant species of timber, served as a stimulus towards organized studies of the physiology of decay organisms and possible means of prophylaxis.

While Nature has been lavish in the supply of fast-growing species, she has also been provident in making such timber more vulnerable to attack by the micro-flora and fauna which act as scavengers for the forests and as conservators for vast quantities of materials which trees take from the soil during their growth period. The necessity of preserving this more easily decayed wood accelerated the search for satisfactory means of protection. This has been especially true in the Bell System where fast-growing but easily rotted southern pine has, to a large extent, been supplanting chestnut and cedar for poles.

In the past the use of certain materials for the preservation of wood was based entirely on their availability or the personal prejudice of proponents for them. This method of selection could result only in widespread waste and oftentimes disastrous consequences, but a wood-preserving industry utilizing certain materials such as coal-tar creosote gradually evolved. The controversies as to what properties of creosote make it an effective preservative still rage, and the problem of choosing and specifying the type of creosote best fitted for the preserva-

194

tion of timber is still urgent. This is particularly vital in that creosote is a loose term covering a congregation of compounds rarely twice the same in quality or proportion.

When in 1927, research on the development of a rapid means of evaluating wood preservatives was initiated in the Chemical Department of these Laboratories, primary consideration was accorded the selection of the best available method for measuring the toxicity of proposed preservatives against wood-destroying fungi. The technique used was one which had been developed and extended to a considerable degree by the workers at the Forest Products Laboratory in Madison, Wisconsin. This petri dish method, described at some length by Richards in 1923,[1] was standardized in 1929[2] at a conference of American workers in St. Louis. Briefly, the method consists in adding various amounts of the toxic agent under test to a nutrient medium in the form of a hot malt-agar solution which is poured into a petri dish, cooled, and the resulting gel inoculated with small sections of the hyphæ of a wood-destroying fungus (Fig. 1). The organism usually used is culture no. 517 from the Forest Products Laboratory but others may be chosen. The excellence of the preservative is based on the lowest concentration which is able to kill or totally inhibit growth of the test organism.

While the petri dish method can be brought to a high degree of efficiency, accuracy and precision by suitable precautions, it is definitely limited in its practical application. It tells nothing of the permanency of the material under test from the standpoint of leaching, evaporation or chemical instability. Nothing is learned of the possible reaction of the preservative with wood, and the dispersion in warm liquid agar which later gels is a far cry from that obtained in wood. There is an axiom of biological assay, that the substratum for *in vitro* tests be as similar as possible to that encountered in nature. Neglect of this principle in the field of antiseptics and germicides has been responsible for many outstanding failures *in vivo* of materials which had given brilliant promise in the culture tube. Doubt concerning the validity of the petri dish test was substantiated when several preservatives highly toxic according to this method failed in outdoor exposure tests. In many cases such failures could not be ascribed to obvious conditions such as high volatility or solubility. Instances were also met wherein materials of little value according to the petri dish method were able to prevent decay in the field. There is no disposition to advise against all use of this method as it is a valuable tool in making initial judgments on a new material; but it should be verified by other means before the expense of a field trial can be justified, and a

[1] Numbers refer to bibliography at end.

proper degree of skepticism should be exercised before condemning a preservative on the basis of this test alone.

Parallel with the use of nutrient substrata of the malt-agar type in this country, there grew up in Europe a technique which utilized the wood itself as a medium for dispersion of the toxic agent. This kolle flask method (Fig. 2) was standardized and accepted by a conference
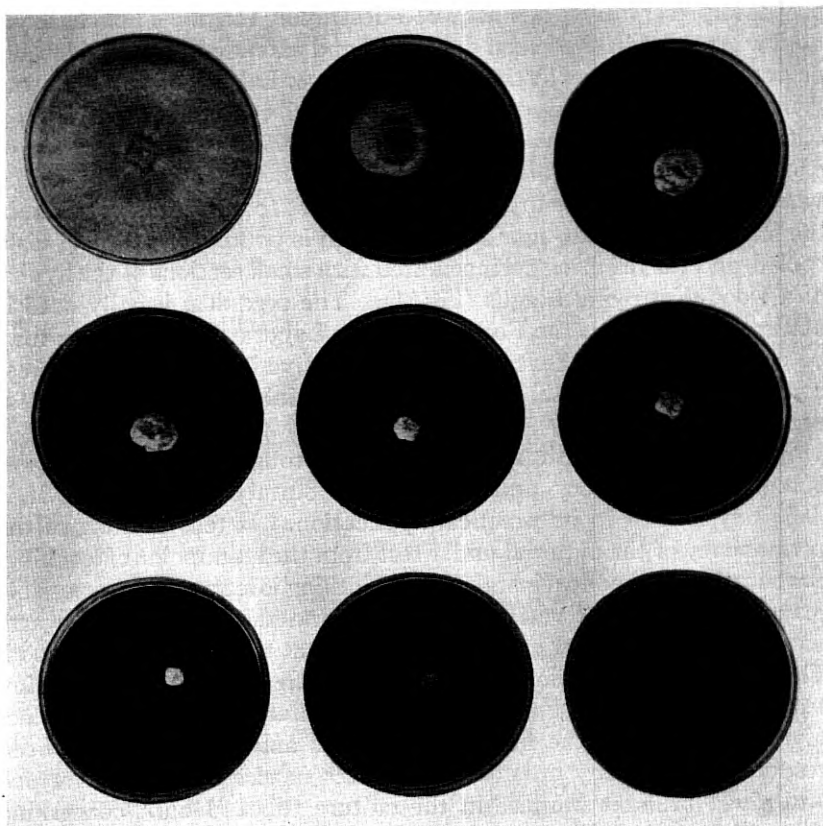
Fig. 1—Assay by petri dish method. Test-fungus No. 517 on increasing amounts of coal-tar creosote.

of European workers at Berlin in 1930.[3] An outline of the method follows: Wood blocks of a convenient size are impregnated with the toxic agent, usually in solution, and after evaporation of the solvent the blocks are placed in kolle flasks and supported on glass rods set in malt-agar covered with the actively growing mycelia of the test fungus. The conference advised the use of *Coniophora cerebella* as the test

fungus, but suggested that at least two species should be used in each test. After three or four months' exposure to the wood-destroying fungi, the blocks are removed from the flasks, freed from adhering mycelium, and the weights taken before and after the test period used as a measure of the amount of decay.

The kolle flask method has much to recommend it, overcoming as it does many of the difficulties inherent in the petri dish technique. However, the test as standardized at Berlin presents serious drawbacks. The kolle flasks are expensive, comparatively fragile, difficult to
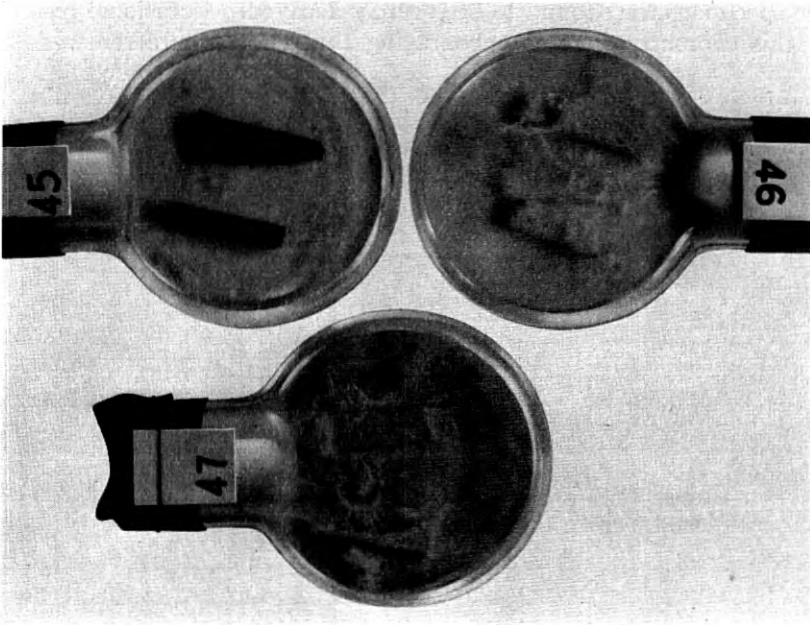
Fig. 2—Assay by kolle flask method. *Poria incrassata* used in comparison of southern pine heartwood versus sapwood.

handle, inconvenient to store, and maintenance of proper moisture conditions is particularly difficult. For really satisfactory results the flasks during the tests should be kept at a constant humidity and temperature. Despite all precautions there is the ever-present danger of excess moisture and resultant lack of decay should the test block touch the agar or any condensed moisture on the flasks. Another unusual problem arose when certain over-ambitious fungi rotted the cotton plugs used to stopper the flasks and even continued to grow into other flasks where they did not belong.

A New Assay Method

Both the petri dish and kolle flask methods had shown definite limitations, and it became apparent that further experimentation on a laboratory assay-method should be directed along somewhat different lines. By chance a few treated pieces which had been removed unscathed after a routine exposure in the kolle flask, were dropped on a beakerful of moist wood heavily infected with a wood-destroying fungus. The beaker was merely covered with a watch-glass and set aside. Growth progressed over the treated blocks with unexpected rapidity and vigor, and when removed at the end of three months, the specimens were found to be severely decayed. Occasional results of this character were so encouraging that efforts were renewed to
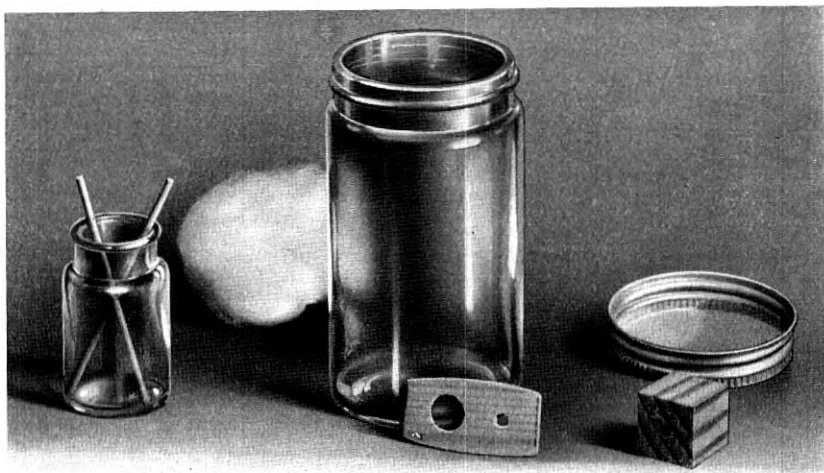
Fig. 3—Apparatus required for modified wood-block method of assay.

develop a technique which would incorporate the use of wood as a secondary substrate together with more favorable moisture control. Experimentation had demonstrated that the amount of moisture in the wood block should be slightly above fibre saturation for optimum growth of the fungus. Inoculated wood placed in air at 100 per cent relative humidity will rot but slowly while too much moisture decelerates and even inactivates the fungal metabolism. The problem therefore was to bring about these optimum decay conditions with low-priced, easily handled equipment. The test in its present state of evolution is inexpensive, easy to manipulate and capable of increased uniformity due to better regulated moisture conditions. The only

equipment necessary consists of a straight-sided screw-capped bottle about 5 inches high and 2 inches in diameter, a smaller bottle 2.5 inches high and 1 inch in diameter, a wad of cotton, a small flat piece of untreated wood and an applicator such as is used by the medical profession for swabs (Fig. 3).

The treated blocks, previously brought to moisture equilibrium, are supported by means of a thin slab of untreated wood on the top of the small bottle which is placed inside the larger screw-topped bottle.

Fig. 4—Assembly of apparatus required for modified wood-block method of assay.

Through holes bored in the test piece and the thin slab of supporting wood are passed the pieces of wooden applicator, which act as a means of anchorage and as wicks for conduction of water to the wood under test. Although not absolutely necessary, cotton is usually wrapped around the small bottle to reduce shock during handling. Water is placed in both bottles and after sterilization of the complete set-up (Fig. 4) the thin slab of wood is inoculated with a portion of

hyphæ of the test-fungus which has been growing on a malt-agar substratum. The bottles are then placed in an incubation room (Fig. 5) at 26–28° C., customarily for a period of 24 weeks. At the end

Fig. 5—Incubator with tests in progress.

of the test period the blocks, freed of adhering mycelium, are again brought to equilibrium at a specified humidity, reweighed and the pieces finally dissected to determine the loss of strength occasioned by the attack of the fungus.

Materials to be tested as possible preservatives are injected in serial concentrations into the blocks of sapwood, commonly southern pine, under conditions simulating as nearly as possible those which would
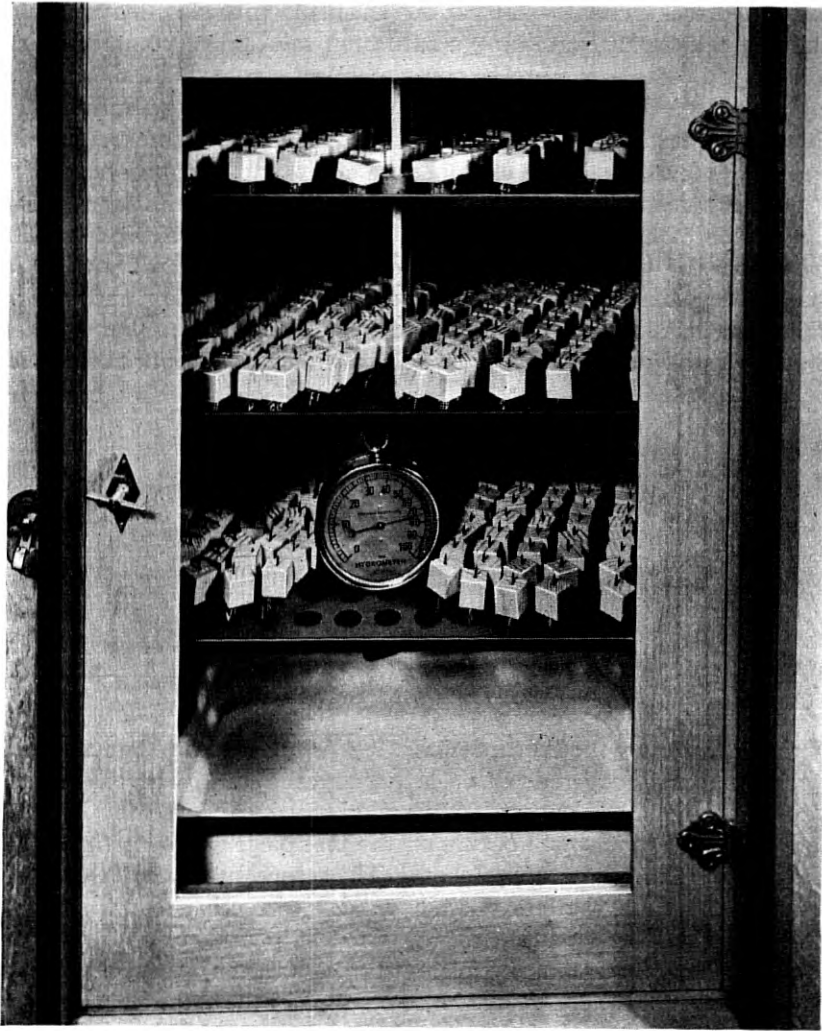
Fig. 6—Constant humidity chamber filled with test blocks.

be used in practice. Due to the variance in the moisture pick-up of wood at different relative humidities, it is necessary to bring the blocks to equilibrium under standard conditions both before and after the

test in order to determine actual weight losses. Since oven-drying is obviously a poor reference standard when volatile materials are under consideration and may also bring about serious changes in the wood, a constant humidity chamber is used for this purpose. An ordinary bacteriological incubator kept at 30° C., fitted with slow-moving fans and a shallow pan containing a saturated solution of common table salt (Fig. 6), has proved to be completely satisfactory in this respect, maintaining a relative humidity of 76 per cent with very little deviation. The test pieces after treatment are placed on racks (Fig. 7) and only a few days in the chamber are necessary for equilibration.

Such a test method allows of three criteria as the basis for judging the degree of attack. First, there is the amount and vigor of the growth of the test-fungus on the wood block, readings of which are made every four weeks. As this is difficult of expression, recourse is had to the classical method of the serologists, wherein plus four denotes the maximum. An attempt is made to evaluate both vigor and extent
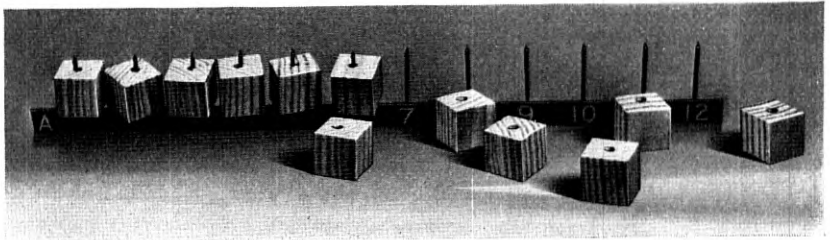
Fig. 7—Test blocks and rack.

of the fungal growth; the notation "2–4" would mean that the test block was partly covered with a heavy mycelial mat, whereas "3–2" would mean almost covered with relatively weak growth (Figs. 8 and 9). Often no growth occurs on the test piece and sometimes the mycelial inoculum is actually killed. The second measure of extent of decay is based on the loss of weight, with corrections for the effect of leaching and evaporation during the test period, computed from data obtained on treated controls put through the entire cycle without inoculation. These controls are also of value in the empirical strength rating made at the end of the test when the pieces are dissected in an effort to judge the remaining strength—a rating of ten indicates no detectable loss in strength as compared to the control and zero denotes complete disintegration.

Long experience with the petri dish method had emphasized the high degree of specificity of the fungi to various toxics. No single

fungus is equally resistant to all preservatives and gross errors are inevitable unless cognizance is taken of this situation. Since it is impossible to use all the organisms which destroy wood, a choice has been made to include genera which are known to be of considerable
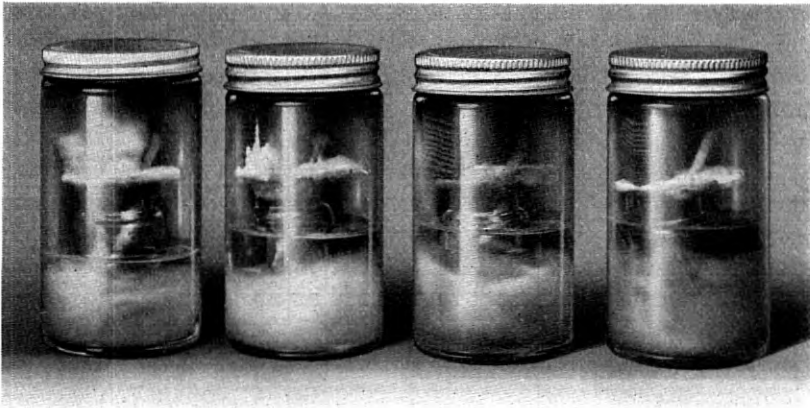
Fig. 8—Assay of a polychlor phenol showing effect of increasing concentration. The test organism *Lentinus lepideus*. The growth ratings from left to right are 4–4, 3–3, 1–2, and √ = no growth on specimen.
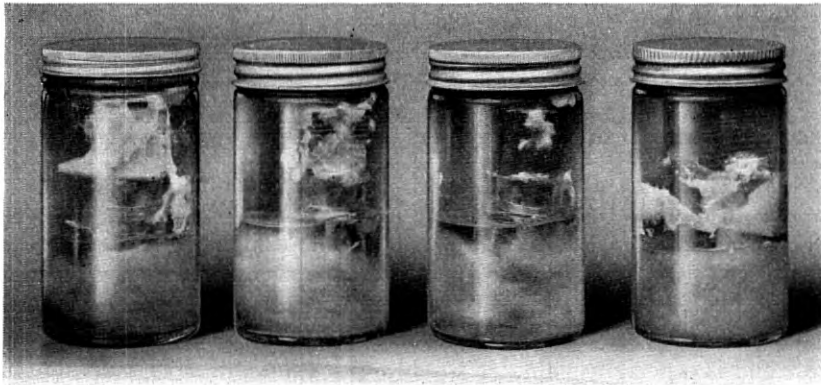
Fig. 9—Same range of concentration as in Figure 8 with U-10 as test fungus. The growth ratings from left to right are 4–4, 3–4, 1–3 and 1–2.

economic importance in the decay of timber or which have been encountered in the actual decay of telephone poles, being sure to include in any given test the fungi which past experience has shown to be resistant to the type of preservative under consideration. Four

organisms in duplicate are used in each test (Fig. 10). *Lentinus lepideus*, cited by Buller,[4] Snell [5] and Humphrey [6] and isolated several times from posts in the Gulfport, Mississippi, test plot,[7] as well as from poles in service, is used in all cases of organic preservatives, but is seldom used against metallic salts, to which it is extremely sensitive. *Lenzites trabea*, another species of great economic importance, Hubert,[8] and also isolated several times from rotted southern pine poles, is somewhat parallel in resistance to *Lentinus lepideus*, but produces a markedly different type of decay. *Polyporus vaporarius*, *Poria incrassata*, and *Coniophora cerebella*, the common "dry rots," although easily killed by many hydrocarbons, are resistant to most inorganic compounds, and at least one of these organisms is included in each test on such materials. *Fomes roseus*, another fungus of wide distribution, reacts in a most inconsistent manner, but its occasional specific virulence is sufficient to warrant its inclusion in all assays of

Fig. 10.—Assay of worthless preservative at maximum concentration. The fungi in duplicate from left to right are *Lenzites trabea*, U-10, *Fomes roseus* and *Lentinus lepideus*.

new and unusual preservatives. Unfortunately the fastest and most versatile decay organism used has no name and masquerades under the designation U (unknown)-10. Isolated several years ago from a decayed pine pole, the identity of U-10 is still a mystery, despite the efforts of many mycological authorities. U-10 is included in every test and is especially valuable when a quick indication of the value of a new preservative is needed, as it is capable of producing an appreciable weight loss in about three months. In addition to the above fungi occasional use is made of such common wood-destroyers as *Trametes serialis*, *Lenzites sepiaria*, *Polystictus versicolor*, *Polyporus sulphureus*, and *Fomes pinicola*.

At the present stage of development this wood block method tells nothing directly about the ability of a wood preservative to resist the action of termites. Most materials which inhibit decay also prevent

termite attack.   In addition all promising leads are verified by means of the sapling test [9] at Gulfport, Mississippi, and here Nature has provided a bountiful supply of these industrious insects.

Fig. 11—Growth on southern pine sapwood controls.   From left to right; *Polyporus sulphureus, Polyporus vaporarius, Polystictus hirsutus* and U-10.
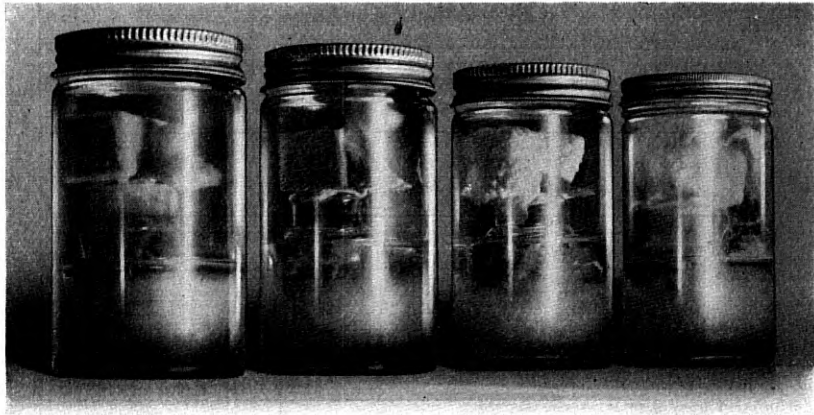
Fig. 12—Growth on southern pine sapwood controls.   *Lenzites trabea, Fomes roseus,* U-10 and *Lentinus lepideus.*

Experimental Results

The above-mentioned fungi have been tested on untreated southern pine sapwood in order to set up standards of comparison (Figs. 11 and 12).   Table I shows individual weight and strength losses effected by our most commonly used organisms in the regular 24-week period. Considerable decay with many of these fungi occurs in a somewhat

TABLE I

WEIGHT LOSSES AND DISSECTION RATINGS ON UNTREATED SOUTHERN PINE BLOCKS EXPOSED TO MOST COMMON TEST FUNGI FOR TWENTY-FOUR WEEKS

Organism	Initial Weight in Grams		Final Weight in Grams		Loss in Per Cent Based on Oven-Dry Weights	Empirical Rating Based on Dissection	Description of Decay
	76% Relative Humidity	Oven Dry	76% Relative Humidity	Oven Dry			
Lentinus lepideus	2.34	2.05	1.87	1.64	20.0	4	Rather advanced decay throughout
	2.35	2.06	1.87	1.64	20.4	4	–ditto–
	2.25	1.97	1.85	1.62	17.8	5	Moderately advanced decay throughout
	2.26	1.98	1.77	1.55	21.7	4	Rather advanced decay throughout
Fomes roseus	2.25	1.97	1.84	1.61	18.3	4	Rather advanced decay throughout
	2.27	1.99	1.84	1.61	19.1	4	–ditto–
	2.22	1.95	1.78	1.56	20.0	4	–ditto–
	2.21	1.94	1.56	1.37	29.4	1	Thoroughly rotted
U–10	2.33	2.04	1.13	0.99	51.5	0	Complete disintegration
	2.33	2.04	1.37	1.20	41.2	0	–ditto–
	2.20	1.93	1.08	0.95	50.8	0	–ditto–
	2.18	1.91	1.19	1.04	45.5	0	–ditto–
Lenzites trabea	2.32	2.03	1.73	1.52	25.1	2	Deep surface disintegration, advanced decay elsewhere
	2.33	2.04	1.76	1.54	24.5	3	Deep surface disintegration, rather advanced decay elsewhere
	2.07	1.81	1.51	1.32	27.1	2	Advanced decay
	2.09	1.83	1.29	1.13	38.3	1	Thoroughly rotted
Polyporus vaporarius	2.12	1.86	1.69	1.48	20.4	4	Rather advanced decay throughout
	2.01	1.76	1.74	1.53	13.1	6	Mild decay throughout
	2.18	1.91	1.78	1.56	18.3	4	Rather advanced decay throughout
	2.26	1.98	1.82	1.60	19.2	4	–ditto–

Growth rating in all cases was 4–4, signifying that the test blocks were covered with heavy normal growth

shorter time, but experience has shown that more consistent results are obtained with the longer period. This is especially true in the case of materials of moderate toxicity, wherein often little growth is seen for two or three months, after which the fungus may become established and rot the test piece.

Using the routine technique, volatile compounds are often found to be practically worthless. This is true of naphthalene, for instance, but when special precautions are taken to insure its presence during the exposure to the fungus, the effective toxicity of this hydrocarbon cannot be questioned. Analysis of control blocks proved that the naphthalene had evaporated quite completely from the test piece even before sterilization. This difficulty can be surmounted satisfactorily in the case of a single compound by injecting a generous quantity and determining the actual amounts of material present from equilibrium weights of the test pieces before treatment and just prior to inoculation. Steam sterilization, of course, would introduce errors under such circumstances, and while the risk of contamination with foreign organisms is high, satisfactory results have been obtained with un-sterilized blocks. In the case of volatile mixtures a similar procedure permits the knowledge of the total evaporation before inoculation, but determination of the loss of the individual constituents is practically impossible.

For all relatively volatile preservatives such as creosotes, the regular method including sterilization can in a way be considered a permanency test. Fortunately this evaporative loss is in the same order of magnitude as that encountered in the field after an exposure of several years, and correlation with outdoor tests is unexpectedly good. Closer control of the amount evaporated would be desirable, but experience has shown this to be difficult of consistent attainment. Artificial weathering machines such as that described by Gillander, Rhodes, King and Roche [10] constitute a reasonably successful attempt to reproduce natural conditions. Leaching is more easily controlled and duplicated than evaporation, and preservatives which by their nature might be considered to be water soluble are subjected to a standard leaching cycle if the initial test has shown them to be promising. Again the close correlation of field results with the laboratory is gratifying.

Of necessity, details of technique have been only sketchily reviewed in this paper; information as to the exact procedure will soon be available in the chemical press together with complete results on several preservatives of interest. Table II contains the results of an assay on a supposedly permanent inorganic preservative before and after

TABLE II

Assay by Wood-Block Method of "Water Insoluble" Preservative Before and After Leaching

Concentration in Pounds per Cubic Foot	Poria incrassata			Coniophora cerebella			U-10			Polyporus vaporarius			Uninoculated
	Growth Rating	Weight Loss in Per Cent	Dissection Rating	Growth Rating	Weight Loss in Per Cent	Dissection Rating	Growth Rating	Weight Loss in Per Cent	Dissection Rating	Growth Rating	Weight Loss in Per Cent	Dissection Rating	Control Weight Loss in Per Cent
2.24 Original	√ √	3.8 7.3	10 10	√ √	5.3 4.1	10 10	√ 2-2	3.4 8.3	10 10	√ √	5.5 4.6	10 10	3.9 5.4
Leached	4-3 4-4	4.0 1.4	10 9	3-2 3-2	1.8 1.7	10 10	2-2 2-2	2.0 0.8	10 9	2-3 3-2	2.1 1.2	10 9	0.8 1.4
1.24 Original	√ √	2.1 2.4	10 10	√ √	1.3 1.9	10 10	√ 3-3	2.2 2.0	10 10	√ √	0.9 3.1	10 10	2.2 1.9
Leached	3-3 3-3	1.2 7.5	10 9	3-3 3-2	9.7 1.9	10 7	3-3 3-3	15.9 6.1	10 5	4-4 3-4	4.7 7.0	10 8	0.4 0.3
0.60 Original	√ √	0.4 1.3	10 10	√ √	0.4 0.4	10 10	√ 3-4	0.4 0.9	10 10	√ √	0.9 1.2	10 10	0.9 0.4
Leached	4-2 4-2	5.1 10.4	10 8	1-1 4-2	0.8 0.8	10 10	3-4 3-4	16.7 15.8	10 4	3-3 3-3	3.2 11.9	10 9	0.0 0.0
0.28 Original	√ √	0.0 0.4	10 10	√ √	0.0 1.0	10 10	√ 4-4	0.0 0.0	10 10	√ √	0.5 0.0	10 10	0.3 0.1
Leached	4-3 4-4	13.6 30.9	10 6	4-3 4-4	17.6 23.5	10 2	4-4 4-4	50.2 12.4	10 0	4-4 4-4	19.8 15.7	10 4	0.0 0.0
0.14 Original	1-1 √	0.0 0.0	10 10	1-1 √	0.0 0.0	10 10	1-2 4-4	0.0 0.0	10 10	√ √	0.0 0.0	10 10	0.0 0.0
Leached	4-4 4-4	22.9 32.8	10 3	4-3 4-3	12.8 26.5	10 6	4-4 4-4	46.4 68.2	10 0	4-4 4-4	26.6 32.8	10 2	0.0 0.0

Ratings under each heading represent duplicate determinations

√ = No growth on specimen

TABLE III

ASSAY BY WOOD BLOCK METHOD OF PROPRIETARY PRESERVATIVE

Concentration in Pounds per Cubic Foot	*Lentinus lepideus*			*Fomes roseus*			U–10			*Lensites trabea*			Uninoculated
	Growth Rating	Weight Loss in Per Cent	Dis-section Rating	Growth Rating	Weight Loss in Per Cent	Dis-section Rating	Growth Rating	Weight Loss in Per Cent	Dis-section Rating	Growth Rating	Weight Loss in Per Cent	Dis-section Rating	Control Weight Loss in Per Cent
12.53	4-2 4-1	3.5 1.7	9 10	2-1 √	0.4 0.4	10 10	1-1 √	0.9 0.4	10 10	√ 2-1	0.5 0.0	10 10	1.7 0.8
10.04	4-4 4-4	9.9 7.1	6 7	4-4 4-4	9.3 7.7	5 6	4-3 4-3	24.5 10.4	3 5	4-2 2-1	11.9 3.2	6 8	0.6 0.3
8.06	4-4 4-4	11.1 8.0	5 6	4-4 4-3	10.6 7.7	5 7	4-3 4-3	5.0 4.3	9 7	4-2 4-1	12.6 10.9	8 5	0.2 0.5
6.64	4-4 4-4	13.4 9.6	5 6	4-4 3-1	7.7 0.5	7 10	4-4 4-4	10.1 9.2	6 6	2-2 4-1	4.5 3.7	8 9	0.1 0.0
4.25	3-4 4-3	6.4 6.2	9 9	4-4 4-4	21.1 19.1	4 4	4-4 4-4	27.6 24.2	3 4	4-4 4-3	30.9 12.9	3 6	0.0 0.0
2.60	4-4 4-4	15.6 8.4	4 7	4-4 4-4	12.9 8.7	4 7	4-4 4-4	38.5 30.6	1 7	4-3 4-4	14.7 10.7	5 6	0.0 0.0

Ratings under each heading represent duplicate determinations
√ = no growth on specimen

TABLE IV

Assay by Wood Block Method of Typical Creosote

Concentration in Pounds per Cubic Foot	Lentinus lepideus			Fomes roseus			U-10			Trametes serialis			Uninoculated
	Growth Rating	Weight Loss in Per Cent	Dis-section Rating	Growth Rating	Weight Loss in Per Cent	Dis-section Rating	Growth Rating	Weight Loss in Per Cent	Dis-section Rating	Growth Rating	Weight Loss in Per Cent	Dis-section Rating	Control Weight Loss in Per Cent
8.82	2-2 2-2	2.7 1.9	10 10	√ √	1.3 0.9	10 10	1-1 √	0.9 0.9	10 10	√ 2-1	1.3 0.9	10 10	1.4 0.8
4.29	3-1 3-2	2.6 1.8	9 9	3-1 2-1	3.2 1.5	9 9	1-1 √	1.0 0.5	10 10	3-2 2-1	0.0 0.0	10 10	0.6 0.3
2.24	4-2 4-2	2.7 2.7	8 8	2-2 3-2	8.8 6.5	6 6	4-4 4-4	38.9 36.1	1	2-1	2.1 0.0	9	0.3 0.1
1.09	4-3 4-3	12.6 11.4	5 5	4-4 4-4	19.4 13.3	8 5	4-4 4-4	44.3 32.1	0	4-4 4-4	30.8 12.1	1 6	0.1 0.0

Ratings under each heading represent duplicate determinations
√ = no growth on specimen

TABLE V

Assay by Wood Block Method of Compound Indicated as Worthless According to the Petri Dish Method

Concentration in Pounds per Cubic Foot	Lentinus lepideus			Fomes roseus			U-10			Lenziles trabea			Uninoculated
	Growth Rating	Weight Loss in Per Cent	Dis-section Rating	Growth Rating	Weight Loss in Per Cent	Dis-section Rating	Growth Rating	Weight Loss in Per Cent	Dis-section Rating	Growth Rating	Weight Loss in Per Cent	Dis-section Rating	Control Weight Loss in Per Cent
2.8	√ 1-1	0.0 0.4	10 10	2-1 2-1	0.8 0.0	10 10	3-2 2-2	0.0 0.0	10 10	3-1 3-1	+0.4 +0.4	10 10	+0.4 0.0
2.1	1-1 1-1	+0.4 +0.4	10 10	2-1 3-1	0.0 +0.4	10 10	3-2 3-2	+0.4 +0.4	10 10	3-1 3-1	+0.4 +0.4	10 10	+0.8 +0.4
0.9	1-1 2-1	1.4 1.4	10 10	3-2 4-2	1.4 0.8	10 10	3-1 3-2	0.0 0.9	10 10	3-1 3-1	0.0 0.0	10 10	0.0 0.5

Ratings under each heading represent duplicate determinations
√ = No growth on specimen

leaching. The losses in weight on the unleached specimens are also present in the controls and are presumably due to an extremely soluble non-toxic salt known to be present. Analysis of the leach waters indicates that the toxic substances were also slowly but definitely soluble. Field results on this same preservative were favorable for a year, but considerable decay was found the second year in all but the two highest concentrations. Table III presents the results obtained with a well-known proprietary preservative of the organic type. The concentrations given are for the preservative as purchased, which consists of a 25 per cent solution of solids in a volatile solvent. This solvent was allowed to evaporate completely before exposure of the test blocks to the fungus. For comparative purposes Table IV illustrates a test of a typical coal-tar creosote. Included as a matter of special interest, Table V outlines the wood-block assay on a material which the petri dish method indicated to be worthless.

This adaptation of the kolle flask method has been in constant use more or less in its present form for the past three years. Hundreds of complete assays have been made with results to date in good agreement with the slower and more expensive outdoor tests. By the use of a range of concentrations the relative efficacy of various preservatives can be judged, but definite expressions of the absolute value of any preservative have been avoided. With conditions controlled for maximum decay, this test is admittedly severe. This very severity, however, is probably an asset in the elimination at the outset of the poor and mediocre materials unworthy of further study.

BIBLIOGRAPHY

1. Richards, C. A.—"Methods of Testing Relative Toxicity," *Proc. Amer. Wood Pres. Assoc.*, **19** (1923).
2. Schmitz, H.—"Laboratory Methods of Testing the Toxicity of Wood Preservatives," *Indus. & Engg. Chem., Analytical Ed.*, **1**, 76–79 (1929).
3. Liese, J. et al.—"Toximetrische Bestimmung von Holzkonservierungs Mitteln." *Z. f. Angew. Chem.*, **48**, 21 (1935).
4. Buller, A. H. R.—"The Destruction of Paving Blocks by the Fungus *Lentinus Lepideus*," *Jour. Econ. Biol.*, **1**, 101–138 (1905).
5. Snell, W. H.—"Studies of Certain Fungi of Economic Importance in the Decay of Building Timbers," *U. S. Dept. Agr. Bull.*, 1053, 1–47 (1922).
6. Humphrey, C. J.—"Timber Storage Conditions in the Eastern and Southern States with Reference to Decay Problems," *U. S. Dept. Agr. Bull.*, 510, 1–42 (1917).
7. Lumsden, G. Q.—"Proving Grounds for Telephone Poles," *Bell Laboratories Record*, **2**, 9–14 (1932).
8. Hubert, E. E.—"Outline of Forest Pathology," 416 (1931), John Wiley & Sons, Inc., New York.
9. Waterman, R. E. and Williams, R. R.—"Small Sapling Method of Evaluating Wood Preservatives," *Indus. & Engg. Chem., Analytical Ed.*, **6**, 413–19 (1934).
10. Gillander, H. E., King, C. G., Rhodes, E. O., and Roche, J. N.—"The Weathering of Creosote," *Indus. & Engg. Chem.*, **26**, 175–183 (1934).

Study of Magnetic Losses at Low Flux Densities in Permalloy Sheet *

By W. B. ELLWOOD and V. E. LEGG

Energy losses in ferromagnetic materials subject to alternating fields have long been considered as due solely to hysteresis and eddy currents. However, at the low flux densities encountered in certain communication apparatus, a further loss is observed which has been variously termed "residual," "magnetic viscosity," or "square law hysteresis." The search for an explanation of this loss has led to precise measurements of hysteresis loops with a vacuum ballistic galvanometer, and of a.-c. losses with inductance bridges. From these results, it appears that that part of the a.-c. effective resistance of a coil on a ferromagnetic core which is proportional to the coil current is strictly identified with the hysteresis loop area as measured by a ballistic galvanometer, or as indicated by harmonic generation in the coil. The hysteresis loop can now be constructed in detail as to size and skewness on the basis of a.-c. bridge measurements. This conclusion was reached previously on a compressed iron powder core, and is now confirmed on an annealed laminated 35 per cent nickel-iron core. Observed eddy current losses for this core exceed those calculated from classical theory by 20 per cent. This excess is ascribed to the presence of low permeability surface layers on the sheet magnetic material. The a.-c. residual loss per cycle (nominally independent of frequency, like hysteresis) is not observed by ballistic galvanometer measurements, although it indicates an energy loss some eight times the hysteresis loss for the smallest loop measured ($B_m = 1.3$ gauss). Analysis of the residual loss shows that it increases with frequency up to about 500 cycles, and remains constant at higher frequencies (to 10,000 cycles per second). Concurrently with the increase of residual loss, the permeability of the alloy is observed to decline with increasing frequency about 1 per cent below the value predicted from eddy current shielding. This effect is most noticeable at frequencies below 1000 cycles.

THE search for an explanation of the excessive magnetic losses observed at low flux densities by alternating current bridge measurement as compared with theoretical indications based on direct-current measurements has led to a more accurate review of both types of measurement.[1, 2, 3] The a.-c. energy loss per cycle which has re-

[1] W. B. Ellwood, *Physics*, **6**, 215 (1935).
[2] V. E. Legg, *Bell Syst. Tech. Jour.*, **15**, 39 (1936).
[3] W. B. Ellwood, *Rev. Sci. Inst.*, **5**, 301 (1934).

ceived most study is the "residual" or "viscosity" loss.[4] It appears related to hysteresis loss because it is nominally independent of frequency, but it differs in being proportional to B_m^2 instead of B_m^3 which would be required by Rayleigh's law for hysteresis loops. Any satisfactory investigation of this anomalous loss demands precise determination of its value, and of its variation with frequency. For this purpose, ballistic galvanometer measurements of the hysteresis loop have been made and compared with bridge measurements of a well annealed 35 permalloy laminated core.

In a previous paper, the magnetic properties of a ring of compressed powdered iron were studied at low flux densities using a sensitive vacuum galvanometer [3] and a multiple swing ballistic method.[1] Hysteresis loops were measured at flux densities B_m ranging from 1.8 to 115 gauss, which showed energy losses proportional to B_m^3 in accordance with Rayleigh's law. Alternating-current measurements agreed with the ballistic measurements as to the magnitude of the energy loss and the proportionality to B_m^3, but in addition showed a residual loss proportional to B_m^2 which was of the same order of magnitude as the Rayleigh hysteresis at these low flux densities.

The analysis of measurements made on the compressed dust core was complicated by the inhomogeneous structure, by the variety of particle shapes and thickness of insulation, and by the mechanical stresses incident to forming the core. To eliminate these objections, the present study was undertaken using a core consisting of well annealed sheet material, for which eddy current losses can be calculated by classical formulae.

SELECTION OF MATERIAL

Considerable a.-c. data were at hand from which to select material for this experiment. The properties of a few representative materials are given in Table I. The constants are defined by the equation

$$\frac{R_f}{\mu_m f L_f} = aB_m + ef + c = \frac{8\pi W}{B_m^2}, \tag{1}$$

where R_f is the difference between the resistances measured with a.-c. and with d.-c. on a toroidal coil with inductance of L_f due to core material of permeability μ_m, when the maximum flux density is $\pm B_m$ and the frequency is f cycles per second. Here the hysteresis coefficient

[4] H. Jordan, *E. N. T.*, **1**, 7 (1924); H. Wittke, *Ann. d. Phys.* (5) **23**, 442 (1935); F. Preisach, *Zeit. f. Phys.*, **94**, 277 (1935); R. Goldschmidt, *Zeit. f. tech. Phys.*, **13**, 534 (1932).

is a, the eddy current coefficient e, and the residual loss term is c. W is the energy loss per cycle in ergs/cm³ of core material. The permeability coefficient $\lambda = (\mu_m - \mu_0)/\mu_0 B_m$.

Table I shows that annealed 35 permalloy in sheet form has the most convenient values of B_r and c/a for further study of this effect. This alloy is of the face centered cubic lattice type common to a large class of magnetic alloys. The numerals preceding the various permalloys give the nickel or alloy percentages, as classified by G. W. Elmen.[5]

The measurement of magnetic losses of 35 permalloy involved further refinements in technique. The high initial permeability required the construction of a special air core mutual inductance to simplify the

TABLE I

Material	Initial Permeability	$\lambda \times 10^4$	$c \times 10^6$	$a \times 10^6$	c/a	$B_r{}^* \times 10^4$.
Compressed Powder Cores						
Grade B Iron.............	35	7.0	110	50.	2.2	13.
81 Permalloy.............	75	1.8	40	5.5	7.3	3.1
Laminated Cores						
35 Permalloy, Annealed.....	1660	30.	60	5.0	12.	62.
38 Permalloy, Hard........	100	7.0	118	9.6	12.	7.2
38 Permalloy, 800° Annealed.	1330	9.0	27	1.5	18.	15.
40 Permalloy, 1000° Annealed	2060	12.0	20	1.4	14.	22.
45 Permalloy, Annealed.....	2550	5.4	14	.43	33.	8.2
78.5 Permalloy, Annealed....	3900	8.1	0	0.6	0	18.
2.4–78 Cr Permalloy, Annealed	14600	6.4	3	.07	43.	7.6
8–79 Cr Permalloy, Annealed.	3025	31.	14	2.6	5.4	60.
45–25 Perminvar, Annealed..	450	0.02	0.0	.002	—	0.0

* These values of remanence were computed from Rayleigh's law as $3a\mu_0 B_m{}^2/16$ for $B_m = 2$.

measuring circuit and increase its stability. The high rate of change of permeability with temperature made it necessary to enclose both the specimen and the air core mutual inductance in a constant temperature box (at $37.1 \pm 0.01°$ C.) throughout the tests.

THE SPECIMEN

The material was melted in a high-frequency furnace, cast, and cold-rolled with intermediate annealings, to strip of thickness $t = 0.0160$ cm. and width 7.62 cm. Analysis showed the following composition: Ni, 35.00 per cent; Fe, 64.25 per cent; Mn, 0.40 per cent; S, 0.030 per cent; Si, 0.02 per cent; C, 0.01 per cent. The resistivity ρ was 82.2 micro-ohm-cms. at 37.1° C. The strip was wound into a tight

[5] *Electrical Engineering*, **54**, 1292 (1935).

spiral core with successive turns insulated from each other by painting with a suspension of fine quartz powder in CCl_4 immediately prior to winding.   The core had an effective magnetic diameter $d = 11.22$ cm., and cross-sectional area of alloy $A = 3.96$ cm.^{2}.   It was annealed in pure hydrogen for one hour at a temperature of 1000° C.

In order to protect the annealed core from mechanical stress during subsequent winding, it was placed on felt in an annular bakelite box which held it without constraint.   The box was wound with a 20-turn magnetizing coil using a flat tape composed of 28 parallel strands of insulated wires connected together at the ends.   This winding prac- tically covered the box with a single layer of wire, and gave a uniform magnetizing force.   It was employed as the magnetizing coil in both the ballistic and the a.-c. bridge measurements.   For the ballistic
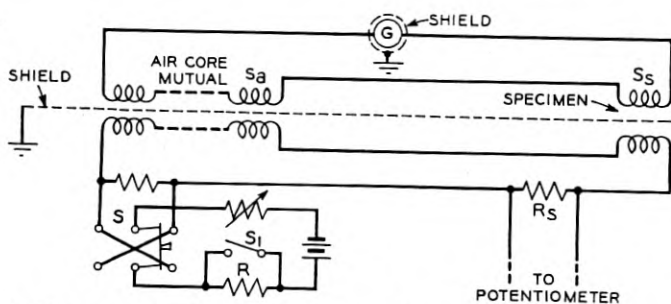

FIG. 1—Ballistic galvanometer circuit, showing adjustable air-core mutual inductance in series-opposition with the test coil.

tests, a layer of insulation was applied over the primary winding before applying the secondary winding.   This insulation consisted of two wrappings of silk tape interspersed with a tinfoil sheath which formed a grounded electrostatic shield between the secondary and the primary winding.   The foil was cut to avoid a short-circuited turn.   The toroidal secondary winding consisted of 5000 turns No. 19 silk-covered enamelled copper wire.

D.–C. Apparatus

In the former experiment,[1] the specimen was compared with a fixed air core mutual inductance in terms of the galvanometer deflection and the primary currents required to obtain approximate balance.   For this experiment, the circuit was modified so that the same current flowed in the primaries of both the specimen and the air core mutual (Fig. 1).   Thus variable thermal effects in the primary circuits were

eliminated and the measuring technique simplified. This required that the mutual inductance be adjustable so as to bring the unbalance onto the galvanometer scale.

The mutual inductance (approximately 0.260 henrys) was constructed for convenience in four separate sections. Each section had a hard wood toroidal core, a low resistance toroidal secondary winding, an inter-winding shield, and sectionalized primary windings on the outside. The secondary windings were connected in series with the galvanometer by a twisted shielded pair of wires. The primary winding groups were also connected in series, and adjusted so that the combination resulted in a mutual inductance of the right value to obtain balance. To eliminate humidity as a source of error each coil was painted with cellulose acetate, covered with silk tape, painted again, baked 48 hours at 108° C. and finally potted in Superla wax in an earthenware jar with only the tops of the terminals exposed. All connections were made by soldering.

During the measurements, the maximum primary current corresponding to H_m was held constant to 0.01 per cent by comparing the voltage drop across R_s with a battery of Weston standard cells. Switching was automatically performed by a photocell and selector switch mechanism previously described [3, 1] but not shown here. These operated switches S and S_1 at the proper time and in the right order. The difference in flux turns between the air core mutual inductance and the specimen was determined in terms of the ultimate galvanometer deflection as before. From this the difference in B between the side of the hysteresis loop and a straight line drawn through its tips could be computed for a given H. A number of values of this difference ΔB were thus determined for different values of H, and plotted to give the hysteresis loop.

A.–C. Apparatus

In order to compare results obtained by the vacuum ballistic galvanometer with those obtained with alternating currents, bridge measurements of resistance and inductance were made over the same range of flux densities at a number of frequencies ranging from 35 to 10,000 cylces. The secondary winding was removed and the special 20-turn primary winding used for most of the measurements. Later an additional 60-turn winding was used for checking the measurements in the low-frequency range. In either case the inductance was low enough to depress any effect of distributed capacitance far below the precision of the measurements.

Measurements were made on a 10-ohm equal ratio arm inductance

comparison bridge,[2] and were verified at low frequencies using a 1-ohm ratio arm bridge. Calibration of the bridge and standard coils was effected by making measurements over the entire frequency range on a calibrated high quality air core coil substituted for the test coil. The maximum correction required on this account was approximately 0.1 per cent of the resistance due to the magnetic core.

The source of alternating current was an oscillator-amplifier supplying approximately 0.4 watt undistorted power, calibrated for these measurements against the Laboratories' standard frequency. The current was adjusted by the insertion of resistance in series with the
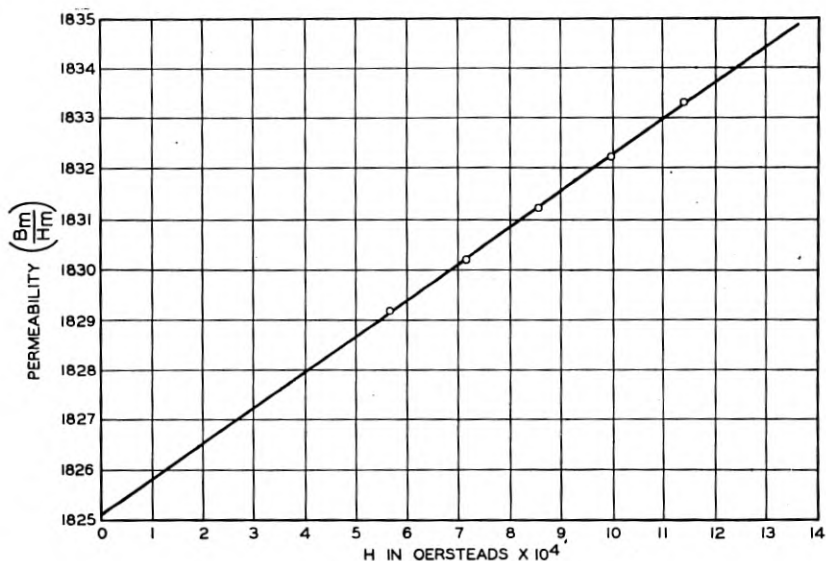

FIG. 2—Core permeability as measured by the ballistic galvanometer.

primary of the bridge input transformer, and was measured by means of a thermocouple between the transformer secondary and the bridge.

The bridge unbalance was amplified by means of an impedance coupled amplifier for the 10-ohm bridge, and by means of a resistance coupled amplifier for the 1-ohm bridge. The amplified unbalance was observed by means of head phones at frequencies above 200 cycles, and by means of a vibration galvanometer at lower frequencies. The d.-c. balance required bridge current of about 3 m.a. in the test coil winding, and had the same precision as the a.-c. balance, viz., ± 0.0002 ohm. The inductance readings were corrected for the air space within the winding, and had a relative accuracy of about 0.03 per cent, and an absolute accuracy of approximately 0.1 per cent.

D.–C. Results

The permeability $\mu = B_m/H_m$ of the specimen is shown as a function of H_m in Fig. 2, on a greatly enlarged scale in which the zero of permeability is not shown. The slope of this line gives $\lambda = 21.5 \times 10^{-4}$.

Values of ΔB are plotted against H for two different hysteresis loops in Fig. 3, from the area of which the energy loss W is computed. For

|	CURVE 1	CURVE 2
B_m IN GAUSS	5.35	2.67
H_m IN OERSTEDS	0.00288	0.00145
W IN ERGS/CC/CYCLE	15×10^{-6}	1.84×10^{-6}
$\dfrac{B_m}{B_r}$	211	423
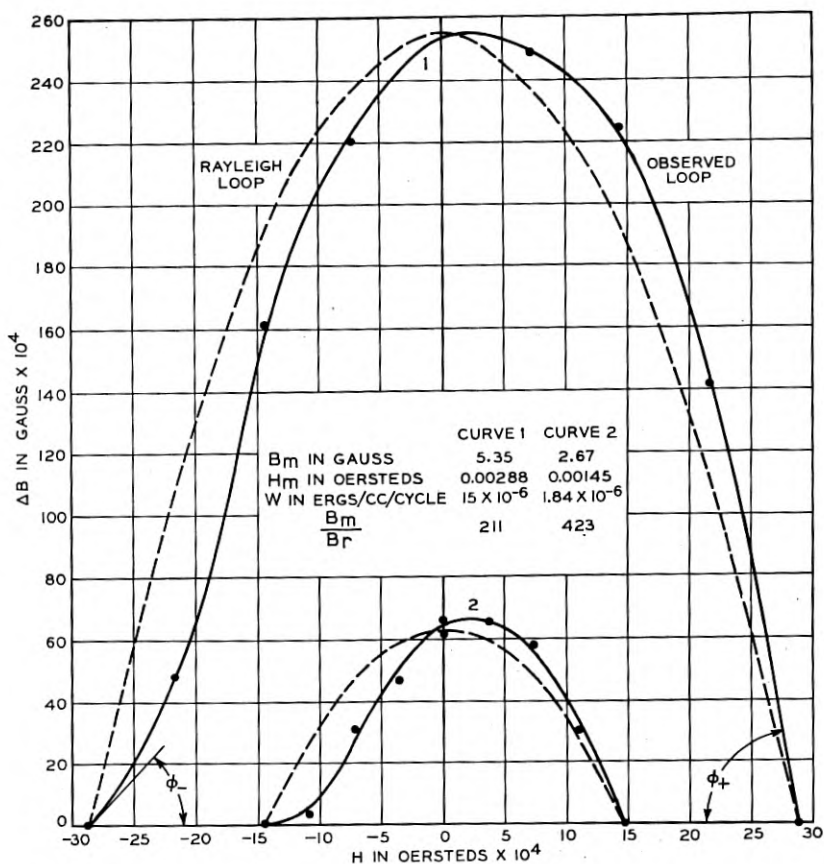
Fig. 3—Two hysteresis (half) loops plotted with reference to a straight line through their tips.

comparison, Rayleigh loops are shown as broken lines. By analysis of the interior angles ϕ_+ and ϕ_- between the ΔB vs. H curve and the H axis at points $+ H$ and $- H$ respectively, it is found that ϕ_+ is larger than for the Rayleigh loop, and is given by the relation tan $\phi_+ = \mu_0\lambda B_m$, while ϕ_- is a corresponding amount smaller than for

the Rayleigh loop. The hysteresis coefficient a and the permeability coefficient, λ are related by the equation $a = 8\lambda/3\mu$ for a loop having parabolic shape, in which case the interior angles are equal, and tan $\phi_{\pm} = \mu_0\lambda B_m$. Since the latter equation applies for ϕ_+ only, on the observed skewed loop, it follows that the Rayleigh relation between a and λ is more or less inaccurate. In fact, the ratio of $8\lambda/3\mu$ to a is a measure of the skewness of the loop. For the present material, this ratio is about 1.15. This result is in accord with our previous data, but was evidently not noted by Rayleigh because the free poles in his magnetic circuit tended to mask the asymmetry. The fact that these hysteresis loops are slightly skewed shows that those processes which produce the familiar S-shaped loop at high flux densities are already present at these low flux densities.

Despite a skewed shape, the area of the observed loop approximates closely the area of a parabola drawn through the remanence and the tips. Hence, supplementary values of energy loss W were obtained from remanence observations at several values of H_m, using the formula $W = 2B_r H_m/3\pi$. The slenderness factor of the loops may be measured by the ratio B_m/B_r, which varies from 211 to 890 for the different loops studied.

The a.-c. resistance introduced by the hysteresis loss of the core material yields the ratio $8\pi W/B_m^2$, as noted in Eq. (1). Values of this quantity computed from the areas of the loops of Fig. 3. and from remanence determinations are plotted in Fig. 4. They agree closely with the aB_m term of Eq. (1) obtained by a.-c. measurements, as shown by the solid line in Fig. 4. The sum of $c + aB_m$ is shown by the broken line. It is evident that the ballistic galvanometer gives no indication of residual loss.

It is interesting to note that the hysteresis loop at low flux densities can now be constructed in detail using the data obtained from a.-c. measurements. The remanence is $B_r = \frac{3}{16}a\mu_0 B_m^2$ and tan $\phi_+ = \mu_0\lambda B_m$. The angle included between the upper and lower branches of the loop at the tips is $(\phi_+ + \phi_-)$ and is given by the equation tan $[\frac{1}{2}(\phi_+ + \phi_-)] = \frac{3}{8}\mu^2_0 a B_m$.

A.–C. RESULTS

Values of R_f and L_f were measured as a function of the current at fixed frequencies. The values of $R_f/\mu_m f L_f$ are plotted in Fig. 5 as a function of current with frequency as a parameter. In order to shorten the vertical scale, the appropriate ordinates are indicated in connection with each line. These form a family of straight lines parallel to one another. This shows that the hysteresis coefficient is practically a

constant over the low flux density range for all frequencies. From the slope of these straight lines the hysteresis coefficient a of eq. (1) is calculated to be 2.6×10^{-6} which agrees with the value 2.53×10^{-6}
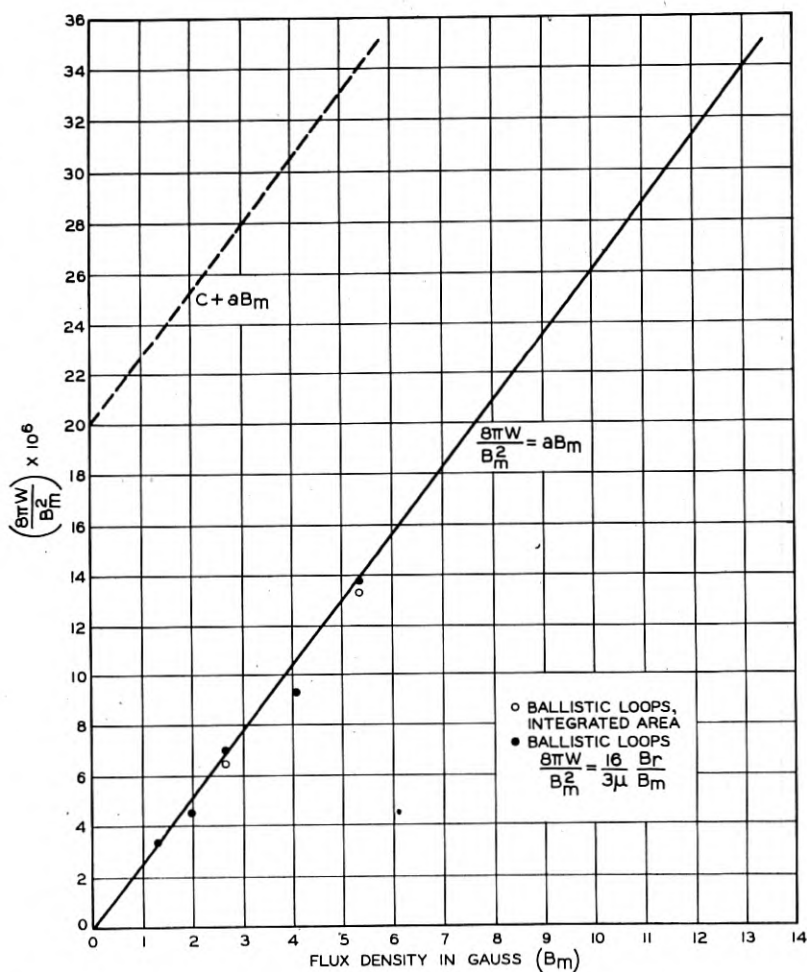

Fig. 4—Comparison of ballistic galvanometer and a.-c. determinations of hysteresis loss. Note absence of residual loss from ballistic observations.

computed from the ballistic tests. The divergence of the data from linearity at higher currents is shown by the dotted curves, which indicate divergence of the hysteresis loop from the Rayleigh form at higher flux densities.
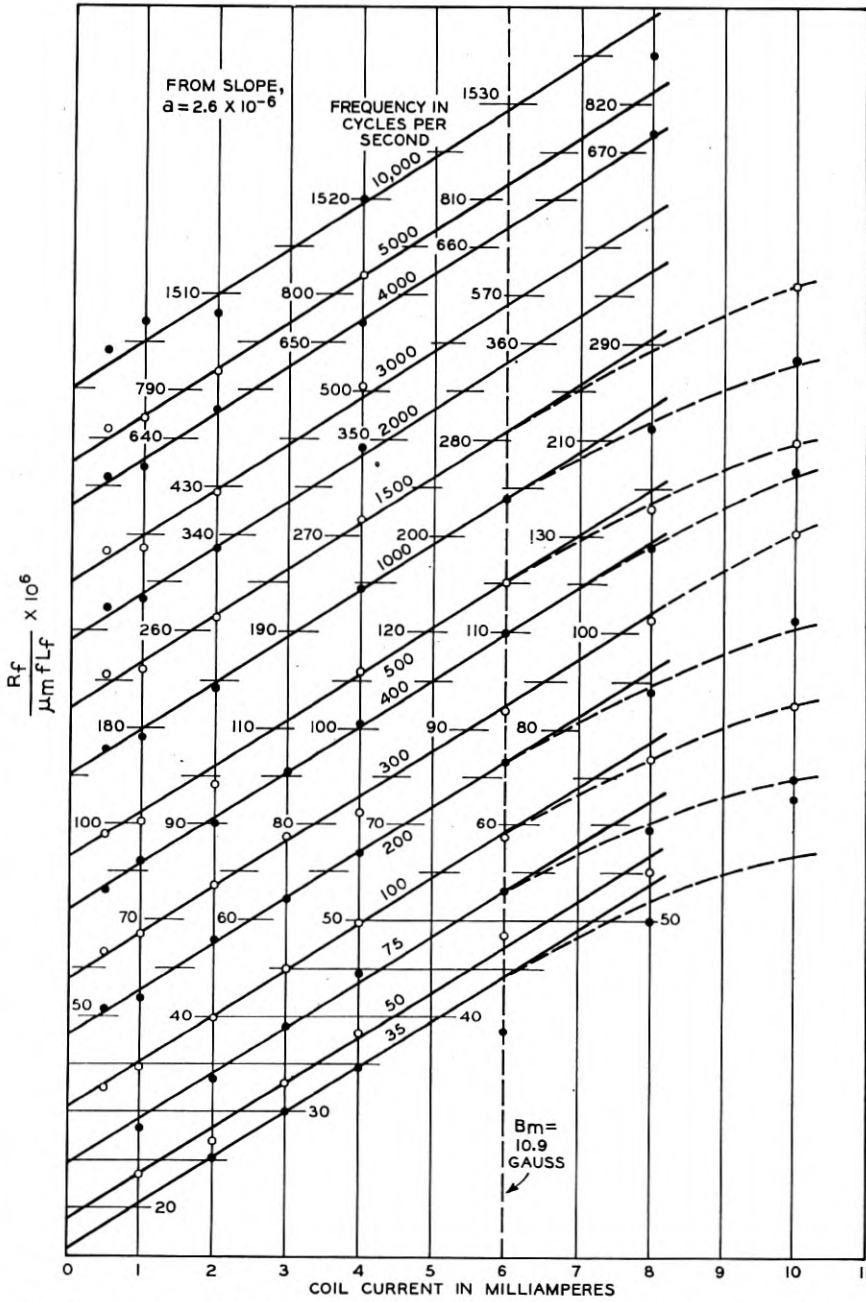
F IG. 5—A.-c. bridge values of $R_f/\mu_m f L_f$ vs. coil current of various frequencies. Slope of the straight parallel lines gives the hysteresis coefficient a.

Further information on hysteresis loss is obtained from measurements of harmonic voltages generated in the coil winding when there is current I_1 of frequency f. It has been shown [6] that the third harmonic voltage for materials with Rayleigh hysteresis loops is

$$E_3 = 0.6\, aB_m\mu_m L_m f I_1,$$

from which the hysteresis coefficient is

$$a = \frac{25\,E_3}{3\,fI_1^2}\sqrt{\frac{Ad \times 10^{-9}}{2\mu_m^3 L_m^3}}.$$

Measurements of third harmonic voltages have been made on the coil described in this paper by P. A. Reiling and the results are shown in Table II.

TABLE II

	I_1 m.a.	E_3 m.v.	$a \times 10^6$	f	I_1 m.a.	E_3 m.v.	$a \times 10^6$
1000	2.0	.0168	2.2	100	3.0	.00447	2.6
	5.0	.133	2.8		5.0	.0106	2.2
	10.0	.55	2.9		10.0	.0473	2.5
					16.8	.1497	2.8
400	1.41	.00335	2.2				
	2.0	.00709	2.3	75	8.0	.0199	2.2
	3.0	.0158	2.3		10.0	.0335	2.3
	5.0	.0457	2.4		18.2	.112	2.4
	10.0	.195	2.5				
				50	10.0	.0359	3.7

The values of a thus obtained show no consistent variation with current or frequency. They give an average value of 2.5×10^{-6}, which is in close agreement with the ballistic and a.-c. bridge results. It therefore appears that that part of the effective resistance which is proportional to current is identifiable with hysteresis loss as obtained by ballistic means, and with that which generates harmonic voltages.

The intercepts for $I = 0$ in Fig. 5 are therefore due to eddy current and any residual losses. They have been plotted against frequency in Fig. 6. The line through these points is generally assumed to be straight, and the eddy current and residual loss coefficients are derived from its slope and intercept. It appears, however, that this line is not strictly straight, but has a somewhat steeper slope at lower frequencies, so that the ordinary graphical method of loss separation fails.

An analytical separation of losses can be made for any frequency interval by returning to the values of $R_f/\mu_0 fL_f$ as obtained from Fig. 5,

[6] E. Peterson, Bell Syst. Tech. Jour., **7**, 762 (1928).

subtracting the value at f_1 from that at f_2 and dividing by the frequency interval $f_2 - f_1$ to give the eddy current coefficient e of equation (1).[7] Figure 6 gives e thus derived, as a function of f, showing a value approximately 20 per cent higher than calculated from the relation $e = 4\pi^3 t^2/3\rho$ at frequencies above 500 cycles, and progressively higher as the frequency approaches zero.

The fact that e is larger than predictable from classical theory has been ascribed to the presence of a low permeability surface skin on
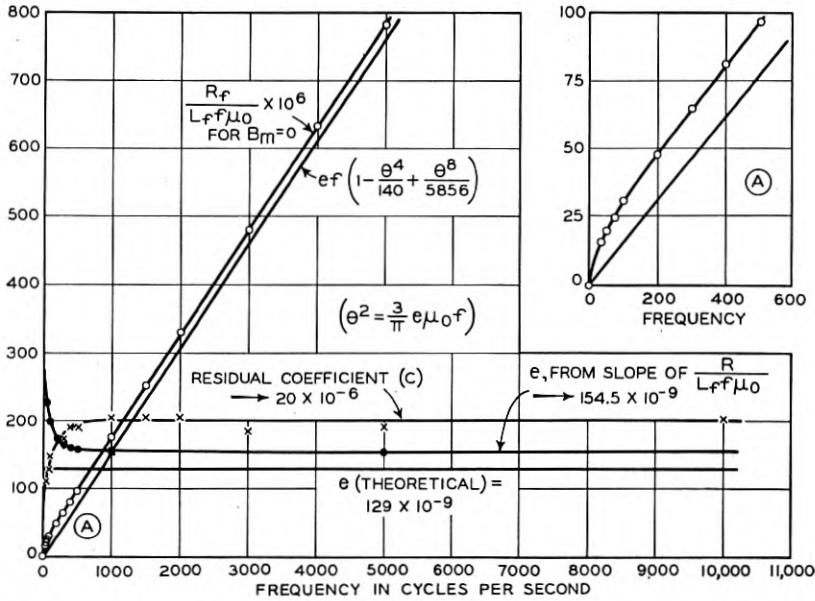

FIG. 6—Intercepts of Fig. 5 vs. frequency. Slope of the curve gives eddy current coefficient e. Residual loss coefficient c varies with frequency near $f=0$.

practically all materials which have been reduced to sheet or wire form by mechanical deformation.[8] But since the eddy current coefficient depends only on the resistivity and effective thickness of the material, any apparent variation of e with frequency can only be interpreted as an indication that the residual loss is varying with frequency.

Taking the value of $e = 154.5 \times 10^{-9}$ characteristic of the higher frequencies, the eddy current loss per cycle has been calculated, and is indicated in Fig. 6. The amount by which the observed loss exceeds

[7] Correction terms must be included at higher frequencies to take account of eddy current shielding as noted in ref. 2.

[8] E. Peterson and L. R. Wrathall, *I. R. E. Proc.*, **24**, 275 (1936).

the calculated eddy current loss gives the residual loss coefficient *c*. Thus, the value of *c* is found to be a constant 20×10^{-6} at frequencies above 500 cycles, but to decline toward zero as the frequency approaches zero, in evident accord with the ballistic galvanometer result.

The inductance due to the core shows a similar frequency effect. The observed inductances for the 20-turn winding are given in Fig. 7. The values at each frequency for the various currents fall on a straight
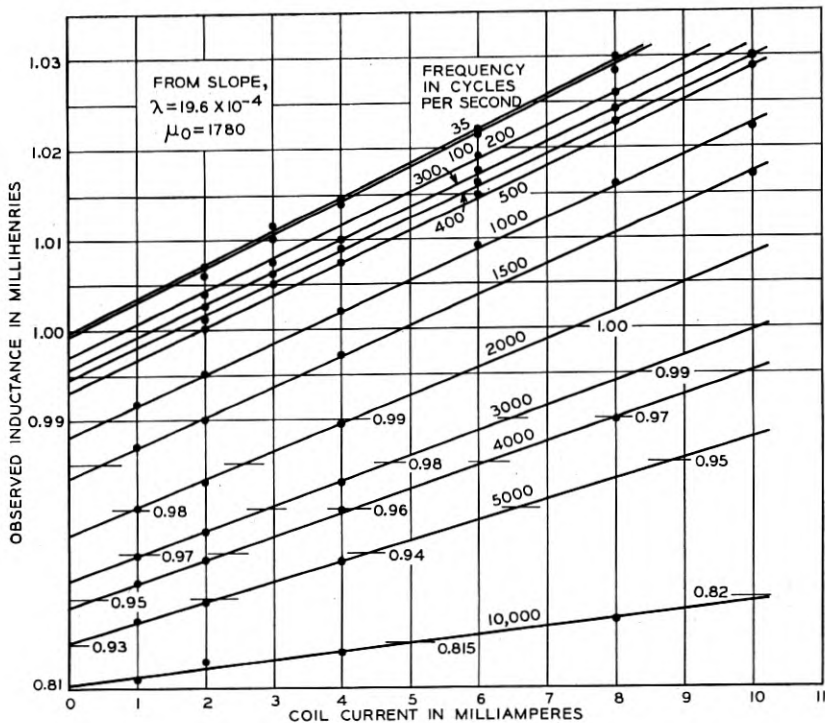

FIG. 7—Inductance observed on 20 turn coil, at various frequencies.

line, the slope of which gives the permeability coefficient, $\lambda = 19.6 \times 10^{-4}$, for the lower frequencies where eddy current shielding can be neglected.

The values of *L* for $I = 0$, obtained from Fig. 7, are plotted against frequency in Fig. 8. The most remarkable feature of this curve is the decline of inductance (or apparent permeability) of about 1 per cent at low frequencies, where very little decrease on account of eddy current shielding is to be expected. The characteristic shielding curve has been

computed using the value of e obtained from the resistance measurements in the relation

$$\frac{L}{L_0} = \frac{1}{\theta}\frac{\sinh\theta + \sin\theta}{\cosh\theta + \cos\theta} = \left(1 - \frac{\theta^4}{30} + \frac{\theta^8}{732} - \cdots\right),^{*}$$

where $\theta = \sqrt{3e\mu_0 f/\pi}$. Using the values of L/L_0 thus computed, the effect of eddy current shielding was eliminated from the observed values, and the results plotted in the upper curve in Fig. 8, showing a rapid
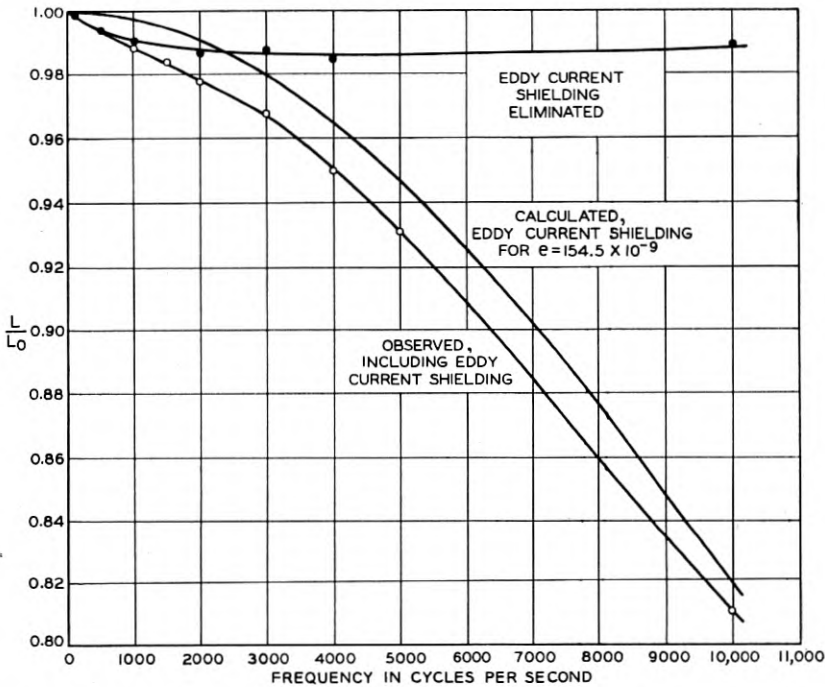

FIG. 8—L/L_0 from intercepts of Fig. 7. Observed values about 1 per cent lower than calculated for eddy current shielding.

decline of inductance or apparent permeability with increasing frequency at low frequencies, and the flattening off to a fairly constant value at higher frequencies.

The initial permeability thus obtained (average of results from the 20-turn and 60-turn windings) is 1780. This is somewhat lower than the value found by the ballistic galvanometer. The difference is due to magnetic aging which was observed to decrease the permeability of

* The series is inaccurate at frequencies above 5000 cycles.

the core at the rate of approximately 1 per cent per month. In contrast, no change of resistivity was detected in an accelerated aging test consisting of a bake at 100° C. for 150 hours.

DISCUSSION

The ballistic data on both the present annealed 35 permalloy sheet core and the previous compressed powdered iron core show that the area of the hysteresis loop varies as B_m^3 in agreement with Rayleigh's law. The magnitude of the loss is not given by the fractional slope λ of the μ,B line as required by Rayleigh's law because the loops are not parabolic in shape. This discrepancy gives a measure of the skewness of the hysteresis loop. The B_m^3 portion of the a.-c. data agrees with the loop areas obtained with the ballistic galvanometer. The threefold agreement between the ballistic data, the harmonic measurements, and the a.-c. resistance measurements indicates that the hysteresis loop is substantially unchanged in shape over a frequency range extending from 0 to 10,000 cycles.

Since the hysteresis loop has a size and shape independent of frequency, and area strictly proportional to B_m^3, it accounts for that part of the effective resistance of a coil on a ferromagnetic core which is proportional to the alternating magnetizing current. The remainder consists of eddy current and residual losses.

The ordinary graphical method of separating these losses is excluded by the obviously non-linear relation between $R_f/\mu_0 f L_f$ and f. Using an analytical method, the eddy current loss is found to be some 20 per cent larger than computed by classical theory, indicating the presence of low permeability surface layers on the sheet material. The residual loss coefficient is found to increase with frequency up to about 500 cycles, and to remain constant at higher frequencies (up to 10,000 cycles).

The observed inductance diminishes with increasing frequency about 1 per cent below the value calculated for eddy current shielding, the most noticeable decrease occurring below 1000 cycles where eddy current shielding is practically absent.

Various theories have been advanced to account for residual loss, as noted in a previous paper.[1] Goldschmidt[9] and Dannatt[10] have attributed the loss to non-homogeneous alloy structure, or preferred axes in such directions as to give a flux component perpendicular to the sheet surface, with accompanying eddy-currents unconstrained by the sheet thickness. This theory fails to account for residual losses in com-

[9] R. Goldschmidt, *Helv. Phys. Act.*, 9, 33 (1936).
[10] C. Dannatt, *I. E. E. J.*, 79, 667 (1936).

pressed powder cores, where eddy-currents are confined to single particles and cannot be increased by a modified direction of magnetic flux.

The most notable feature of residual loss is its large value for unannealed materials, and its extremely small values for well annealed alloys, particularly 78.5 permalloy and 45–25 Perminvar. (See Table I.) The permeability is increased by annealing while both c and a are decreased. On the other hand B_r is slightly increased. The decreases in hysteresis and residual loss are attributed to the decrease in work done against internal strains, which also tend to limit initial permeability.[11]

This suggests that residual loss may be due to elastic hysteresis or even simple mechanical friction, with magneto-striction providing the necessary coupling between the elastic or frictional variables and the magnetizing field, as pointed out in our previous paper.[1] Thus, in addition to losses from eddy-currents and magnetic hysteresis, mechanical work is done by the alternately expanding and contracting core— work expended on itself and its supports and insulation. Since the ballistic galvanometer measures only equilibrium values of B and H, this work is not revealed in the area of the ballistic loop. However, in the a.-c. loop the magnetostriction strains produce stresses too rapidly to be relieved, so that B lags behind H with an absorption of energy into the surroundings. This results in an additional effective resistance beyond that due to magnetic hysteresis and eddy-currents. For a sufficiently slow process in well annealed material supported with minimum constraint, the stresses may relieve themselves by thermal agitation and do very little work. But for sufficiently rapid traversals of the loop, all the magnetostrictive stresses will do the same amount of work on the core and its surroundings every cycle. Unannealed materials, or materials rigidly constrained, should continue to show residual loss at very low frequencies. The magnitude of c and its variation with frequency thus should depend on the magnetostrictive constant for the material, and on the types of dissipative constraints.

[11] R. M. Bozorth, *Elec. Eng.*, **54**, 1251 (1935).

Moisture in Textiles

By ALBERT C. WALKER

Evidence is presented that for a cotton hair structure of the specific type described, calculations are in such close agreement with many experimental data as to suggest the following tentative conclusions:

1. The moisture content necessary to form a monomolecular layer on all internal surface of the cotton hair appears to be slightly more than 1 per cent of the hair weight.

2. Less than half the internal surface, that termed fibril surface, appears to be involved in moisture adsorption which causes appreciable transverse swelling of the cotton hair. Upon this surface multimolecular chains of water seem to condense, the length of such chains increasing progressively up to saturation with corresponding increases in hair diameter throughout the whole of this range, each hydroxyl group in the cellulose surface being the base of a water chain, with separations between these chains along the surface corresponding to the arrangement of the hydroxyl groups on the cellulose surface.

3. Moisture adsorbed on surfaces within the cellulose aggregates composing the fibrils does not appear to be involved in transverse swelling, but may be responsible for the slight longitudinal swelling exhibited by cotton. The capacity of the cotton hair for this type of adsorption suggests that its locus is the ends of crystallites and therefore within the body of the fibrils. To account for the slight swelling, it is assumed that only a monomolecular layer can be adsorbed on these surfaces.

4. A theory is proposed to explain the dependence of the electrical properties of textiles upon their moisture adsorbing properties, and upon the surface distribution of moisture within the submicroscopic structure.

1. Introduction

A STUDY of the electrical properties of textiles and their dependence on atmospheric conditions and naturally-occurring impurities in the material has resulted in important economies and improvements in the use of textile insulation in the telephone industry. Recently, calculations have been made as to the moisture content and swelling of cotton at various equilibrium conditions, based on assumptions, first as to the structure of the cotton hair,* then as to the

---

* In keeping with recognized terminology, the individual cotton fiber is called a hair, suggestive of its morphological origin.

location and distribution of the internal surface upon which moisture might condense, and finally as to the manner in which moisture may be held upon this internal surface.

From this rather specific picture of the cotton hair structure it has been possible to calculate moisture contents and swelling properties
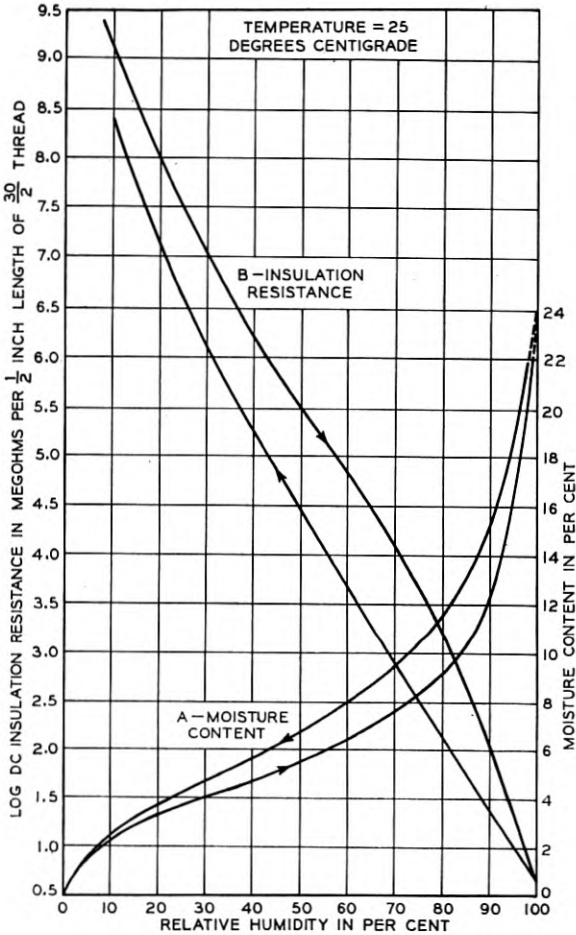

Fig. 1—Moisture sorption and electrical properties of raw cotton.

consistent with experimental data. It has been possible, also, to present a more comprehensive explanation of the change in the relations between electrical resistance and moisture content of cotton over the whole range of atmospheric humidity than that given in

previous publications from these Laboratories.* It is therefore con-
sidered that such a picture should contribute towards a better under-
standing of the moisture-sorbing † properties, not only of cotton, but
also of other similar fibrous materials, despite the hypothetical nature
of some of the assumptions upon which the calculations are based.
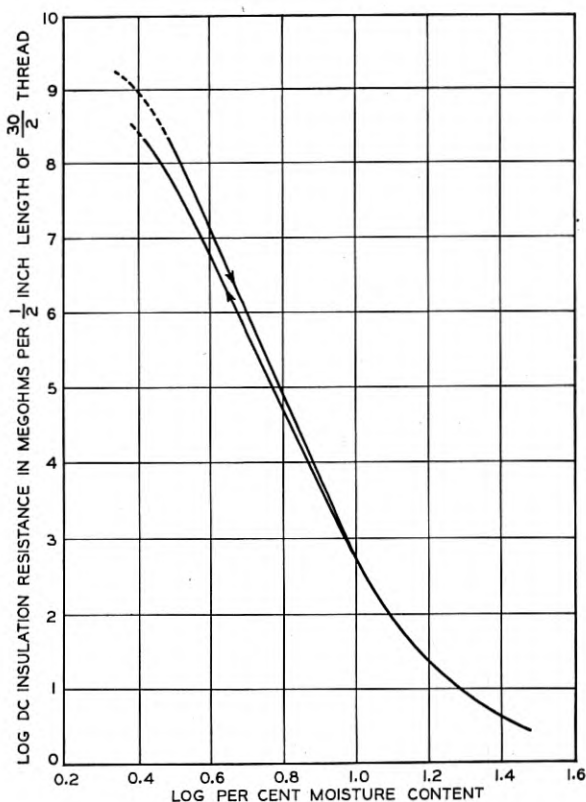

Fig. 2—Effect of previous history on resistance of raw cotton.

The electrical insulation resistance of textiles, when dry, is enormous
compared with the resistance observed under atmospheric conditions.
A change of but 1 per cent in atmospheric relative humidity (R. H.),
equivalent to between 0.1 per cent and 0.2 per cent change in moisture
content (M. C.), causes a change of about 25 per cent in resistance of

* See references 1 and 2 of the list with which this article concludes.
† "Adsorption" is here defined as the taking up of a gas or vapor by a solid,
"desorption" the giving up of a gas or vapor, and "sorption" the general process
without special indication of gain or loss. The use of these terms implies no as-
sumptions with regard to the mechanism of the processes they denote.

cotton. With silk the corresponding change in resistance is somewhat greater, and although silk sorbs materially more moisture than cotton at any equivalent atmospheric condition, it is much the better insulating material. Small amounts of naturally-occurring, water-soluble salts in cotton, such as NaCl and K_2SO_4, seriously impair the resistance of this textile. Traces of acids or alkalies left after degumming have a similar effect on silk. By washing these materials in water, their electrical properties are greatly improved.

Figure 1-*A* shows the familiar equilibrium relation between relative humidity and moisture content for cotton, including the hysteresis loop. A similar hysteresis characteristic, Fig. 1-*B*, in the relative humidity-resistance relation has been discussed in previous publications.[1,2] Figure 2 shows more clearly, as suggested by a comparison of the two types of curves in Fig. 1, that the resistance of cotton is critically dependent upon its moisture content. The curves in Fig. 2 show another important fact. The resistance of cotton may have, not one, but a *range* of resistance values for a single moisture content, depending upon the previous treatment or "history" of the sample.

This fact, which is one of great practical importance, is illustrated in Table I. Eleven samples of cotton, taken successively from the same spool, were dried to constant weight at 100° F., in a current of dry air, then equilibrated together under very carefully controlled conditions, first at 87.7 per cent R. H., then re-dried as before and re-equilibrated at 84.3 per cent R. H. several days later. The moisture contents of these samples were as follows:

TABLE I.

Sample No.	% Moisture Contents	
	at 87.5% R. H.	at 84.3% R. H.
1	10.95	10.1
2	10.8	10.0
3	10.7	9.9
4	10.8	9.8
5	11.1	10.2
6	11.0	9.9
7	11.8	10.8
8	10.7	10.1
9	10.85	9.8
10	11.0	10.0
11	10.7	9.9

The moisture contents of these samples showed small but definite differences, persisting even between tests several days apart. One of the samples had apparently been treated slightly differently from the others in preparation, since it preserved a marked difference in moisture content in both tests. Since a change of only 0.1 per cent in M. C.

may cause a change of about 10 per cent in resistance, these data are considered significant in such testing methods as are used for electrical textiles.

In a previous publication [2] a series of simple equations was formulated to show the quantitative relations between moisture content,
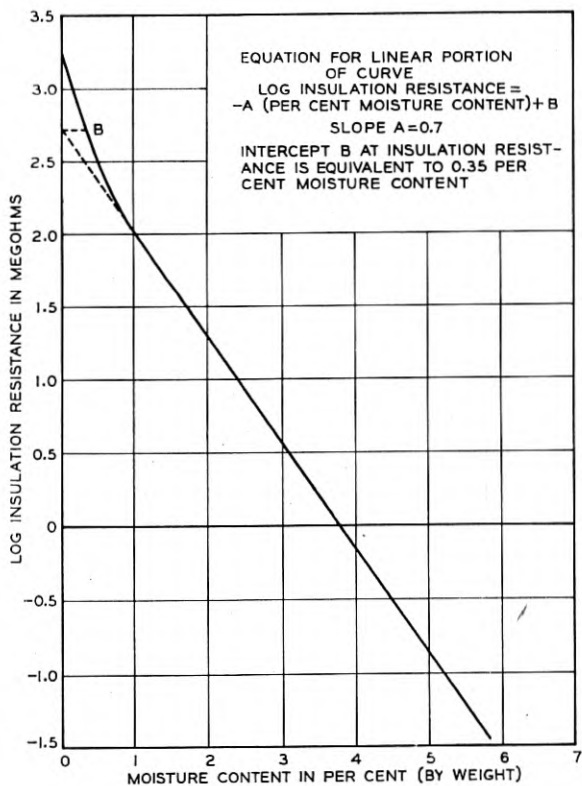

Fig. 3—Moisture content-resistance relation for rag paper.

relative humidity, and the resistance (Ω) of cotton:

$$\log \Omega = -A(\% \text{ M. C.}) + B, \tag{1}$$

$$\log \Omega = -a(\log \% \text{ M. C.}) + b, \tag{2}$$

$$\log \Omega = -\alpha(\% \text{ R. H.}) + \beta. \tag{3}$$

Equation 1 was considered as applying for moisture contents in the vicinity of 3 per cent, Equation 2 between 3 per cent and 10 per cent M. C., and Equation 3 from 10 per cent M. C. to saturation.

The ranges of application of Equations 2 and 3 are evident from Figs. 2 and 1-*B*, respectively; but since the resistivity of cotton becomes enormously high as the moisture content approaches zero, it has been difficult to verify the application of equation 1 below about 2 per cent. However, a recent study along somewhat different lines has provided us with information on this portion of the moisture content curve down to as low as 0.04 per cent M. C. It will be seen from Fig. 3 that equation 1 holds between 1 per cent and 6 per cent M. C. Below 1 per cent M. C., however, the resistance increases more rapidly with decreasing moisture content than is consistent with equation 1.

The data from which Fig. 3 was secured completes a chain of evidence upon which is based a theory of moisture adsorption which appears adequate to explain many properties of cotton. This theory involves, in addition to the data just discussed, a rather specific picture of the cotton hair structure.

2. Structure of the Cotton Fiber

According to Balls,[3] the cotton hair is formed by the outward extension of a single cell from the epidermis of the seed-coat; this extension, unaccompanied by any cell division may continue until the hair is 2000 times as long as it is broad. Up to about half maturity, the cell wall remains very thin but the hair attains most of its length; during the remaining half of the growth period (about one month) the wall thickens from the outside in until it appears to consist of about 30 to 35 concentric "growth rings" (see Fig. 4). Each growth ring consists, further, of parallel strands of fibrils, which run continuously in spiral form from end to end of the hair making one complete turn around the hair in about three diameters, and with periodic reversals in the direction of this spiral. Balls also suggests that side by side in each growth ring, there are about 100 fibrils, each separated from its neighbor by an air space. These fibrils are described by Balls as "dominoes" laid down one on top of the other in a pile-up of growth rings extending from the wall of the central canal or lumen to the outer wall of the fiber. Thus the front and back of each domino are growth ring boundaries, and each domino is separated from its neighbor by an air space. There are also air spaces between each domino in a growth ring. These air spaces are identified as the so-called pits in the wall structure. They are visible under a microscope, and appear to extend from the outer surface of the cotton hair down to the lumen. These air spaces are far larger in magnitude than those separating the front and back of each domino. Only by swelling the fiber in

(a) CROSS SECTION

SLIP SPIRAL
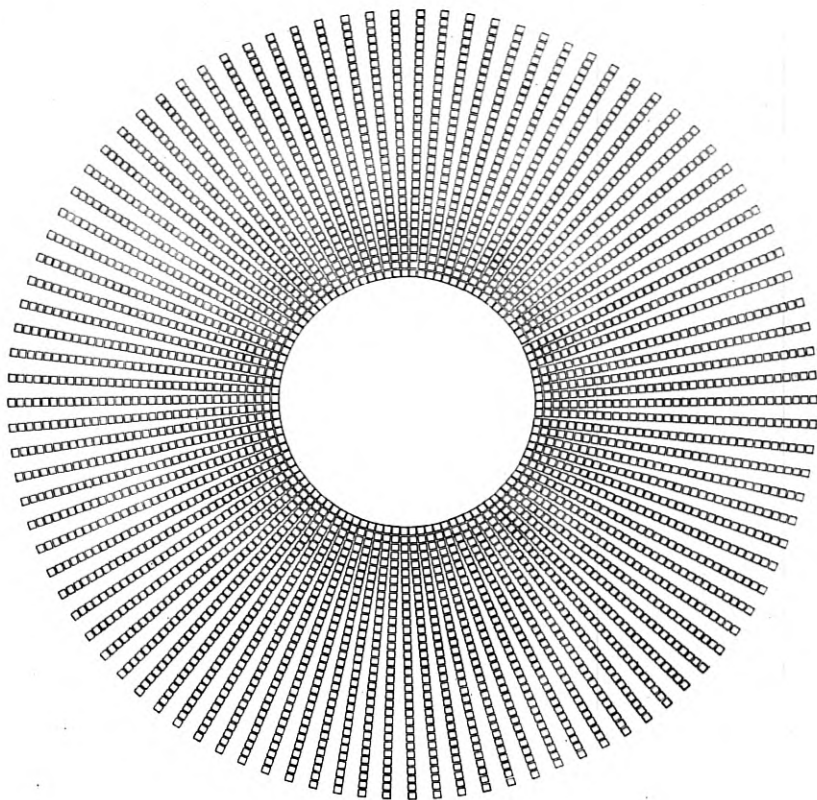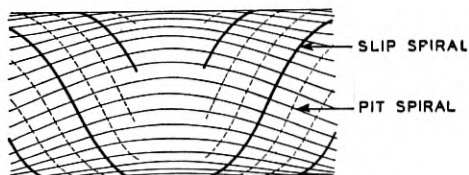
PIT SPIRAL

(b) SIDE VIEW SHOWING PIT SPIRAL REVERSALS

Fig. 4—The fiber structure of cellulose.

(a) An idealized cross-section of the cotton hair. The domino-like blocks shown in cross-section are arranged according to Ball's conception.

(b) The spiral arrangement of these domino-like blocks or fibrils is shown, together with the separating pits in the wall, and the slip-spiral effect along the fibrils.

Obviously these conventional type figures do not represent the true shape of the cotton of commerce, but they approximate the shape during the growth period, before the boll is opened. As the hair dries out, the central lumen collapses and the hair twists.

caustic soda can a differentiation be detected in the cross-sectional structure of the fiber to indicate this growth-ring character. Thus the fibrils are considered as being separated by air spaces on all sides, the whole cotton hair is spongy, and the surfaces of cellulose bounding these air spaces are internal surfaces of the fiber.

Slip spirals are visible in the hair surface at high magnification. Though decidedly irregular, they appear to cross the pits at approximately right angles, suggesting that there are additional internal surfaces at these points.

Cellulose from all sources appears to consist of definitely arranged crystallites or micellae.* Haworth [9] suggested that cellulose is composed of an elementary group consisting of two $C_6H_{10}O_5$ units, called cellobiose (Fig. 5-*A*). Figure 5-*B* indicates how these cellobiose units are joined together end to end to provide the fibrous structure of native cellulose.
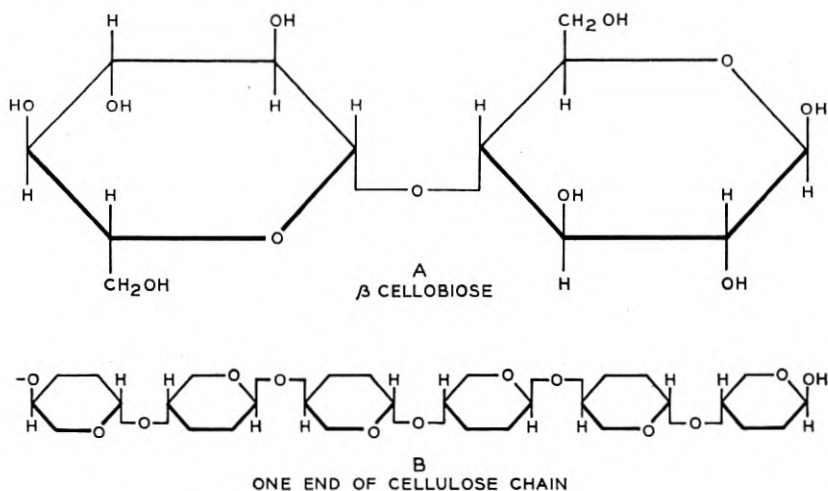

Fig. 5—Molecular structure of cellulose.

Diffraction and chemical evidence indicate that the cellobiose units are arranged parallel to the *b*-axis of the unit cell, with one cellobiose group at each common edge of adjacent cells and one through the center of each cell. These form long primary valence chains arranged parallel to the fiber axis and are held together laterally by cohesive forces. Figure 6 shows this conception of the unit cell as given by Meyer and Mark.[5]

* Sponsler and Dore,[4] Meyer and Mark,[5] Freudenberg,[6] Herzog,[7] Polanyi.[8]

3. Moisture Adsorption on Fibril Surfaces

It appears reasonable to assume that moisture will first adsorb on dry cotton on the outer surface of the hair, and by diffusion in the vapor state will penetrate into the pits and adsorb on the pit walls. Since cotton swells appreciably in a transverse direction, but hardly at all lengthwise, it is further assumed that moisture in the pits will next penetrate between the fibrils which are contiguous to one another in the radial direction. At equilibrium with any humidity below that required to form a monomolecular layer, it is assumed that the water molecules will be distributed at random on active points over all of the internal surface. For humidities above this value, polymolecular chains of uniform thickness are assumed to adsorb at active points on the fibril surfaces only, since moisture on the growth ring surfaces of these fibrils appears to be responsible for the transverse swelling of the cotton.

The equilibrium moisture content of cotton is reduced if the hydroxyl groups on the cellulose molecules are acetylated or otherwise esterified. Consequently it seems reasonable to assume that each water molecule adsorbed on the cellulose surface is held by a force originating in the oxygen atom of a surface hydroxyl group. As may be seen from Fig. 5-*A*, there are six hydroxyl groups per cellobiose unit, and the percentage moisture equivalent to a monomolecular layer covering the surface of the fibril structure with each water molecule satisfying forces of a surface hydroxyl oxygen will now be estimated.

The fibril cross-section is estimated to be 1240×1300 AU, based on average dimensions of the cotton hair.* Assuming the cellobiose units arranged with the *a*-axis parallel to the fibril width (Fig. 6), there will be $1240/8.3 = 150$ unit cells across the fibril, and $1300/7.9 = 165$ unit cells down through the fibril. Therefore the total number of oxygen atoms per unit cell length in the four fibril surfaces is:

$$6 \times 150 \times 2 + 6 \times 165 \times 2 = 3780.$$

From this the moisture content equivalent to a monomolecular layer is:

$$\frac{3780}{2 \times 150 \times 165} \times \frac{18}{324} \times 100 = 0.42\%.\dagger$$

* The considerations upon which these and subsequent calculations are based are given in detail in separate publications which will appear in the April and May issues of *Textile Research*.

† The Angström unit AU is 10^{-8} cm. From Fig. 6 it appears that only the equivalent of one cellobiose unit may be available for surface adsorption per unit cell in the fibril surface. Furthermore, since molecules in solid or liquid surfaces are subject to unbalanced forces (surface tension) it is assumed that all surface cellobiose units are so oriented that all 6 hydroxyl groups have surface forces capable of adsorbing water molecules.
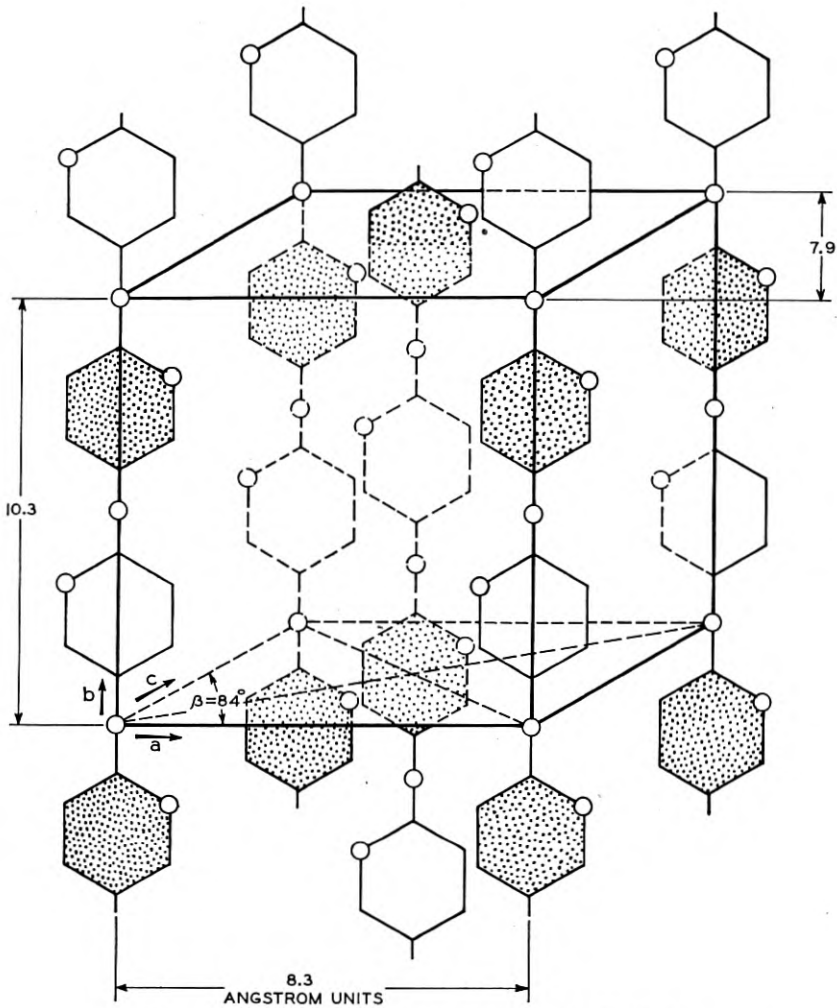
Fig. 6—The cellulose unit cell or crystallite structure.

4. Hair Swelling due to Fibril Surface Moisture

The diameter of the water molecule is reported as 3.8 AU. The surfaces of adjacent fibrils along growth ring boundaries must be separated at least $2 \times 3.8 = 7.6$ AU when a monomolecular layer of water is present on each contiguous surface. This corresponds to a total increase in hair diameter of $33 \times 2 \times 7.6 = 500$ AU. The percentage diameter increase in the hair is:

$$(500/125000) \times 100 = 0.4\%.$$

where 125000 AU is taken as the mean diameter of the dry cotton hair.

According to Collins,[10] the coefficient of hair diameter increase with humidity is about 0.11 per cent per 1 per cent R. H.   Therefore, an increase of 0.4 per cent in hair diameter is found at 0.4/.11 = 3.6 per cent R. H.   From adsorption data (Fig. 7) by Urquhart and Williams,[11] this relative humidity corresponds to between 1.1 per cent and 1.2 per cent moisture content.   The difference in this value and that
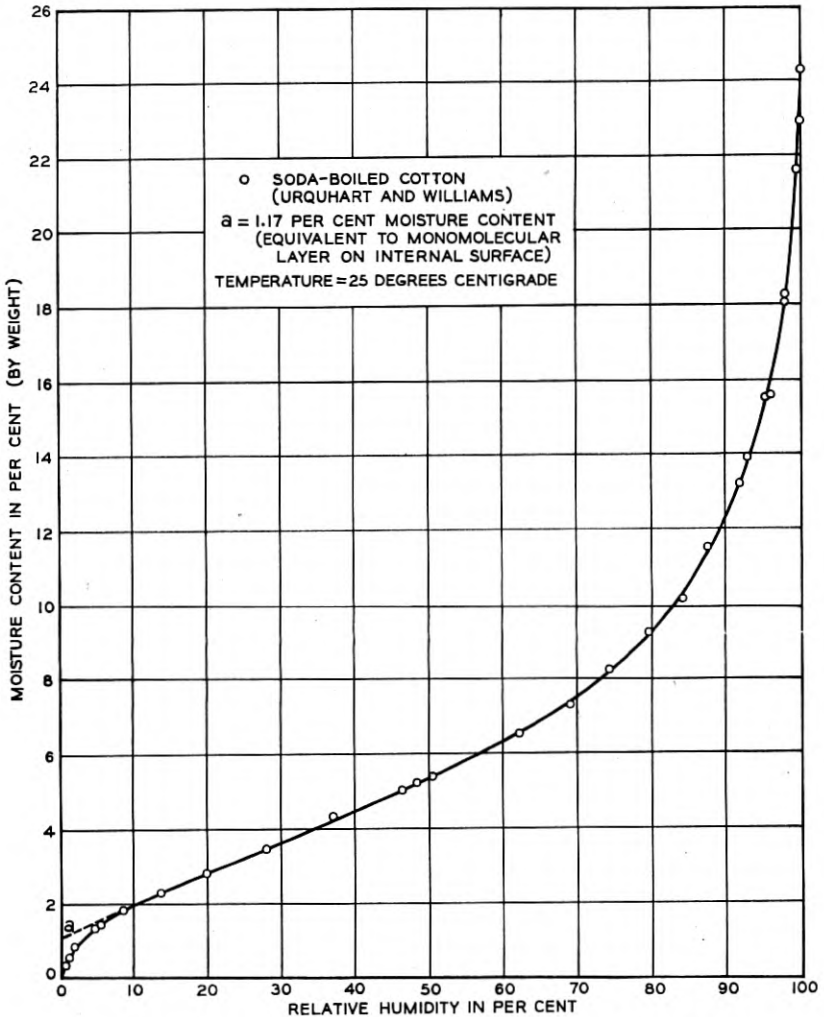

Fig. 7—Moisture adsorption-humidity relation for cotton at 25° C.

calculated under Section 3 is between 0.7 per cent and 0.8 per cent, suggesting that there is additional internal surface within the hair structure upon which moisture may be held without manifesting itself by an increase in diameter. This suggestion appears to be confirmed by quite different considerations.

Brunauer and Emmett[12, 13] consider it likely that the linear portion of van der Waals adsorption isotherms for nitrogen on the surface of ammonia catalysts indicates the building up of additional layers of adsorbed molecules. They state that extrapolation of this linear portion to zero pressure indicates the amount of gas needed to form a monomolecular layer upon this surface. Between 3 per cent and 50 per cent relative humidity the adsorption isotherm for cotton in Fig. 7 is very nearly linear. Applying this method to cotton the intercept (a) has values between 1.4 per cent and 0.35 per cent, depending on temperature. The average value is about 1 per cent being of the same order as that estimated from swelling data.

Since the estimated moisture content equivalent to a monomolecular layer on the internal surface of the cotton hair is so nearly the same when determined by two independent methods, it seems reasonable to postulate an additional internal surface in the cotton hair, amounting in extent to somewhat more than that corresponding to the fibril surfaces.

Slip spirals along the hair, crossing the pits at approximately right angles (see (b) of Fig. 4) suggest that there are discontinuities in the length of the fibril structure, hence further internal surface. Since the additional internal surface suggested by the preceding calculations and estimates does not appear to be involved in the transverse swelling of the cotton hair, it is suggested that this may be held upon the ends of crystallites or micellae which compose the fibril structure.

It is considered of much less importance to pursue the detailed calculations of this possibility than it is to point out that some such distribution of surface within the body of the fibril structure may be involved in adsorption of a small amount of moisture, and this picture is of material value in accounting for some of the properties of cotton.

5. MULTIMOLECULAR LAYERS

It is further assumed that above 1.5 per cent moisture content, addition of moisture simply increases the thickness of the moisture layer upon the surfaces of the fibrils. The thickness (n) of the moisture layer on each fibril, expressed in number of water molecules, and the percentage moisture content at 50 per cent R. H. may readily be obtained. At 50 per cent R. H. the hair diameter increase is 5 per cent
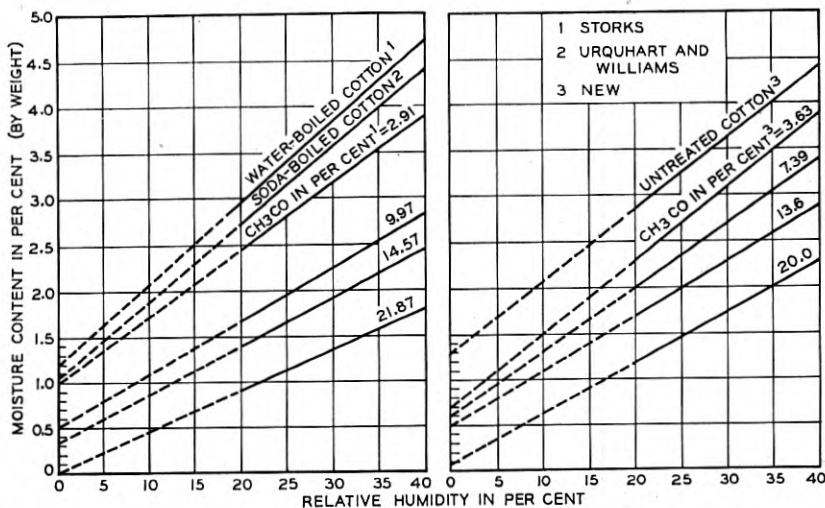
Fig. 8—Moisture adsorption intercepts for acetylated cottons indicating amounts of internal surface.

8. Theory of Conduction of Electricity Through Cotton

It now appears possible to provide a more comprehensive theory for the conduction of electrical current through the moisture paths in a textile than has been suggested previously.[1,2]

Below 1 per cent moisture content it is likely that equation 1 fails to hold, due to obvious discontinuities in the moisture paths over surfaces containing less than a monomolecular layer of water.* Above 1 per cent, it is not to be concluded, however, that a continuous moisture film exists. It appears that some space is still available between certain water molecules, and the space pattern of water distribution is determined by the type of solid surface and the arrangement of active points or zones upon which each water molecule is held. In the case of cotton, such active points are considered to be hydroxyl groups; for silk they may be amino or carboxyl groups or both, and from Astbury's discussion [16] of the chain structure of these two materials it seems likely that their space patterns for moisture adsorption are different. Furthermore, it is assumed that each of these active points may be anchorage not only for a single water molecule, but for a chain of such molecules, the length of the chain being deter-

* It is of interest to note that if the linear portion of the curve shown on Fig. 3 is extrapolated to the insulation resistance axis, the insulation resistance corresponding to this intercept is found at 0.3 per cent M. C. (see a—Fig. 3), this being of the same order of magnitude as that estimated to cover fibril surfaces with a monomolecular layer, suggesting that the linear portion of the curve is specifically related to moisture adsorption on the fibril surfaces.

mined by the relative humidity. This conception is much like the picture of acid or oil molecules standing as a film on a water surface, with the polar end in the water.

Some such function as equation 1 may apply since simply increasing the length of the water chains will not cause a proportionate decrease in the resistance. It seems evident from Fig. 5-*a* that small increments of water might be expected to sufficiently lengthen water chains of minimum separation so as to establish contacts between them along the current path, but that larger increments of water are necessary to accomplish the same result between more widely separated anchorage points. This would explain the gradual change from the relation of equation 1 at low moisture contents to equation 2 at intermediate moisture contents. At some point along the humidity curve it is conceivable that capillary condensation occurs in the pits so that at progressively higher humidities the increasing cross-section of these pits plays a more important part in current conduction than the adsorbed chains of water molecules. This may explain why equation 3 is found to apply at highest humidities.

Adsorption, however, appears to continue throughout the whole of the humidity range, consistent with the hair swelling relations. Thus it is shown that adsorption and capillary condensation need not be considered separately but may go along together with a gradual shifting in importance from one to the other in the current conduction process.

Evershed [17] explained the decrease in resistance of a textile with increasing applied potential as being due to elongation of pools of water in the material under electrical stress forming more continuous current paths. This deviation from Ohm's law may be explained also as being due to the influence of increasing electrical stress upon the oscillation of the free ends of moisture chains, bringing more of them into orderly alignment along the line of applied potential, and establishing shorter current paths through the structure.

The difference in electrical behavior of different textile fibers may be illustrated by a comparison of the adsorption of moisture on cotton and silk surfaces. From Astbury's pictures of the structure of protein molecules as compared with cellulose molecules it appears that although there may be more points per unit surface for moisture to condense upon on protein surface, there are also possibilities of separation of adjacent moisture chains in a manner similar to that discussed for cellulose, and furthermore, there appear to be side chains of hydrocarbons interspersed in the protein chain which may act as barriers to the ready contact of adsorbed water chains on either side

of these hydrocarbon chains. This may explain why silk has a higher resistance than cotton for a given moisture content. It might be expected that silk, due to these hydrocarbon barriers in the current path might also have a higher dielectric breakdown under potential stress.


TAN ψ = APPARENT POWER FACTOR
TAN ψ_r = ABSORPTION COMPONENT
TAN ψ_i = CONDUCTION COMPONENT
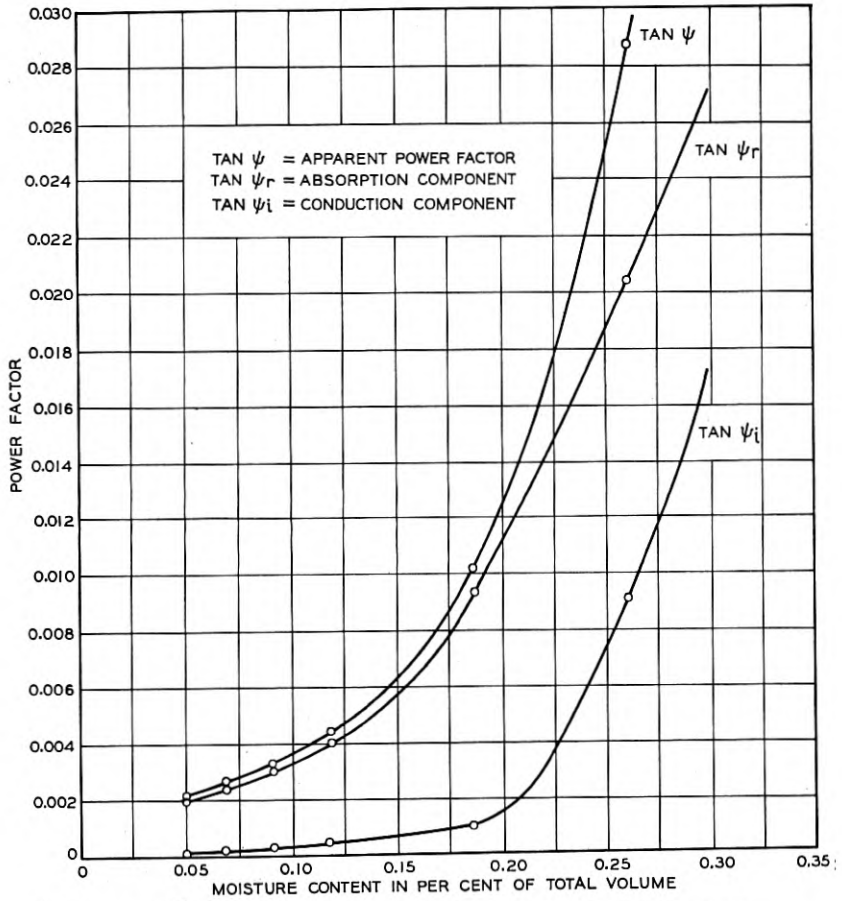
Fig. 9—Relation between power factor components of cable paper and moisture content.

Whitehead,[18] in a study of the effects of moisture on power cable paper insulation, obtained data on the change of power factor with increasing moisture content. Figure 9 shows this relation. It will be noted that the conduction component (tan ψ_i) of the power factor rises sharply as the moisture content of the paper exceeds 0.2 per cent

by volume (about 0.3 per cent by weight). This increase occurs in the range consistent with the completion of the monomolecular layer of moisture on the internal surface of the material, particularly since the internal surface of paper and cotton appears to be of the same order of magnitude.

9. GENERAL DISCUSSION OF THEORY

Peirce [19] proposed a two-phase theory for the adsorption of moisture by cotton, based upon the facts that a small quantity of water is adsorbed by dry cotton very much more rapidly than the same amount added to cotton with a moderate water content, that it has much greater effect on the elastic properties, evolves more heat, and is more difficult to remove. He regards the moisture attached to the hydroxyl points as in phase (a) while that in phase (b) consists of an indefinite number of molecules adsorbed in a looser fashion over all available surfaces, limited only by the conditions of space and of equilibrium with the external concentration of aqueous vapor.

The differentiation between fibril and other internal surfaces is considered as giving a more definite explanation of such two-phase adsorption than that proposed by Peirce. The (a) phase may be pictured as moisture added to the active hydroxyls which lie on the fibril surfaces where such surfaces are readily available for moisture adsorption, while the (b) phase is associated with a definite number of active hydroxyls but within the body of the fibrils and therefore less accessible than those on the surface. As has been pointed out, it is quantitatively reasonable to suppose these available internal hydroxyls to be located at the ends of the crystallites.

According to the cotton hair structure presented in this paper, there is actually more than twice as much internal surface available for moisture adsorption from the dry state as there is in cotton already in equilibrium with a 1 per cent moisture content. The slow diffusion of moisture to those surfaces most deeply buried in the fibrils may account for the fact that while cotton very nearly reaches equilibrium with any given humidity in a relatively few minutes, the final establishment of equilibrium conditions, involving a change of less than 1 per cent in moisture content, may take more than 24 hours. The first water molecule to attach itself to an active hydroxyl might be expected to evolve more heat than subsequent molecules in the chain since the interaction is between water and cellulose hydroxyls, not between water and water. Also, water held within the fibril structure no doubt is the most difficult to remove since it must diffuse out through this fibril structure.

This picture of moisture adsorption seems to provide a reasonable explanation for a variety of practical problems.

Thus it is known that if fibrous materials, such as wood, paper or fiber board are dried below a certain critical moisture content, permanent changes may be expected in the structure; even serious damage may result from too thorough drying at low temperatures. It seems evident that when the moisture content of such more or less dense structures is reduced to a point where the outer layers have less than 1 per cent of moisture, the internal surfaces of these layers may begin to lose the monomolecular layer of water. The valence forces of surface hydroxyl groups are now no longer satisfied by water molecules, so that such hydroxyls on contiguous surfaces may stick together. On readsorption of moisture, portions of these surfaces may be so permanently attached to one another that swelling will no longer occur in just the same way as originally, and cracking and warping may result.

BIBLIOGRAPHY

1. Murphy and Walker, *Jour. Phys. Chem. 32*, 1761 (1928).
2. Walker, *Jour. Text. Inst. 24*, T145 (1933); also *Bell Sys. Tech. Jour. 12*, 431 (1933).
3. Balls, "Studies of Quality in Cotton," Macmillan & Co., p. 24 (1928); also *Egyptian Cotton Supplement, 14*, 10 (1927).
4. Sponsler and Dore, Colloid Symposium Monograph, *4*, 174 (1926).
5. Meyer and Mark, *Ber. Deut. Chem. Gesell. 61*, 593–614 (1928); also "Der Aufbau Der Hochpolymeren Organischen Naturstoffe auf Grund Molekular-Morphologischer Betrachtungen," Leipzig (1930).
6. Freudenberg, *Ber. 54*, 764 (1921).
7. Herzog, *Ztschr. Phys. Chem.* (A) *139*, 235 (1928).
8. Polanyi, *Ztschr. Phys. 7*, 149 (1921).
9. Haworth, *Nature*, p. 430, Sept. 19, 1925; also *Jour. Soc. Dyers and Colourists, Jubilee Issue*, 1884–1934, 16–23.
10. Collins, *Jour. Text. Inst. 21*, T313 (1930).
11. Urquhart and Williams, *Jour. Text. Inst. 15*, T559 (1924).
12. Brunauer and Emmett, *Jour. Amer. Chem. Soc. 57*, 1754 (1935).
13. Emmett and Brunauer, *ibid. 57*, 2732 (1935).
14. Coward and Spencer, *Jour. Text. Inst. 14*, T30 (1923).
15. New, *Electrical Communication, 13*, 216–225, 370 (1935).
16. Astbury, "Fundamentals of Fiber Structure," pp. 50 and 96, Oxford Press (1933).
17. Evershed, *Jour. Inst. Elec. Engrs.* (London), *52*, 51 (1914).
18. Whitehead, "Impregnated Paper Insulation," J. Wiley & Sons, p. 31 (1935).
19. Peirce, *Jour. Text. Inst. 20*, T133 (1929).

Abstracts of Technical Articles from Bell System Sources

Determination of Ferromagnetic Anisotropy in Single Crystals and in Polycrystalline Sheets.[1] R. M. BOZORTH. Following the work of Akulov and of Heisenberg on the magnetic anisotropy of cubic crystals, it is shown that by taking account of an additional term in the expression for the energy of magnetization the [110] direction may under certain conditions be the direction for easiest magnetization in a crystal, instead of [100] or [111] as given by previous theory. This is in accord with experiment. Magnetization curves for single crystals are calculated using the additional term and some peculiarities are recorded. The anisotropy constant appropriate for a single crystal (of iron) has been calculated from measurements on hard-rolled sheet in which there is preferred orientation of the crystals.

Impact Bend Testing of Wire.[2] W. J. FARMER and D. A. S. HALE. This paper comprises a discussion of a machine designed to make rapid determination of the ability of wire to resist permanent deformation by bending.

Two types of machine used in the industry for wire bend testing are described and their features discussed with regard to their suitability for use as standard test methods.

A bend tester operated by the impact of a pendulum has been developed by the Bell Telephone Laboratories in collaboration with Subcommittee IV on Mechanical Tests of the Society's Committee B–4 on Electrical-Heating, Electrical-Resistance and Electric-Furnace Alloys. Results of typical tests with this machine are given, together with information gathered from ultra-rapid motion pictures taken of the machine in operation.

It is concluded that the impact bending machine described offers a simple, rapid and accurate means of measuring the bending properties of wire and that the information acquired from the test is directly applicable to design problems.

Positions of Stimulation in the Cochlea by Pure Tones.[3] JOHN C. STEINBERG. The relation between tone frequency and position of

[1] *Phys. Rev.*, December 1, 1936.
[2] *Proc. 39th Ann. Mtg. Amer. Soc. for Testing Materials*, Vol. 36, 1936—Part II, Technical Papers.
[3] *Jour. Acous. Soc. Amer.*, January, 1937.

stimulation on the basilar membrane has been calculated from data on differential pitch sensitivity. The calculations involve assumptions concerning the choice of the upper and lower pitch limits of hearing and the choice of tone levels which should be used in obtaining differential pitch sensitivity data. It is shown that for quite different assumptions the positions of stimulation for tones in the range from 500 to 10,000 cycles are not greatly affected. Outside this range the positions depend on the assumptions. The calculated positions for tones of 1000, 2000 and 4000 cycles fall, respectively, at points on the membrane about $\frac{1}{3}$, $\frac{1}{2}$ and $\frac{2}{3}$ of its length away from the helicotrema. The calculated positions are compared with positions obtained from post-mortem studies of human cochlea and with positions obtained from electric response measurements on the cochlea of anesthetized guinea pigs. The differences between various methods for the most part are no larger than calculated differences between observers.

Some Uses of the Torque Magnetometer.[4] H. J. WILLIAMS. The history of torque measurement as an index of ferromagnetic anisotropy is outlined. A simple magnetometer for torque measurement is described in detail and uses for the instrument are discussed. These include the measurement of anisotropy constants, coercive force, complete magnetization curves for single directions, and rotational hysteresis losses. With auxiliary ballistic measurement residual inductions and demagnetizing factors are obtainable.

[4] *Rev. Scientific Instruments*, February, 1937.

Contributors to this Issue

EDWIN H. COLPITTS, who has recently retired as Executive Vice President of the Bell Telephone Laboratories, scarcely needs an introduction. In 1899 he left Harvard to begin his career of research and development in the Bell System. In 1907, when development work was transferred from Boston to the Engineering Department of the Western Electric Company in New York, he also transferred and headed the Physical Laboratory. Later, with the formation of a Research Department, he became its head. In 1933, preliminary to the consolidation of the Department of Development and Research of the American Telephone and Telegraph Company with the Laboratories, Dr. Colpitts was appointed Executive Vice President.

W. B. ELLWOOD, A.B., University of Missouri, 1924; M.A., Columbia University, 1926; Ph.D., Columbia University, 1933. Bell Telephone Laboratories, 1930–. Dr. Ellwood has been engaged in various investigations relating to magnetic materials and measurements.

C. N. HICKMAN, A.B., Winona College, 1914; M.A., Clark University, 1917; Ph.D., Clark University, 1922. Physicist, Bureau of Standards, 1919–22; Physicist, U. S. Navy Yard, 1922–24; Research Physicist, American Piano Company, 1924–30; Bell Telephone Laboratories, 1930–. Since 1930 Dr. Hickman has been engaged in the development of special acoustical instruments.

C. M. HILL, B.S. in Chemistry, Princeton University. American Telephone and Telegraph Company, Long Lines Department, 1929–30; Bell Telephone Laboratories, 1930–. Mr. Hill's work has been on the biometrical problems of wood preservation.

VICTOR E. LEGG, B.A., 1920, M.S., 1922, University of Michigan. Research Department, Detroit Edison Company, 1920–21; Bell Telephone Laboratories, 1922–. Mr. Legg has been engaged in the development of magnetic materials and in their applications, particularly for the continuous loading of cables, and for compressed dust cores.

JOHN LEUTRITZ, B.S. in Chemistry, Bowdoin College, 1929; A.M. in Botany, Columbia University, 1934. U. S. Navy, Medical Corps, 1921–25. Bell Telephone Laboratories, 1929–. Mr. Leutritz' interest has been along biological lines, primarily in respect to wood preservation.

E. L. NORTON, S.B. in Electrical Engineering, Massachusetts Institute of Technology, 1922; M.A., Columbia University, 1925. Western Electric Company, Engineering Department, 1922–25; Bell Telephone Laboratories, 1925–. Mr. Norton has been engaged in the study of network and transmission problems. His present work is in connection with signaling circuits and apparatus.

TODOS M. ODARENKO, University of Technique in Prague, E.E., 1928. New York Telephone Company, 1928–30; Bell Telephone Laboratories, 1930–. Mr. Odarenko has been engaged in the measurement and study of transmission characteristics of existing and newly developed types of transmission lines.

S. A. SCHELKUNOFF, B.A., M.A. in Mathematics, The State College of Washington, 1923; Ph.D. in Mathematics, Columbia University, 1928. Engineering Department, Western Electric Company, 1923–25; Bell Telephone Laboratories, 1925–26. Department of Mathematics, State College of Washington, 1926–29. Bell Telephone Laboratories, 1929–. Dr. Schelkunoff has been engaged in mathematical research, especially in the field of electromagnetic theory.

ALBERT C. WALKER, B.S., Massachusetts Institute of Technology, 1918; Ph.D., Yale University, 1923. Bell Telephone Laboratories, 1923–. Dr. Walker has been engaged in developing and applying methods of improving the electrical properties of textile insulation and methods for the inspection control of commercially purified textiles for telephone apparatus.

R. E. WATERMAN, B.S. in Chemical Engineering, Williams College and Massachusetts Institute of Technology. Western Electric Company, 1922–25; Bell Telephone Laboratories, 1925–. Mr. Waterman has been engaged in organic and biochemical investigations and for the past few years has been in charge of a group studying the chemical phases of wood preservation.